

Aus dem Pathologischen Institut der
Ludwig-Maximilians-Universität München
Direktor: Prof. Dr. med. Thomas Kirchner

**Biopharmaceutical Characterization of
Porcine Mesenchymal Stromal Cells
as a Model System for a Human Cell Therapy Product**

Dissertation
zum Erwerb des Doktorgrades der Humanbiologie
an der Medizinischen Fakultät der
Ludwig-Maximilians-Universität zu München

vorgelegt von
Christoph Prinz
aus Köln
2017

Mit Genehmigung der Medizinischen Fakultät
der Ludwig-Maximilians-Universität München

Berichterstatter:

Prof. Dr. med. Dr. h.c. Ralf Huss

Mitberichterstatter:

Priv. Doz. Dr. Dorit Nägler

Mitbetreuung durch den
promovierten Mitarbeiter: Dr. phil. nat. Felix Hermann

Dekan: Prof. Dr. med. dent. Reinhard HICKEL

Tag der mündlichen Prüfung:

12.03.2018

Betreuer Prof. Dr. med. Dr. h.c. Ralf Huss

Datum, Unterschrift

Eidesstattliche Versicherung

Ich erkläre hiermit an Eides statt,
dass ich die vorliegende Dissertation mit dem Thema

*“Biopharmaceutical Characterization of Porcine Mesenchymal Stromal Cells
as a Model System for a Human Cell Therapy Product”*

selbständig verfasst, mich außer der angegebenen keiner weiteren Hilfsmittel bedient und alle Erkenntnisse, die aus dem Schrifttum ganz oder annähernd übernommen sind, als solche kenntlich gemacht und nach ihrer Herkunft unter Bezeichnung der Fundstelle einzeln nachgewiesen habe.

Ich erkläre des Weiteren, dass die hier vorgelegte Dissertation nicht in gleicher oder in ähnlicher Form bei einer anderen Stelle zur Erlangung eines akademischen Grades eingereicht wurde.

Unterhaching, den 11.04.2018

Prinz, Christoph

„Was lange währt, wird gut. Selten besser.“

Wolfgang Mocker

Für meine Familie,

Karola,

Lara

Content

1	Introduction	1
1.1	Multipotent Mesenchymal Stromal Cells (MSCs)	1
1.2	The Identity of MSCs and Their Heterogeneity	3
1.3	MSCs Change their <i>in vivo</i> Phenotype by <i>ex vivo</i> Manipulation	5
1.4	A Drug-Delivery System: Pharmacokinetics of MSCs	7
1.5	Therapeutic Gene Modification of Stem Cells and Usage of Inducible Promoters	11
1.6	The Suicide Gene “Herpes Simplex Virus Thymidine Kinase” and Apoptosis of Cells	13
1.7	The Pig and its Role as Large Animal Model (LAM) for Preclinical Studies	15
1.8	Modelling human MSCs: Porcine MSCs (in contrast to rodent MSCs)	17
2	Aim of This Work	20
3	Summary	21
4	Abbreviations & Units	23
4.1	Abbreviations	23
4.2	Units	25
5	Material	26
5.1	Consumables / Liquids (Media, Solutions, Kits, Chemicals)	26
5.2	Equipment and Software	27
5.3	Cell Lines	27
5.4	Antibodies	27
6	Methods	28
6.1	Isolation of Adherent, Mononuclear Cells from Bone Marrow	28
6.1.1	Donor characterization	28

6.1.2 Isolation of human MSCs	29
6.1.3 Isolation of porcine MSCs	29
6.2 <i>In Vitro</i> Cultivation	31
6.2.1 General.....	31
6.2.2 Thawing of cells	31
6.2.3 Standard <i>in vitro</i> cultivation and detachment of cells.....	31
6.2.4 Cell count determination	32
6.2.5 Isolation of single cell line clone (after transduction with a GFP gene)	32
6.2.6 Calculation of the population doubling time	33
6.3 Insertion of Genes.....	34
6.3.1 Transduction by direct seeding (Method A)	34
6.3.2 Transduction on PLL plates (Method B)	35
6.3.3 Transduction in suspension (Method C)	35
6.4 Selection, Expansion and Cryopreservation of Cells	36
6.4.1 Selection.....	36
6.4.2 Expansion and cryopreservation.....	36
6.5 Differentiation into Osteocytes and Adipocytes and Staining.....	37
6.5.1 Staining of osteocytes and analysis.....	37
6.5.2 Staining of adipocytes and analysis.....	37
6.6 Measurements by Flow Cytometry	38
6.6.1 Identification of surface markers	38
6.6.2 Intracellular staining of the HA-tag.....	39
6.6.3 Differentiation of apoptotic and dead cells in a single or several cell populations.....	40
6.7 Treatment of Cell Populations with GCV	42
6.7.1 Titration of cell sensitivity to GCV by using the MTT-assay.....	42
6.7.2 Mono-cultivation: characterization of apoptosis under the treatment with GCV.....	43
6.7.3 Co-cultivation: proof of the bystander effect	44
6.8 Isolation and Quantification of DNA.....	45
6.8.1 Isolation of DNA from cells and photometric quantification	45
6.8.2 Quantification of genomic DNA or a sequence of interest by real-time PCR	45
6.8.3 Determination of the mean retroviral vector insertion rate of a population	47
6.9 <i>In Vivo</i> studies and Histopathological Staining	49
6.9.1 Infusion of MSCs into pigs, clinical observation and pathology	49

6.9.2 Immunohistochemistry (IHC) on porcine tissues	50
6.10 Statistical Analysis of Results	50
7 Results	52
7.1 Strategy and Batch Production.....	52
7.2 Adherent Bone-Marrow MNCs from the Pig are MSCs.....	54
7.2.1 Porcine and human MSCs were plastic adherent and showed similar morphology	54
7.2.2 Surface markers of both species were nearly identical	56
7.2.3 HLA-DR presentation on human MSCs was inducible – not in porcine MSCs.....	59
7.2.4 Porcine MSCs differentiated with human stimulation media.....	60
7.2.5 Doubling time of porcine MSCs was comparable to human MSCs	65
7.3 Insertion of the Therapeutic Gene into Porcine MSCs was Controllable and Comparable to Human MSCs	66
7.3.1 Same vector / cell ratios lead to comparable transduction rates	66
7.4 Human-derived Promoters worked comparably in Porcine MSCs	69
7.4.1 Proof of functional human PGK promoters in porcine MSCs.....	69
7.4.2 Up-Regulation of RANTES in porcine MSCs was feasible	71
7.4.3 Porcine HSV-TK expressing cells showed higher sensitivity to ganciclovir	71
7.5 Porcine MSCs showed the same Mode of Action under GCV Treatment	75
7.5.1 Activated GCV initiated the apoptotic cascade in both species in a comparable manner.....	75
7.5.2 Population doubling time correlated with the efficacy of HSV-TK induced cell death	81
7.6 Proof of a Therapeutic Effect <i>in vitro</i> for Porcine MSCs.....	82
7.6.1 Inter species killing: porcine and human HSV-TK MSCs killed human cell line (HT1080) and porcine cell line (K67)	82
7.6.2 Both species induced the apoptotic cascade in co-cultivated cell lines.....	84
7.7 Experimental <i>in vivo</i> Studies: Biodistribution of intravenously infused MSCs in the Mini-Pig	86
7.7.1 Freshly thawed MSCs were stable for 90 min in the cryopreservation medium.....	86
7.7.2 Intravenously infused MSCs were detectable in the peripheral blood stream	87
7.7.3 Pathological report showed pneumonia in pig 2	91
7.7.4 Immunohistochemically analysis showed MSCs in lung and spleen	92

8 Discussion	95
8.1 The Identity of Humans´ and Pigs´ MSCs – Comparing Apples and Oranges?	95
8.2 Controllability of Gene-Modification Realizable in Porcine MSCs comparable to Human MSCs	100
8.3 Functionality of Human-Derived Promoter and Therapeutic Gene in Porcine MSCs ..	102
8.4 Programmed Cell Death by GCV– Do Both Species Go the Same Way?	104
8.5 Infusion of MSCs into Mini-Pigs indicate Lung-Passage Dependent Delay	110
8.6 Conclusions and Outlook	115
9 Acknowledgements	119
10 References	121
11 Supplemental	141

Figures

Figure 1: Here, a schematic description of the therapeutic cassette pEMTAR.bi-RANTES.tk including the selection gene is shown. The LTR sequences were part of the viral system facilitating an insertion of the gene, which was embedded between both LTR sequences. The HSV-TK gene was under the control of an inducible promoter, called RANTES. This RANTES promoter generally is inducible with pro-inflammatory cytokines e.g. TNF α and IFN γ . The HA-tag was attached to the kinase, which allowed a detection with accordant antibodies for measurement through flow cytometry. The enzyme PAC deactivated the cytoxin puromycin by acetylation. This enzyme was expressed continuously because it was under the control of a constitutive promoter (pPGK) allowing a selection by puromycin during cultivation. The WPRE sequence enhanced the stability of the transcribed transgene increasing protein expression [278]..... 34

Figure 2: This flow chart presents the comparison approach of the human and the porcine-derived cell therapy products. Both species cells derived from the bone marrow and were produced in the same way. After the first detachment, the cells were split into a naïve line and into a line that was transduced with the HSV-TK vector. Testing was performed on several different steps of the MSC product. *In vivo* studies were performed with porcine MSCs only..... 53

Figure 3: Before the first media change, no adherent cells were visible (A) since erythrocytes completely masked the plastic surface. The successive media changes reduced the amount of suspension cells dramatically until only adherent cells remained in the cultivation flask. Here, stromal cells (B) built up adherent colonies that showed a circular proliferation with a high cell density at the inner part. Within days, the colonies grew up until they got in touch with each other. Not later than 14 days, the cells were split and scattered for further proliferation. Scale bar: (A) 100 μ m and (B) 500 μ m..... 54

Figure 4: Porcine (A, batch: Porcine 0) and Human MSCs from donor 1 (B, batch: Human 1) in low-density seed showed fibroblast-like morphology. Microscopy showed that human MSCs tended to be larger than their porcine counterparts and were slightly more spindle-shaped. After seeding, both species showed nearly complete adherence in less than 2 h. Scale bar: 250 μ m.55

Figure 5: The human donor 2 (A, batch: Human 3) and donor 3 (B, batch: Human 5) were comparable in morphology to donor 1 and the porcine MSCs. Comparing donor 2 to the other human donors, a more flattened and enlarged size was visible. Scale bar: 250 μ m..... 55

Figure 6: In general, porcine and human MSCs showed a similar set of surface markers (also viability). The criteria of the ISCT were fulfilled. In contrast to CD90, CD105 was significantly less presented on porcine MSCs, which was further evaluated in Figure 7. CD45+, a typical haematopoietic marker, was not present on both species. HLA-DR was found on human MSCs

(see Figure 8) but not on porcine MSCs. More comparison stainings could not be performed due to the lack of commercially available antibodies for porcine cells. Statistics: two-way ANOVA... 57

Figure 7: In contrast to other positive MSC markers like CD90 (A), a small sub-population of CD105 negative porcine MSCs (B) could be observed (see arrow). The porcine MSCs showed a single population overlapping with the isotype control. A second population of positive cells could be discriminated..... 58

Figure 8: The presence of TNF α and IFN γ induced no up-regulation of HLA-DR on porcine MSCs in contrast to human MSCs. MSCs of both species were cultivated w/wo pro-inflammatory cytokines and stained for HLA-DR. The naïve and genetically modified batches were grouped. Porcine MSCs did not show any HLA-DR presentation on their surface whether stimulated or not. Human MSCs increased HLA-DR presentation under stimulation significantly. Statistics: two-way ANOVA. 60

Figure 9: Both porcine (A) and human (B) MSCs showed an adipogenic lineage potential. Defined stimulation media induced the cell differentiation. After 10 d, first fat vacuoles were observed. Not earlier than 14 d after the start of differentiation, the cells were washed and stained. The reddish colour of the droplets was caused by the red oil, which was used to detect the fat vacuoles more easily. The same commercial differentiation media were used for both species (the used media were indicated for human MSCs only). The human donors generally showed more lipid vacuoles than the pig (see Table 15). The human batch 1 (C) showed a significantly higher sensitivity for differentiation because the appearance large fat vacuoles was observable. In addition, small vacuoles lined up in a row (see arrows) at the edge of nearly all cells. (D) Appropriate controls showed no red oil staining although very small vacuoles could be observed in some sections. Scale bar: 250 μ m for (A,B,C) and 25 μ m for (D) (all sections had the same optical magnification)..... 62

Figure 10: Both species (porcine (A), human (B)) showed strong calcium enrichment. No significant difference between the batches and species could be observed. The porcine MSCs were equivalent to the human MSCs in their osteogenic potential with the human stimulation media. (C porcine, D human) Controls for both species showed no calcium enrichment if cultivated with the accordant standard media. Scale bar: 250 μ m..... 63

Figure 11: The mean population doubling time (PDT) of porcine and human MSCs was comparable. The mean PDT of the porcine batches was 62 h and while it was 58 h for the human batches. Obviously, a donor dependency could be observed indicating different doubling times for each donor. The porcine batches showed a similar population doubling time. Both batches of each donor showed similar population doubling times varying from 30 h to 100 h. Statistics: two-tailed, unpaired t-test. 65

Figure 12: Successful transduction was identified by flow cytometry measuring a second population (B) in contrast to a single population of naïve cells (A). (A) Naïve cells showed a typical negative population in the SS / fluorescence plot. (B) The heterogeneous cell population of transduced and naïve cells showed a partial shift creating a diffuse second population. Isotype-controlled gating showed more than 46% cells expressing the transgene. 67

Figure 13: (A) Transducing MSCs with the same vector/cell ratio and the same method led to comparable mean transgene rates in both species. The human batches 2 and 6 had slightly reduced insertion rates, whereas Human 4 was quite similar to Porcine 4. (B) If only the method of transduction was changed (same vector / cell ratio), the insertion rate varied significantly. Method B showed the highest efficiency while method A and C did not show any statistical relevant changes. Statistics: (A) ordinary One-Way ANOVA and (B) ordinary Two-Way ANOVA. 68

Figure 14: (A) The selection by puromycin killed most of the adherent cells visible as detached, spheric units. (B) As soon as the selection medium was depleted and a standard medium was given into the culture, the MSCs started to proliferate again, indicated by small, not flattened cells. Scale bar: 250 µm. 69

Figure 15: (A) Naïve porcine cells showed a typical population distribution in the fluorescence / SS depiction. (B) After transduction and selection without RANTES activation, background expression of the not induced promoter was detectable (37%). Here, the cells distributed on both sides of the gate. (C) If pro-inflammatory cytokines were given into the medium, a single population of porcine HSV-TK expressing cells was identified. 70

Figure 16: Stimulation of the human RANTES promoter with pro-inflammatory cytokines led to increased HSV-TK expression in both species. Although the RANTES promoter was isolated from human cells, it showed functionality in porcine MSCs. Slight background expression was detectable in both species in comparison to naïve cells as the negative control. Statistics: paired t-test for columns A/B and C/D and Welch's test (unpaired t-test, non-equal stdv) for the comparison of porcine to human batches. 71

Figure 17: Porcine (A) and human MSCs (B-D) expressing HSV-TK showed a higher sensitivity to GCV than their naïve counterpart. Increasing the GCV concentration in a logarithmic scale showed an earlier effect on transduced MSCs, decreasing the amount of living cells. The cell line HT1080 and the porcine cell line K67 did show a GCV sensitivity profile (E) like naïve MSCs. Statistics: nonlinear regression (dose response inhibition), *goodness of fit* for each figure A-E: $R > 0.9$ 73

Figure 18: The EC50 (half-maximal effectivity of GCV) of all non-transduced MSCs and cell lines were more than 100-fold lower than HSV-TK expressing cells. The porcine cells showed sensitivity

differences of nearly 1000-fold. Statistics: standard deviation bases on the 95% confidence interval of the nonlinear regression..... 74

Figure 19: (A) Naïve porcine MSCs did not react with massive apoptosis if GCV was added to the medium. The naïve cells showed good adherence and only occasional deatchment was visible although GCV was present. (B) The treatment of HSV-TK expressing MSCs with GCV led to a massive accumulation of cells and cell debris in the supernatant, which could be seen on day five. (C) Depleting the medium only occasionally showed adherent cells. Scale bar: 250 µm. ... 76

Figure 20: The treatment (pro-inflammatory cytokines + GCV) of HSV-TK expressing cells showed significant reduction in cell proliferation in contrast to also treated naïve cells. All groups were additionally cultivated without treatment as negative control. At the end of the assay, the cell counts of the treated groups were normalized to the negative control and the reduction was calculated. Both species showed a comparable percentage of killed cells during treatment for HSV-TK expressing and naïve cells. Statistics: paired t-test for columns Porcine 1 / Porcine 2-4 (HSV-TK) and Human 1,3,5 / Human 2,4,6 (HSV-TK) and Welch´s test (unpaired t-test, non-equal stdv) for the comparison of porcine to human batches..... 77

Figure 21: GCV-treated, HSV-TK expressing porcine MSCs in contrast to non-treated MSCs: Morphological changes correlated with different stages of apoptosis. (A) Non-treated MSCs were characterized by one population in the FS / SS plot. (B) If this population was stained for 7-AAD and Annexin-V, a slight drift to Annexin-V positive cells was observable. Very small amounts of cells were 7-AAD positive indicating dead cells. (C) Since no further populations were visible, the gating showed no cells. (D) Treatment of HSV-TK expressing cells generated a second, smaller but more granular population in the FS / SS plot. (E) Staining with 7-AAD and Annexin-V for cells gated on the “normal population“ showed mainly Annexin-V positive cells and a smaller Annexin-V and 7-AAD negative population indicating living cells. 7-AAD cells were increased if compared to the amount of 7-AAD in (B). (F) Gating on the smaller and more granular population (here “shrunk population“) showed that nearly all cells were 7-AAD and Annexin-V positive. A smaller sub-population was Annexin-V positive only..... 78

Figure 22: Porcine and human HSV-TK expressing MSCs became smaller and more granular if they were treated with pro-inflammatory cytokines and GCV. In this figure, the distributions of the cells in the FS / SS are summarized for all batches after treatment following the gating strategy of Figure 21. Naïve cells of both species primarily showed a normal morphology in the FS / SS with more than 80% in the “normal population” gate in spite of the treatment. HSV-TK expressing MSCs showed a change to more granular and smaller cells. Human HSV-TK MSCs showed about 30% of shrunk cells but porcine HSV-TK MSCs showed up to 70% of shrunk cells. Statistics: two-way ANOVA; following comparisons did not show a significant difference: Porcine 1 and Human 1,3,5 for normal and shrunk population (p=0.34 and p=0.56); Human 1,3,5 and

Human 2,4,6 for shrunken population ($p=0.05$). All other comparisons did show a significant difference ($p<0.05$)..... 79

Figure 23: (A) Annexin-V stains phosphatidylserine as apoptotic marker and was significantly higher presented on HSV-TK expressing MSCs under treatment. All naïve and HSV-TK expressing batches were cultured with or without treatment on day three, four and five. On day five, the cells were detached and stained with Annexin-V. In contrast to naïve cells under treatment, the increase in Annexin-V for all HSV-TK expressing batches was significant. If naïve cells were treated, they showed a trend to be more Annexin-V positive although this was not statistically significant. (B) HSV-TK expressing cells showed also a statistically significant shift to 7-AAD. All batches were treated the same way as described in section 7.5. Here, only Annexin-V positive cells were gated for 7-AAD following the described gating strategy (see Figure 21). This increase was statistically significant only in porcine cells. Human MSCs expressing HSV-TK showed the tendency to be more 7-AAD positive, which cannot be confirmed statistically ($p=0.23$). Statistics: two-way ANOVA. 80

Figure 24: The growth speed of a population correlated with the reduction of cells due to GCV-initiated apoptosis. All HSV-TK expressing batches were counted before seeding and after cultivation in the standard medium (after harvest). This growth is described by percentage in the horizontal axis. All HSV-TK expressing batches were treated over five days. The amount of killed cells of each batch was normalized to the seeded cells cultivated in the standard medium. Irrespective of the species, the killing efficacy correlated with the growing speed of a population. Statistics: linear regression, $R^2=0.92$ 81

Figure 25: Porcine and human HSV-TK MSCs reduced the amount of the porcine and the human cell line during co-cultivation and treatment. (A) If HT1080 were co-cultivated with naïve cells, no significant shifts could be observed between porcine and human cells. But there were less HT1080 cells present in the population if cultivated with porcine cells. The killing of HT1080 cells by both species was comparable. (B) K67, the porcine cell line, was killed by both species with the same efficacy. In contrast to naïve porcine MSCs, the naïve human cells also showed anti-proliferating effects: the batch Human 5 and, partially, Human 1 showed an inhibition of the proliferation since less than 50% K67 cells were left after treatment although no HSV-TK expressing cells were present. This effect was species-specific as no similar observations could be made if co-cultivated with naïve porcine MSCs. Statistics: ordinary one-way ANOVA for each graph, referring to first column in graph A and to second column in graph B. 83

Figure 26: MSCs of both species induced the apoptotic cascade in HT1080 as shown by a simultaneous increase of Annexin-V and 7-AAD. (A) Naïve porcine or human MSCs did not induce any significant increase of Annexin-V or 7-AAD in HT1080 cells. HT1080 cells in mono-cultivation served as control. HSV-TK expressing human and porcine MSCs raised the mean percentage of Annexin-V positive HT1080 to 93% respectively 88%. (B) Also, the amount of 7-

AAD positive cells increased in the presence of HSV-TK expressing MSCs. Human HSV-TK expressing MSCs did not induce a statistically significant increase ($p=0.06$). Porcine HSV-TK expressing MSCs caused an accumulation of 7-AAD positive cells of 40%. Statistics: two-way ANOVA. 84

Figure 27: As well as HT1080, K67 cells were killed by in an apoptotic mode of action by both species. (A) Annexin-V was significantly increased for HSV-TK expressing, porcine and human MSCs. But also naïve human MSCs showed an increase of Annexin-V positive K67 cells in contrast to naïve porcine MSCs. This effect differed significantly from HSV-TK expressing human MSCs. (B) 7-AAD was increased, too, although it was overall lower than observed for HT1080. Statistics: two-way ANOVA. 85

Figure 28: Porcine MSCs (A) and Human MSCs (B) showed no significant reduction in proliferation if they stayed in the cryopreservation medium for 120 min (A) or respectively 90 min (B) after thawing. On day one, one vial of each batch was thawed and left for 180 min in the cryopreservation medium. A defined amount of cells was sowed out in triplicates every 30 min. After four days, all wells were harvested and counted. (A) Porcine MSCs showed a significantly reduced amount of cells, if the cells were left for 150 min. Human MSCs already showed a significant difference after 120 min in contrast to the same amount of cells, which were sowed out immediately after thawing. Statistics: one-way ANOVA (all data were compared to point in time 0 min). 87

Figure 29: (A) Blood samples were aspirated through a peripheral venous catheter, which was implanted into an ear vein (see arrow). (B) The cells were infused into the jugularis vein by a catheter that was fixed at the nape to reduce possible damage by the pigs' movement after waking up. (C) A sleep-inducing drug was injected to allow the correct placement of the intravenous access and to reduce the stress for the animal. The sleeping agent's activity lasted for about two to four hours until the pigs woke up again. This immobilization allowed for a simplified blood sampling during the first hour of infusion. From day two on, the blood sample counts were deliberately low. Otherwise, the stress for the animals would have been too high. On day three, respectively five, the animals were euthanized in the *Institut für Tierpathologie der Ludwig-Maximilians-Universität München* and pathologically examined..... 89

Figure 30; Fig 1: Intravenously administered cells could be detected in the peripheral blood stream by accurate isolation and quantification through real-time PCR. Pig 1 received a dosage of 5.1×10^6 MSCs / kg bodyweight. Blood samples were aspirated at different points in time before and after injection. The detection limit of the method was 450 MSCs per mL due to the preparation of the sample for measurement. Assuming an even distribution of all cells in the blood stream, the maximal expectation would be about 22,000 MSCs per mL blood (supposing 6% blood volume / bodyweight). MSCs could be identified at 2 min and 6 min after infusion. In the following minutes to hours, infrequent signals could be detected. In the end, a strong signal could be identified after

30 h. Statistics: none, descriptive only; three analysis (each consisting of five measurement) are depicted. 90

Figure 31, Pig 2: In contrast to pig 1, no significant consistent signals could be detected in the peripheral blood. Pig 2 received a dosage of 5.9×10^6 MSCs / bodyweight. Although the dosage was increased, only signals next or under the detection limit were identified. At no point in time the measured signals were higher than the detection limit. Statistics: none, descriptive only; three analysis (each consisting of five measurement) are depicted. 90

Figure 32: Anti HA-tag immunohistochemistry detected HSV-TK expressing MSCs in spleen (A; animal 1) and lung (B, animal 2); identifiable by a brownish colour (see arrow). Lung, spleen and liver of both animals were sent into an external laboratory for immunohistochemical examination. Several histo-pathological sections were analyzed to detect any MSCs in the tissues in question (see Table 19). In addition, three tissue samples of a mini-pig that received no MSCs were sent as control, too. As a second negative control, all stainings were compared to an appropriate antibody isotype (C, D). 93

Figure 33: Construct #65 was used as plasmid for the clinical grad vector carrying the therapeutic gene HSV-TK under the control of the Rantes promoter. HSV-TK was fused with HA to allow an identification of the enzyme by flow cytometry mediated by antibodies. The selection gene for degrading the antibiotic puromycin is controlled under the constitutive promoter hPGK that shows continuous expression. The WPRE enhances the mRNA stability of the transcribed gene. 141

Figure 34: The eGFP containing plasmid was used to tag the cell lines HT1080 and K67. The GFP signal was used during flow cytometry analysis to distinguish cell lines and MSCs. The expression of GFP was under control of the EFS, a constitutive, promoter. 141

Tables

- Table 1: This overview represents the nomenclature and properties of human and porcine MSCs in the generation of the cell products. The human donors were chosen based on a thorough medical anamnesis following the accordant laws (actual, german tissue and transplantation law). The pig's cells isolation was performed by members of the *Lehrstuhl für Biotechnologie der Nutztiere* from the *Technische Universität München*. The mini-pig derives from an isogenetic inbreed. This animal is isogenetic to the pigs that were used during the biodistribution study (see 7.7)..... 28
- Table 2: Description of the cultivation media. Bio-1 was used for human MSCs. This media does not contain FBS but platelet lysate that is based on a patent, referenced in 4.1. All other media, also for porcine MSCs, had FBS as an ingredient. The recipe for the porcine MSCs cultivation media is based on personal communication with the working group of *Prof. Angelika Schnieke* of the *Technische Universität München* leading the "Chair of Livestock Biotechnology" 32
- Table 3: Description of the cryopreservation media used for different types of cells [279]. 10% DMSO was used for all cell types to reduce the amount of crystallization during the freezing process. Hydroxyethyl starch served as the cryoprotective supplemental protecting the cell surface [280]. 36
- Table 4: The staining of porcine MSCs for flow cytometry measurement was performed with the following fluorophore-conjugated antibodies and 7-AAD. All stainings were performed as single stains to reduce compensational work. All antibodies were generated from murine cell lines as declared by the manufacturer. 38
- Table 5: The staining of human MSCs for flow cytometry measurement was performed with the following fluorophore-conjugated antibodies and 7-AAD. The stainings were done by multiple stainings per tube, so called master mixes. All antibodies were generated from murine cell lines. Accurate compensation was done as needed. 39
- Table 6: The staining of the HA-tag for flow cytometry measurement was performed with the following fluorophore-conjugated antibodies. The antibody was generated from a murine cell line as declared by the manufacturer. 40
- Table 7: The staining of apoptotic and dead cells was performed utilizing Annexin-V and the dye 7-AAD. These markers / dyes allow a distinction of apoptotic and necrotic cells. Mediated by Ca^{2+} , Annexin-V binds phosphatidylserine on the cell's surface if presented. Apoptotic cells can not be stained with 7-AAD since these cells still have an intact lipid bilayer. 40
- Table 8: GCV was given into a serial dilution and added to the media to quantify the GCV sensitivity. All cells were treated following the same GCV dilutions..... 42
-

-
- Table 9: Each cell line and each batch of MSCs was measured for GCV sensitivity in a 96-well plate. Five parallel cultures were generated to take the assay variance into account. The accordant GCV concentrations are listed in Table 8. A staining control (st ctrl) without any cells was performed to consider staining artefacts. PBS was given in the outer rows and columns to reduce evaporation effects..... 43
- Table 10: To characterize the apoptotic pathway under the treatment with GCV, the cells were to reach a confluency of less than 25%. Because the size of a cell also depends on its origin, species and “*in vitro* age”, different cell seedings were chosen. 44
- Table 11: Single-copy genes or a defined sequence of interest allowed the quantification of DNA by specific real-time PCR. Because photometric measurements unspecifically measure the whole DNA in a sample, the defined quantification of a DNA or a sequence of interest was performed by real-time PCR [281]. To measure the insertion rate into a population, the therapeutic gene was quantified by the amplification of the transgene enhancer WPRE [278], which generally is not present in naïve cells. 46
- Table 12: The following master mixes were used for the quantification of single copy genes or the transgene sequence WPRE. All mixes were tested with different concentration of primers and probes / dyes to optimize the amplification and the robustness of the result. 47
- Table 13: This overview summarizes the difference between data sets that were entitled as statistically significant or not. If the assumed normal distribution of two data sets differed for more than 95% from each other, the difference was assessed to be significant. If the statistical differences of the distributed values were even 99% or higher, it was described with the accordant symbol to underline this difference..... 51
- Table 14: Here, a detailed list of all measured, present and absent marker of both species is shown (as well as viability in the measured populations). For porcine cells, the variety of commercially available antibodies was very low in contrast to human MSCs. Most of the markers were described before (see 1.2). Hematopoietic markers e.g. CD45 and CD34 were absent for both species (CD34 could only be measured for human MSCs). Statistics: With the exception of batch Porcine 1, all groups are described by their mean value and standard deviation. 59
- Table 15: Overview of differentiation potential of both species. All batches were differentiated following the same protocol. After differentiation, the populations were fixed, stained and representative sections (~750 µm × 1000 µm) were counted for differentiated cells. All batches kept their differentiation potential whether transduced or not. If the cells were cultured with standard media, no signs of differentiation could be observed. The porcine cells could be differentiated following the same protocol and same differentiation media designed for human MSCs. After the induction time, porcine MSCs generally showed less adipogenic potential than human MSCs.
-

Only donor 2 (Human 3 / 4) was as weak as the porcine MSCs. Coloration: red ≥ 25 , orange 15-25, yellow ≤ 15	64
Table 16: Different transduction methods led to different transduction rates although the vector / cell ratio was equal. Method C and A showed transduction rates that obviously did not differ as much as method B. Statistics: none, descriptive only.	67
Table 17: This table shows all relevant facts about the pigs and the cells used for the biodistribution study. Two clinically healthy mini-pigs were chosen for the study. Two intravenous catheters were implanted into each pig to separately inject the cells into the jugularis vein and aspirate blood samples from the ear vein (see Figure 29). After positive results were generated in the first animal (see Figure 30), the amount of blood samples was increased and the second animal's life-time was expanded to five days. After three, respectively five days, the pigs were euthanized and necropsied at the <i>Institut für Tierpathologie der Ludwig-Maximilians-Universität München</i> . 88	88
Table 18: At the end of the life-time, both animals were necropsied for histo-pathological examination. The main anatomical and histological findings and the final pathological expertise are described in the table. Pig 1 showed a pericarditis and pig 2 showed a high-grade pneumonia and a chronic gastritis. During the study, no clinical observations by the responsible veterinarian (member of the <i>Institut für Molekulare Tierzucht und Biotechnologie der Ludwig-Maximilians-Universität München</i>) were noticeable. The pathological and histological assessment was performed by members of the <i>Institut für Tierpathologie der Ludwig-Maximilians-Universität München</i>	91
Table 19: The immunohistochemical analysis of lung, spleen and liver showed MSCs in both animals. Several sections were analyzed before MSC-positive slices were identified. The number of sections represents the count which was positive for MSCs. Pig 1 showed MSCs in lung and spleen. Pig 2 showed MSCs in the lung only.	94
Table 20: This overview concludes all <i>in vitro</i> tested parameters and the generated results within this work. For both species, all tested parameters were assessed against each other. Porcine MSCs showed to be a well-usable platform for human MSCs because they had many similarities regarding identification, production and therapeutic efficacy <i>in vitro</i> . Most of the <i>in vitro</i> generated results showed the comparability of both species.	115

1 Introduction

1.1 Multipotent Mesenchymal Stromal Cells (MSCs)

Friedenstein *et al.* described multipotent stromal or mesenchymal stem cells for the first time in 1968 [1]. These are non-haematopoietic, multipotent cells that were isolated from the bone marrow and could easily be cultured due to their plastic adherence. Friedenstein *et al.* could show that these cells support the haematopoiesis and are able to differentiate into osteogenic cells [2].

More than 45 years of research on MSCs have been performed since discovery. In spite of all efforts, the clear identity and all *in vivo* functions are still unclear [3]. The “International Society of Cell Therapy” (ISCT) defined the nomenclature and essential properties of MSCs to harmonize controversies and to get a uniform understanding. The three criteria: plastic adherence, differentiation potential and defined surface proteins gave an important but minimalistic basis [4, 5]. The heterogeneity of the population [6], the pro- or anti-inflammatory switching phenotype [7, 8] and the numerous tissues from which so-called MSCs were derived [9] are still questionable and cannot be answered by the ISCT criteria alone. Also regulatory authorities understand the inconsistencies of MSC-based medicinal products as an important question [10]. Unlike HSCs, the MSC role in the bone marrow stem cell niche is still under investigation and it seems that they are strong supporters of the HSC niche [11]. The proof of a highly primitive stem cell character – as it is shown for HSC’s bone marrow re-population in irradiated mice [12-14] – could not be performed yet since defining accurate assays is complex although transplantation of so called “heterotopic ossicles” could be performed [15].

Despite the biological questions in the field of MSCs, the enormous therapeutic potency of these cells becomes obvious when treating Graft-versus-host disease (GvHD) [16] or *osteogenesis imperfecta* [17]. In 2012, Prochymal® was the first approved MSC-based drug showing a benefit treating pediatric patients suffering from advanced GvHD [18, 19]. Many successful applications and treatments of inflammatory diseases like Crohn’s [20], joint diseases [21] or other autoimmune diseases [22] underlined the immunomodulatory and regenerative capability of MSCs. Moreover, the constant increase of clinical trials, which are listed on www.clinicaltrials.gov with the term “mesenchymal stem cell”, is raising hope to patient’s needs.

Even if many therapeutic applications are promising, it is a path of trial and tribulation [23-25]. Many cornerstones are still unknown and clinical setbacks have to be overcome. The hallmark of MSCs, a real stem cell defining set of surface proteins and the control of their variable properties are still milestones in this field [26].

1.2 The Identity of MSCs and Their Heterogeneity

First, these cells were called non-hematopoietic, “osteogenic cells” and later on the term “stromal stem cells” was established [2, 27]. Arnold Caplan broadened the concept to “mesenchymal stem cells” [28]. Because of many controversies and a little accordance in the nomenclature, the *ISCT* suggested “multipotent mesenchymal stromal cells” in 2005, excluding the word “stem” since the real stem cell character could not be shown yet [4].

One year later, the *ISCT* also demanded a by now generally accepted, valid set of requirements, which *ex vivo* expanded MSCs have to fulfill. Firstly, the cells must adhere to plastic. A simple seeding of the bone marrow or other tissue shows colony forming units (CFUs). Secondly, defined media with stimulating cytokines and drugs can induce a differentiation into adipocytes, osteocytes and chondrocytes [5, 29]. After a defined incubation time with an e.g. adipocyte stimulation media, fat vacuoles are observed in the cells and are easily stained with lipophilic dyes. Even if these assays show the multipotency of MSCs, there is still criticism regarding functional proofs of the differentiated cells [30]. The most valuable and last assay of the *ISCT* proposal is the verification of certain surface proteins discriminating MSCs from hematopoietic cells. While CD90 (Thy-1), CD73 (ecto 5' nucleotidase) and CD105 (endoglin) are typical positive marker, other proteins like CD45 (pan-leukocyte marker), CD34 (primitive hematopoietic progenitor), CD14 and CD11 β (monocytes and macrophages) CD79 α and CD19 (B-lymphocyte marker) must not be identified *in vitro*. Appropriate flow cytometry can easily recognize an MSC population by suitable antibody staining [5].

Following the fundamental requirements of a medicinal product from a pharmaceutical point of view, the active substance must be described by identity, purity and content. The minimal criteria are helpful to describe MSCs, but recent publications show that these are not sufficient because the pharmacological activity of MSCs is highly variable and does not mandatorily correlate to known markers [31-33]. Therefore, the hidebound check for the previously defined surface proteins to determine e.g. the purity of the active substance may raise false-positive results, as these markers may not present the desired phenotype [34]. The preparation of MSCs by adherent culture is a source of heterogeneity since the donor, the chosen tissue, purification steps, culture media, cytokines, passaging and expansion time have great impact on the phenotype of the cells without losing the *ISCT* prerequisites [6, 35]. Therefore, accurate potency assays for the intended indication characterizing the wanted properties rightly are heavily needed [36, 37] since describing the identity is obviously a tough task.

MSCs react on IFN stimulation by expressing immunomodulatory cytokines and presenting MHC-II on their surface. Additionally, MSCs are able to switch from their mostly observed anti-inflammatory to a pro-inflammatory phenotype expressing different interferons (IFNs) [31, 38, 39]. This can be induced by an anti-inflammatory milieu [39, 40]. Nonetheless, transient markers which correlate with the actual phenotype are lacking and hence the phenotype of MSCs has to be described mostly by functional assays e.g. a T-cell proliferation assay [41]. This *ex vivo* change of the phenotype is described in 1.3.

Apart from the phenotype, the heterogeneity of the isolated, adherent cells [42, 43] requires a unique stem cell marker which may identify the “true” stem cell sub-population. Great efforts are made screening for the most potent subset of cells. SSEA-3 (stage-specific embryonic antigen-3) [44] and CD146 (cell surface glycoprotein MUC18) [45] are auspicious markers that were found on MSCs sub-populations [46]. Especially CD146 showed a good CFU-F enrichment after sorting [42]. Other markers like CD349 (frizzled-9) [47], GD2 (a neural ganglioside) [48] or CD49f ($\alpha 6$ -integrin) [49] correlate with better CFU-F enrichment or a more effective differentiation. But all these markers are also presented on other cell types too and are therefore helpful, but not unique. Additionally, the subset of positive markers differs from tissue to tissue from which MSCs are derived [46].

Unless a sole marker correlating to a stem cell-like sub-population was identified by accurate functional assays, it makes sense to follow the ISCT recommendations and to call the adherent cells “multipotent mesenchymal stromal cells” and to exclude the term “stem”. MSC is hence a concept, which describes the whole population of all adherent cells from an isolation fulfilling the minimal ISCT criteria [4, 5].

1.3 MSCs Change their *in vivo* Phenotype by *ex vivo* Manipulation

The *in vivo* phenotype of MSCs is still not fully understood [3]. Often, these cells are directly linked to pericytes [50, 51] or fibroblasts [34, 52, 53] since they share many similarities. Especially pericytes are in the focus because they are able to beneficially stimulate their tissue site with a panel of cytokines. There is increasing evidence that MSCs remain also in a perivascular niche [50] and are activated if the tissue site is injured [54]. Studies in animal models underline the vascular thesis since the CFU-F of MSCs and the blood vascular density seem to correlate [55].

MSCs are highly affected by *ex vivo* expansion [35]. On one hand, it is difficult to understand how the used protocols impact the MSCs and leads to unwelcomed stimulation. On the other hand, MSCs may be understood as a platform, ready to be conditioned for treating a chosen indication. Several studies investigated the impact of elemental culture manipulations: hypoxic conditions, addition of pro- or anti-inflammatory cytokines and the mechanical interaction with 2D- or 3D-layer. These culture conditions led to different profiles and amounts of secreted cytokines, reviewed by Madrigal *et al.* [32].

MSCs cultured under hypoxia express several growth factors like vascular endothelial growth factor (VEGF), fibroblast growth factor 2 (FGF-2), hepatocyte growth factor (HGF) and insuline like growth factor 1 (IGF-1) in dependence of NF-kappa β . These growth factors support angiogenesis, anti-apoptosis and may maintain the stem cell character of MSCs [56-58] as well as the immunomodulatory capacities mediated by increased expression of indolamine 2,3 deoxygenase (IDO) [59]. This modulated phenotype is also *in vivo* significant and may lead to better neuronal regeneration after brain injury [60] or reduces the effects of diabetic cardiomyopathy [61]. In general, hypoxic condition is a potent manipulation to enhance regenerative effects of MSCs [60].

It is well described that human, but also canine and murine MSCs are HLA-DR positive [62] and show MHC-II on their surface and an increase of IDO expression if stimulated with IFN γ and TNF α [63-65]. These cytokines are potent inducers to generate an anti-inflammatory phenotype [31], which can be proofed by the T-cell proliferation assay [41]. IDO, as well as prostaglandine-2 (PGE-2), transforming growth factor β (TGF- β) and galectin-9 (Gal-9) are prominent anti-inflammatory markers [66-68] and are essential for the anti-inflammatory potency.

GvHD is a life-threatening disease and is often successfully treated with MSCs. These treatments are well studied [16, 18, 19, 69, 70]. Increasing the potency on these indications

with pre-stimulation may promise better efficacy [71] in these critical, inflammatory indications.

Beside the chemical-biological milieu, the mechanistic interaction of MSCs with their environment may have great impact, too. 3D-culture systems mimic the stem cell niche more than standard 2D monolayers do. These spheroid cultures stimulate the secretion of trophic factors. For example, TNF-stimulated gene 6 protein (TSG-6), an anti-inflammatory protein, is only expressed in 3D culture flasks, which may vary the treatment outcome [72]. Although, the diversity of culture systems will differently impact the cells properties, spheroids in general seems to promote an anti-inflammatory phenotype [73, 74].

1.4 A Drug-Delivery System: Pharmacokinetics of MSCs

The pharmaceutical industry regularly designs new drugs following the “*Rule of Five*” to enhance a good systemic absorption after oral intake [75]. These drug properties are investigated in extensive studies on absorption, distribution, metabolism and elimination (ADME) [76]. New to this field, biopharmaceutical products gain also center stage in ADME evaluations [77].

The pharmacokinetics of small molecule drugs is passive, controlled by the biology of the body and its biochemical processes. This fact challenges the pharmaceutical industry for appropriate design of small molecules because little alterations on the chemical compound may have great impact on the drugs pharmacological profile [75, 78]. Beside vaccines, antibodies are the first generation of biologicals, which found their way into clinical pharmacy. Therapeutic antibodies show a great field of usage in cancer therapy as drug delivery systems e.g. Adcetris® or as agents acting directly against the tumor e.g. Erbitux®. Nevertheless, antibodies follow the rules of passive diffusion gradients as well as small molecules and only increase their therapeutic efficacy by their high specificity to target structures. In contrast to these classical medicinal product groups, many research groups promise a new class of pharmacokinetics for cells, especially for MSCs: directed targeting respectively the so-called homing.

Successful clinical results treating *osteogenesis imperfecta* showed the therapeutic potency of the bone marrow and its cells in the early 2000s [17, 79]. Good clinical response of MSCs-treated children indicated an engraftment of the donor cells into the patients’ bone after intravenous administration. This basic proof of concept – the feasibility of treatment with MSCs by intravascular application– facilitated many new clinical approaches and applications for other indications suitable for MSC treatment e.g. GvHD [80], cancer (MSCs as drug-delivery system) [81-83] or regenerative indications [84]. Systemic transplantation of MSCs seemed to be performed quite easily. Since then, many *in vivo* studies have been performed to examine the pharmacokinetics of MSCs, summarized in several reviews [85-88].

Beside the therapeutic success, the method of detection is a major hurdle to track MSCs *in vivo* and to define the biodistribution of MSCs. Approaches range from labeling with radioactive systems, fluorescent vital dyes, contrast agents, reporter genes or cell-specific DNA markers (microsatellites) [89-93]. Some of the detection systems can only be used for

short time-intervals or do not distinguish between living and dead cells. This makes the evaluation of the generated data difficult.

In spite of the tracking method challenges, it is well understood that intravenous administered MSCs mainly reside in the lungs' vascular system for the first hours after administration [72, 94, 95]. It is still a matter of debate whether the cells' size or surface proteins regulate this interaction. The average diameter of MSCs is about 16-53 μm dependent on tissue origin, culture conditions, passage and several other factors [96]. HSCs are about 4 - 12 μm large. Therefore, obstructive processes in the pulmonary capillaries (<10 μm diameter [97]) are probable. Preclinical studies proofed a pulmonary first-pass effect after systemic infusion in small and large animal models [72, 92, 98, 99]. This effect might be reduced if a vasodilation is performed by administration of nitroprusside [100] underlining the importance of the cells' size and the steric interaction.

In spite of these steric issues, it is evident that surface molecules of MSCs also interact with endothelial cells. Although CXCR4, a prominent homing receptor, is absent on culture-expanded MSCs [101, 102] (and is only broadly present after induction [103]), adhesion molecules like vascular cell adhesion molecule (VCAM-1) are involved in endothelial interaction [101]. VCAM-1 and the surface protein very late antigen-4 (VLA-4) are immanent for the firm adhesion of MSCs to the endothelium [104]. Studies on different enzyme treatment during harvesting show the important role of the adhesion markers. Different enzymes used for detachment alter the lung clearance significantly [105]. This was also underlined by results indicating a correlation between the whole surface profile and its markers and lung clearance [106]. In contrast to intravenous administration, intra-arterial applications avoid the first-pass effect in the lungs and show an increased uptake in inflammatory sites [107] and therapeutic efficacy [108, 109]. But, intra-arterial infusions are more complex to be handled in a clinical setting.

After the first hours to days in the lungs vascular system, MSCs relocate throughout the body. Here, inflamed tissues seem to attract the - mostly immunosuppressive - cells [89, 110]. Tumors and their immunological microenvironment are highly complex and seem to be an attractive target for MSCs [111-114]. The physiological role of stromal cells as e.g. tumor-associated fibroblasts is still unclear although there is evidence that MSC can inhibit or contribute to growth of solid tumors dependent on the preclinical setting. It is obvious that MSCs play a role in the tumor microenvironment. *Niess et al.* evaluated these contradictory reports in a review [115]. This involvement of MSCs in the tumor stroma led to therapeutic approaches bringing a suicide gene next to the tumor cells. Several authors examined this

MSC based drug-delivery system [116-118]. The efficiency of homing (and the efficacy of the therapeutic suicide gene) is still challenging this therapeutic approach.

Preclinical models with myocardial infarction allow a good insight into the MSC homing. Here, MSCs have been observed to accumulate at ischemic sites [119, 120]. Interestingly, transgenic mice expressing CCR2 in cardiac muscle cells have a significant higher recruiting rate of MSCs [121]. But, it is still unclear if MSCs are temporarily or constantly incorporated into the cardiac tissue.

More cues than evidences have been shown for kidney diseases. Although the therapeutic usability of MSCs in kidney indications was proofed, the mechanisms beyond that are not yet understood [122]. The fact that also MSC derived microvesicles showed therapeutic effects in an acute kidney injury mouse model [123] as well as MSCs themselves [124, 125] queries direct correlations between pharmacodynamics and pharmacokinetics and therefore the homing of MSCs into the site.

Gholamrezanezhad *et al.* provided evidence of the biodistribution in humans by measurement of radioactive ¹¹¹In-oxine labeled MSCs [110]. Here, the cells passaged the lung successfully. Hours to days later, the MSCs migrated into the liver of patients with liver cirrhosis. Cells could also be detected in the spleen. Intriguingly, a recruitment of cells into the injured liver of mice could not be shown [126] underlining the difficulty of translational studies.

The work of Horwitz and colleagues [17, 79] indicated a successful engraftment of MSCs into the bone marrow of children with *osteogenesis imperfecta* as referenced before (see 1.1). In contrast to these data, it is evident that donor MSCs do not generally engraft in allogeneic hosts [127-129]. Especially long-time culture can reduce the homing capacities of MSCs dramatically [130].

Besides the fact that MSCs show an accumulation at inflamed sites, the ratio of homing MSCs vs. infused MSCs is still hard to determine. The methodological limits often reduce the meaningfulness of quantitative assessments. Descriptive data are mostly relative to the accordant methodological controls only allowing vague statements. Systemically infused MSCs show both migration to the pathological site [110, 121, 131] and distribution throughout other organs [89, 93, 132]. Absolute cell numbers are seldom stated in publications.

The possibility of using cryopreserved MSCs for clinical trials is very popular since planning and therefore costs may be reduced. At any given moment, the medicinal product may be

freshly thawed just before administration. But, cryopreservation also alters the physiological activity and cellular structure and therefore the biodistribution. Galipeau *et al.* published disillusioning results of cryopreserved MSCs in contrast to living MSCs regarding desired pharmacokinetics [133] and good pharmacodynamics [134, 135] suggesting to use cultured MSCs for immunosuppressive indications. Several working groups got aware of this challenge and tried to optimize their cryopreservation and thawing protocols to improve cell viability and function for their MSC based products [136-138]. The pro of cryopreservation to save costs and the con of reduced migration capabilities and therefore therapeutic efficacy of MSCs should be carefully weighed and possibly answered by appropriate dosing.

1.5 Therapeutic Gene Modification of Stem Cells and Usage of Inducible Promoters

In general, gene modification can be separated into an *in vivo* and an *ex vivo* approach. The *in vivo* way is the direct administration of gene modifying particles into the body. *Ex vivo* approaches include a cultivation step of the target cells outside the body. During this phase, the gene modification of the cells is performed before they will be given back to the patient. In contrast to germ cells (e.g. sperms, eggs), stem cells (e.g. HSC, MSC) are also a possible target of gene therapy from a regulatory point of view.

Both approaches, *in vivo* and *ex vivo* have proven their usability treating difficult diseases despite setbacks in the past. Trials like the CUPID study (Calcium Up-Regulation by Percutaneous Administration of Gene Therapy in Cardiac Disease) showed a safe application of adeno-associated virus carrying a therapeutic gene for heart failure in a phase 2b clinical trial [139, 140]. *Ex vivo* approaches did surely dominate the treatment of monogenic diseases. Severe diseases like the severe combined immunodeficiency (SCID) [141] or Wiskott-Aldrich syndrome [142] were successfully treated in the past and become to be first line therapy [143]. The increasing number of gene therapy clinical trials is impressive: before 2000, overall 484 studies were initiated. Since beginning of 2000, 1729 studies were recorded with more than 60% treating cancer. The second largest group build up the monogenic diseases (10%) followed by cardiovascular and infectious diseases (each 7%) [144].

Although adenoviral vectors or naked DNA are often used as delivery system, they are not integrating into the DNA and therefore do not show a stable expression. For stable expression, integrating vector systems e.g. gamma-retroviral or lentiviral vectors are prevalent. Lentiviral vectors integrate more safely into dividing and non-dividing cells but are more complex to manufacture than gamma-retroviral vectors and are therefore more expensive for clinical usage [144]. In addition, gamma-retroviral vectors have the tendency to integrate into transcriptional start sites in contrast to lentiviral vector, which obviously choose safer sites [145] [146]. This implies a potential higher risk for insertional mutagenesis for gamma-retroviral delivery systems. Especially, if high vector copy number in the target population is achieved, the possibility of a clonogenic outgrowth raises. A small vector copy numbers leads to high insertions rates in a very small fraction of a transduced population. [147, 148] [149]. But, risk mitigation by controlled transduction conditions and an appropriate vector system is realizable. Known titers of vector supernatant and a defined cell count allow constant transduction processing. Also, the development of better vectors

e.g. self-inactivating vectors (SIN) that have weaker enhancers (LTR regions) [150, 151] or targeted gene editing system e.g. nucleases like ZFN or TALENs [152] can increase the safety and reduce the risk of Insertional mutagenesis. The therapeutic approach itself can also lead to a higher safety profile e.g. suicide gene therapy systems. Cells with transgene integration after exposure to a viral vector will be killed due to the suicide gene system [153]. Here, sponsors of these kinds of studies potentially have more safety arguments that may answer regulatory demands better.

Promoters used for gene therapy are mainly divided into two groups: constitutive and inducible promoters. Constitutive promoters allow a constant expression independent of the cells status. They often derive from eukaryotic cells (e.g. elongation factor-1 (EFS), eukaryotic translation elongation factor 1 alpha 1 (EF1alpha) or phosphoglycerate kinase 1 (PGK)) or can be isolated from viruses (e.g. cytomegalovirus (CMV) or simian vacuolating virus 40 (SV40)). Viral derived promoters often show very high expression rate in the beginning but become quickly silenced in eukaryotic cells due to inherent mechanisms against infections. In contrast, EFS, EF1alpha or PGK do not show the same level of expression but are less silenced and therefor allow a more stable expression over time [154, 155].

Inducible promoters either increase expression if certain cytokines are present (e.g. RANTES (regulated upon activation, normal T-cell expressed and secreted) promoter) [156] or are activated if the cell differentiates e.g. Tie2-expressing monocytes [157]. In contrast to other systems like “Tet-On” promoter, which react very tightly on the presence of tetracycline [158, 159], the RANTES promoter reacts on different pro-inflammatory signals [156, 160].

The advantage of inducible promoter is the selective activation of the therapeutic gene in a defined environment or in a defined status of the cell. Especially pharmacological highly active agents that typically show large side effects can be introduced reasonably by cell-based delivery systems. A controlled, tissue-specific expression of the active protein or an enzyme, which regulates the translation of a prodrug, can reduce adverse effects [161].

1.6 The Suicide Gene “Herpes Simplex Virus Thymidine Kinase” and Apoptosis of Cells

GCV (Cymeven®) is authorized as standard treatment of cytomegalovirus infections and therefore widely used. GCV acts as a competitive inhibitor of deoxyguanosine triphosphate inhibiting viral DNA synthesis after intracellular activation and leading to cell death if incorporated into the genome DNA [162-165]. Besides that, the HSV-TK / GCV system has been established as a suicide gene therapy approach in clinical trials. After insertion of HSV-TK into the target cells by retro- or adenoviral vectors, GCV is administered intravenously days later. HSV-TK expressing cells translate GCV into its toxic counterpart and induce cell death by DNA damage [166-169]. Tested *in vitro* and *in vivo*, many therapeutic approaches aimed to treat difficult diseases e.g. glioblastoma [170, 171].

Although the safety and the proof of concept of direct viral transfection of the pathological tissue could be shown, the results were not as satisfactory as desired. This raised the idea of cell-based drug delivery systems e.g. MSCs [172, 173] to increase the efficacy at the desired site. Gap junctions between migrated MSCs and the target cell mediate the transfer of activated cytostatic agents (“bystander effect”) like phosphorylated GCV [174-176] and initiate the apoptotic cascade in MSCs and tumor cells [177-180]. The amount of intercellular connections is critical for the desired therapeutic effect [181]. The execution of apoptosis itself is led by mitochondrial perturbation [182] after previous rise of p53 and can be inhibited by accordant resistance mechanisms of the tumor cells [183, 184]. Additional apoptosis inducing signals strongly enhance the initiation of the cell death e.g. TNF or TRAIL [185].

During apoptosis, the cell passes through different membrane alterations and morphological changes. These changes can be accordantly identified and quantified by flow cytometry [186-189]. Especially, the differentiation between necrotic and apoptotic cells can be made by single cell measurement. Staining of Phosphatidylserine (PS) can be measured as direct indicator for the stage of apoptosis. PS is normally arranged asymmetrically on the bilayer membrane by ATP-dependent flippases and orientated to the inner site. During apoptosis, a mega-channel opening of the mitochondrion leads to an irreversible loss of the cells vital function: the production of ATP. This “point of no return” represents the commitment of apoptosis of the cell [190-192]. Also the activity of the ATP-dependent flippases stops, allowing PS to turn to the outer site of the bilayer. If exposed on the surface, it serves as “eat-me” signal of apoptotic cells for phagocytic cells [193-195] (PS has also other function e.g. regulating the blood coagulation on thrombocytes [196]).

These PS lipids on the membrane surface can be stained with Annexin-V conjugates in dependency of calcium and easily measured by flow cytometry [197, 198]. In later stages of apoptosis, the cells membrane also becomes permeable for DNA dyes like 7-AAD. This combination allows the differentiation between earlier and later stages of apoptosis in a cell population and differentiate necrotic from apoptotic cells [199, 200].

In spite of the surface changes, apoptosis induces a cytoplasmic volume condensation. This shrinkage is due to volume-regulatory chloride and potassium channels, which have altered activities during apoptosis resulting in more granular and smaller cells. At the end, the apoptotic process leads to the death and a total integrity loss sets all remaining, intracellular structure free [201-203].

1.7 The Pig and its Role as Large Animal Model (LAM) for Preclinical Studies

Regulatory Authorities demand toxicological studies in non-rodent mammals before entering clinical trials [204]. Ethical aspects regarding preclinical studies with non-rodent mammals e.g. the pig are therefore first to address before these trials may be performed [205]. Any concerns should be discussed seriously. A thorough literature research should be done to evaluate the most compliant animal model with the best chances to generate valid data. Then, a risk-benefit analysis for the planned studies should be the basis for any preclinical testing. In sum, the design of preclinical studies should follow the 3R-principle by Russell and Burch described in 1959: “replacement, reduction and refinement” as it was laid down in European law [206].

Compared with other large animal models like horses or non-human primates, pigs have a little reproduction time and grow very fast in their first year after birth. Already after six months, they are sexually matured and a new generation of pigs is available after four months of pregnancy. In the field of gene and cell therapy, a lot of working groups prefer the pig, particularly the mini-pig, since it shows physiological and anatomical comparability with humans [207-211]. Regulatory authorities demand toxicological data for medicinal products before clinical trials may be initiated. Regarding large animal models, the pig with his high comparability makes it to a well-reputed animal for toxicological testing [212-214].

Also surgical interventions were often tried for the first time in the swine to develop new therapy options. Still, medical training is frequently performed on pigs. The close physiological relation is also found in the field of medicinal products: porcine insulin was used regularly for diabetes patients (e.g. *Insulin Hypurin Porcine®*) and cardiac valves from the pig are still an option as biological alternative to synthetic imitations [215].

In spite of surgical indications, the research in the swine and its biology made significant advances over the last decades: the whole genome of pigs is known [144], induced pluripotent stem cells are available [216-218], transgenic animals have been developed and somatic cell cloning to replicate identical animals is possible [219-221]. As all animal models, every species has its own model history for its typical field of diseases. Pigs are often related to cardiovascular or metabolic diseases and many trials have been performed to treat e.g. ischaemic diseases of the heart on a cell-based approach [222]. Furthermore, the spectrum of genetically modified pig models for human diseases becomes constantly wider [223, 224] e.g.: models for skin inflammatory diseases [225], diabetes [226], severe

combined immunodeficiency (SCID) [227], cystic fibrosis [228] and further indications like *alzheimer's* disease, *retinitis pigmentosa* or spinal muscular atrophy are available as listed by Prather *et al.* [229]. Altogether, the pig is an attractive model for preclinical studies [211, 213, 214] although the cost per animal is obviously significant higher than e.g. per mouse. In contrast to rodents, the reproduction time of several months makes strategic planning more difficult since the flexibility to design preclinical studies and the time needed to generate new data is longer.

At the end, it should be mentioned that the public sees less ethical concerns on preclinical testing with pigs than with e.g. non-human primates or dogs.

1.8 Modelling human MSCs: Porcine MSCs (in contrast to rodent MSCs)

The immunological barrier of a healthy animal is a major hurdle for preclinical testing of ATMPs. If the human cell therapy product is administered into animals, immunological reactions may vary preclinical results in an undesired manner. Homologous MSCs offers an alternative, avoiding any immunological effects. Still, poor cell characterization of the animal species may lead to false results since they could show other pharmacokinetics and -dynamics than expected as for their human counterpart. It is hard to define accurate models and homologous products [230].

The good characterization of the animals' cells is a major key to perform relevant preclinical studies and to overweigh potential arguments that these cells are not the "original" cells. Moreover, the characterization and applicability of animal MSCs must be shown sufficiently to convince the regulatory authorities approving the initiation of clinical trials [212, 230]. These circumstances are often complicated by poor literature for homologous cell products since publication mostly concentrate on preclinical experiments and not on the cells characterization. Nevertheless, several working groups did characterization work for porcine MSCs as follows.

Like human MSCs, porcine MSC were already isolated from different tissues e.g. bone-marrow [231-234], umbilical cord blood [235, 236], endometrium [237], skin [238-240] or adipose tissue [241, 242]. Comparison analyses between these origins regarding proliferation, differentiation, functional properties or molecule markers showed significant differences and potential influence on preclinical study outcomes might be relevant [243-245] – as it is for human MSCs [46, 246-248]. In pigs, the adipose tissue offers easy isolation practices since they naturally gain weight easily [249]. The identification of porcine MSCs is equivalent to human MSCs following the ISCT criteria for different markers e.g. CD70+, CD90+, CD105+, CD45- [5]. The scarce availability of commercial, porcine specific antibodies unfortunately limits the characterization of surface markers to smaller panels. Beside the plastic adherence, the trilineage differentiation of porcine MSCs is essential for defining MSCs. This could be also shown well for porcine MSCs [235, 240, 243, 250, 251]. But, the differentiation potential is highly affected by the used protocol and tissue origin, which makes comparison hard between different working groups regarding differentiation efficacy [251], also summarized by *Barthi et al.* [252].

In preclinical studies, the pig is well known for its suitability in cardiovascular disease modelling. Mostly pigs and their cells generated great value in cell-based therapy approaches for ischaemic infarcts, extensively reviewed by van der Spoel *et al.* [222]. Although dog and sheep participated in this development, studies with pigs constitute the majority. Porcine MSCs proofed their preclinical value also in other indications with therapeutic need such as liver failure [249, 253], skin regeneration [254, 255] or osteochondral defects [255, 256]. Also, pharmacokinetics studies in the pig showed great significance [99].

Even though there are good evidences for high comparability of other mammals, inconsistencies between the results of clinical trials and preclinical studies with MSCs occurred [257]. Comparison studies on the immunomodulatory properties of MSCs from different species showed varieties, e.g.: IDO synthesis in human and monkey MSCs increases if they are stimulated with pro-inflammatory cytokines. Mice MSCs mainly react with an increased expression of inducible nitric oxide synthase (iNOS) to mediate an anti-inflammatory effect [258]. IDO and prostaglandin E2 play a major role for the immunosuppressive properties of human MSCs [259]. Connected to that, it could be shown that antibacterial properties of human MSCs, which are mediated by an increase of IDO, are not present in murine MSCs [260]. Furthermore, there are evidences that murine MSCs have other intracellular pathways to react on cytokine stimulation [63].

Rodent MSCs also differ in the expression of surface proteins like CD90 and CD73 in dependency of passage and tissue [261]. This observation was also made for human MSCs from different origin. Although all markers suggested by the ISCT were present, the expression rate differed significantly [262]. Interestingly, the presence or absence of CD105 directly correlates with functional properties of this sub-population in murine MSCs [263].

Beside functional properties and presence/absence of surface markers, murine MSCs show spontaneous transformation into malignant cells. This expansion phase can endure several weeks. Transformations were already observed during cultivation passage three or four [264-267]. Subsequent *in vivo* experiments showed the malignant potential of these murine cells [268]. Chromosomal stability of MSC culture is essential to meet the specifications and cell dosages as defined in clinical protocols of more than 0.5×10^6 cells/kg bodyweight [69, 81]. It is probable that this critically affects preclinical studies and their value for clinical trials.

Spontaneous transformation of human MSCs is still in an open discussion although there are several cues indicating no spontaneous transformation of human MSCs. There are data

negating malignancy [269] and showing a cultivation until senescence of human MSCs [270]. Working groups describing an occurrence of high proliferating, spheroid-forming cells [271, 272] had to contradict themselves since this cell line was a contaminant during long time culture in the laboratory [273, 274]. Until now, no reports are available describing results of long-time cultivated porcine MSCs regarding possible transformation.

It is quite obvious that porcine MSCs show high potential to be a feasible cell model system in contrast to murine MSCs. Availability of transgenic and disease-modelling pigs as well as the high comparability of the pigs' physiology to humans underlines this usability for modelling cell-based therapeutics.

2 Aim of This Work

Mesenchymal Stem Cells are the basis for a new class of cell therapy products and offer novel opportunities to treat difficult diseases. These MSC-based drugs are regulatory called “Advanced Therapy Medicinal Products” (ATMPs) and have to be tested in preclinical studies before they may enter clinical trials. These studies have to give proof of a safe and efficient drug product *in vitro* and *in vivo*. Especially, safety should also be shown in large animal models [204].

Testing the clinical human-based product in animals may lead to undesired immunological reactions, which are not representing the clinical setting correctly. The option of immune-compromised or -deficient rodents may mitigate these reactions, but significantly changes the model system and interactions between the immune system and the cell-based therapeutic. Testing the animal-based cell product of a chosen species in the species itself requires sufficiently characterized cells because they possibly do not correctly represent the “human” product [275]. In addition, the costs and the dependency of human bone marrow donors complicate the preclinical testing program.

The miniature pig is known to be highly comparable to humans in regard to anatomy and physiology – especially in contrast to other small or large mammalians. It is therefore a very attractive model for preclinical drug testing. Although the usefulness is highly indicated, no systematic characterization to proof the suitability of this cell model platform for an MSC-based suicide gene therapeutic was done before.

The aim of this work was to show that porcine MSCs represent a good model system for the characterization and manufacturing of a cell therapy product. Here, the HSV-TK system is described for the first time in porcine MSCs in parallel with the product for a clinical trial [81]. This question of comparability was evaluated in three *in vitro* and one *in vivo* part discussing the model product only:

1. Characterization of adherent cells as MSCs
2. Controlled insertion of therapeutic suicide gene and proof of functionality
3. Characterization of the therapeutic effect
4. Experimental *in vivo* investigation on pharmacokinetics

3 Summary

Model cells in syngeneic animals are a potential alternative in the field of preclinical development of ATMPs (Advanced Therapy Medicinal Products) because they do not trigger any immune response. But these model cells have to mimic the human derived counterpart sufficiently. To assure this, a previous characterization of the model cells is required to allow a translation of these results into clinical trials.

In the present work, porcine MSCs (Mesenchymal Stromal Cells) expressing HSV-TK (Herpes Simplex Virus Thymidine Kinase) are described and compared to human MSCs, which are engineered for a human cell therapy product [81]. It was the aim of this work to show that the porcine HSV-TK MSCs cells are comparable and therefore useful for preclinical development of an equivalent human cell-based therapeutic. This goal was systematically pursued comparing the human MSCs with the pig-derived model MSCs during production and testing of the generated batches. The suicide gene therapy concept was also investigated and subsequently characterized *in vitro* comparing both species. Consecutive *in vivo* studies in the mini-pig were performed in an experimental approach with porcine MSCs.

It could be shown that porcine MSCs share nearly all properties with human MSCs regarding identity as they match the specifications of the *International Society for Cellular Therapy*. The plastic adherence and the fibroblast-like morphology could be clearly shown. The general presence of CD90 and CD105 and the absence of CD45 were similar with human MSCs. A sub-population of CD105 negative porcine MSCs was observed that was not described for human MSC but for murine MSCs before. HLA-DR (Human Leukocyte Antigen – antigen D Related) expression could not be shown whether the cells were induced with cytokines or not. The differentiation into adipogenic and osteogenic cells was successful using commercial available differentiation media that were compiled for human MSCs. A similar population doubling time could be shown, too, although the human derived batches highly varied. The examined MSCs of human and porcine origin showed many similarities although slight differences in the surface marker were observed, as it is also known for other animal-derived MSCs.

The successful transduction with the same retroviral vector enabled the expression of the HSV-TK gene that was also used for human MSCs. The resulting vector-copy numbers were comparable after a successful selection. The inducible RANTES (Regulated upon Activation, Normal T cell Expressed and Secreted) promoter isolated from human cells was

inducible in both species and showed comparable up-regulations. It could be clearly shown that HSV-TK expressing cells are multiple fold higher sensitive to GCV (Ganciclovir) than naïve cells. Here, the porcine MSCs were even more sensitive. Resulting apoptosis due to activated GCV was comparable and could be well described by appropriate Annexin-V and 7-AAD (7-Aminoactinomycin) staining. Cell count reduction occurred also in co-cultured cell lines that did not express HSV-TK. It could be proven throughout all species arrangements of HSV-TK expressing MSCs that the targeted cell lines undergo apoptosis. As control for these apoptosis experiments, naïve MSCs were used. Interestingly, in one setting also naïve human MSCs showed anti-proliferative effects on the porcine-derived cell line.

The following experimental *in vivo* studies with mini-pigs confirmed the expectation that intravenously (i.v.) infused MSCs show extra-ordinary pharmacokinetics. Before the cells were systematically available, a delay could be observed. MSCs interact with the epithelium of the lungs vascular system before they enter the peripheral arterial bloodstream. This first-pass effect of i.v. administered MSCs is well described in the literature. This phenomenon was not reproducible in a second animal. Here, a severe pneumonia was identified. The well-known migration of MSCs to pro-inflammatory tissues could have led to an enduring engraftment in the lung. Remaining MSCs in the bloodstream probably undercut the detection limit of the assay.

Altogether, this work shows the usability of porcine MSCs as a model system for a clinical cell therapy product *in vitro* and also *in vivo*. It could be proven that porcine MSCs are modeling human MSCs beside minor differences.

4 Abbreviations & Units

4.1 Abbreviations

7-AAD	7-Aminoactinomycin D
ADME	absorption, distribution, metabolism, elimination
ANOVA	Analysis of Variance
ATMP	advanced therapy medicinal product
BALT	Bronchus-associated lymphoid tissue
Bio-1	Expansion Medium for CD34-Negative Stem Cells (Patent, US201101834141 A1)
CCR2	C-C chemokine receptor type 2
CD	Cluster of Differentiation
CFU	colony forming units
CT	cycle threshold
DMEM	Dulbecco's Modified Eagle Medium
EC50	half maximal effective concentration
ECD	phycoerythrin-Texas Red conjugate
EDTA	ethylenediaminetetraacetic acid
EFS	elongation factor short
EMA	European Medicines Agency
FBS	fetal bovine serum
FFPE	formalin-fixed paraffin-embedded
FGF-2	fibroblast growth factor 2
FITC	fluorescein isothiocyanate
FS	forward scatter
(e)GFP	(enhanced) green fluorescent protein
HEPES	4-(2-hydroxyethyl)-1-piperazineethanesulfonic acid
HT1080	human, fibrosarcoma cell line
HSV-TK	herpes simplex virus thymidine kinase
ICH	International Council for Harmonisation
iNOS	inducible nitric oxide synthase
ISCT	International Society of Cellular Therapy
K67	Neo3-14/K67/1.1+cMyc; immortalized porcine cell line
LAM	large animal model
LTR	long terminal repeats

LSM	lymphocyte separation media
MFI	mean fluorescence intensity
MGH	Massachusetts General Hospital
MHC	major histocompatibility complex
MNC	mononuclear cells
MOI	Multiplicity of Infection
MSC	multipotent mesenchymal stromal cell
MTT	3-(4,5-dimethylthiazol-2-yl)-2,5-diphenyltetrazolium bromide
NADH	nicotinamide adenine dinucleotide
NADPH	nicotinamide adenine dinucleotide phosphate
NEAA	Non-Essential Amino Acids
PAC	puromycin N-acetyl-transferase
PBS	phosphate-buffered saline
PC7	phycoerythrin cyanine dye 7
PCR	polymerase chain reaction
hPGK	human phosphoglycerate kinase
PE	phycoerythrin
PI	propidiumiodide
PLL	poly-L-lysine
PS	phosphatidylserine
RANTES	regulated upon activation, normal T-cell expressed and secreted
real-time PCR	real-time polymerase chain reaction
SCG	Single Copy Gene
SCID	severe combined immunodeficiency
SS	side scatter
STDV	standard deviation
ST CTRL	staining control
TD	transduced / transduction
TC treated	Tissue Culture treated
TRAIL	TNF-related apoptosis-inducing ligand
TRIS	Tris(hydroxymethyl)-aminomethan
qPCR	<i>see real-time PCR</i>
VCAM-1	vascular cell adhesion molecule 1
VCN	vector copy number (mean transgenes per cell)
w/wo	with or without
WPRE	Woodchuck Hepatitis Virus Posttranscriptional Regulatory Element

4.2 Units

°C	degrees Celsius
%	percentage
cm	centimeter
cm ²	square centimeter
CT value	quantity of PCR doublings before detection of significant fluorescence
d	days
h	hours
L	liter
mL	milliliter
min	minutes
M	molar
µg	microgram
µL	microliter
µm	micrometer
µM	micro molar
nm	nano meter
g	standard acceleration due to gravity
sec	seconds

5 Material

5.1 Consumables / Liquids (Media, Solutions, Kits, Chemicals)

Solutions, Media and Chemicals	Manufacturer
2-Propanol 99.9%	Carl Roth
10% Formalin, neutral buffered	Sigma Aldrich
10cm dishes, TC-treated	Corning
96-well flat clear bottom black polystyrene plates	Greiner Bio One
Alizarin Red S	Sigma Aldrich
BacT/ALERT SA, Standard Aerobic	bioMérieux
BacT/ALERT SN, Standard Anaerobic	bioMérieux
Blood & Tissue Kit	Quiagen
CellSTACK (1, 2 or 5 layer), TC-treated	Corning
CellTiter 96® Non-Radioactive Cell Proliferation Assay	Promega
Centrifugation Tubes / Falcons (1.5°mL, 2°mL, 15°mL, 50°mL)	Eppendorf / Corning
Culture Flasks (25°cm ² , 75°cm ² , 175°cm ² , 225°cm ²), TC-treated	Corning
Culture well plates (6-, 12-, 24-, 48-, 96-wells), TC-treated	Corning
Cytofix/Cytoperm Fixation and Permeabilization Solution	BD Biosciences
Deionized Water	Laboratory Water System
Discovery DAB Map Detection Kit	Roche Diagnostics
DMEM	Biochrom
FACS buffer (1% FBS, 99% PBS)	see FBS and PBS
FBS	Biochrom
HEPES Buffer Solution [1M]	Gibco
Mayer's Hematoxylin	Sigma Aldrich
Non-essential amino acids	Gibco
Red Oil	Sigma Aldrich
PBS Dulbecco	Biochrom
Perm/Wash Buffer	BD Biosciences
Pipet Tips (10µL, 20µL, 100µL, 200µL, 1000µL)	Greiner Bio One
Pipets (Serological, 2°mL, 5°mL, 25°mL, 50°mL)	Corning
PLL 0,01%	Sigma Aldrich
Puromycin	Sigma-Aldrich
StemMACS AdipoDiff Media, human	Miltenyi Biotec
StemMACS OsteoDiff Media, human	Miltenyi Biotec
Trypan Blue	Sigma Aldrich

5.2 Equipment and Software

Equipment / Software	Manufacturer
Balance	EW 600 2M
BX51 microscope	Leica
Centrifuge	Heraeus Fresco 21 Thermo Fisher Scientific
Centrifuge	Eppendorf Centrifuge 5810R
CO ₂ -Incubator (#1)	Sanyo MCO-20AIC
CO ₂ -Incubator (#2)	ThermoScientific Heaerus BBD6220
Counting Chamber	C-Chip Disposable Hemocytometer NanoEnTek
DML6000B microscope	Leica
DNA / RNA safety working bench	DNA/RNA UV-Cleaner UVC/T-M-AR Biosan
Flow Cytometry Cytomics FC 500	Beckman-Coulter
Kaluza	Beckman-Coulter
Infinite 200 PRO microplate reader	Tecan
Laminar Flow Working Bench	HeraSafe HS15 Heraeus
Las X	Leica
Lightcycler 480 II	Roche
Mr. Frost Freezing Container	Thermo Fischer Scientific
NanoPhotometer	Implen
Pipets	Eppendorf
Pipetboy	Integra
Waterbath	Memmert WNB 14

5.3 Cell Lines

Cell Line	Description	Supplier
HT1080	Human Fibrosarcoma cells	ATCC
K67	Neo3-14/K67/1.1+cMyc; immortalized porcine cell line; generated originally from a pMSC (Pietrain Landrace Pig) [276]	Technical University of Munich (Working Group, Prof. Dr. Schnieke, Anja Saalfrank, Chair of Livestock Biotechnology)

5.4 Antibodies

Antibodies are listed within the accordant Methods.

6 Methods

6.1 Isolation of Adherent, Mononuclear Cells from Bone Marrow

6.1.1 Donor characterization

The following table shows all specifications and characteristics of the human and porcine donors from whom MSCs were isolated. A batch nomenclature was introduced to differentiate gene-modified batches from naïve batches.

Table 1: This overview represents the nomenclature and properties of human and porcine MSCs in the generation of the cell products. The human donors were chosen based on a thorough medical anamnesis following the accordant laws (actual, german tissue and transplantation law). The pig's cells isolation was performed by members of the *Lehrstuhl für Biotechnologie der Nutztiere* from the *Technische Universität München*. The mini-pig derives from an isogenetic inbreed. This animal is isogenetic to the pigs that were used during the biodistribution study (see 7.7).

Species	(Mini-) Pig <i>Sus scrofa domesticus</i>				Human <i>Homo sapiens</i>					
Tissue	Bone marrow Both <i>Femur</i> and <i>tibia</i>				Bone marrow <i>Iliac crest</i>					
Volume	Unspecified (whole marrow taken)				Each 75-100 mL					
Method Of Harvesting	Narcotization and necropsy, then Flush and Scrape out				Aspiration under short-time anaesthesia					
Donor	1				1	2	3			
Gender	Male				Male	Female	Female			
Age	3 months				31 years	32 years	20 years			
Health Status	no clinical observations by veterinarian				according to german law: healthy; based on blood, urine, serum measurements and medical anamnesis, also free of relevant infectious markers (e.g. CMV, HIV, hepatitis virus, etc.)					
Batch Nomenclature	Porcine 1	Porcine 2	Porcine 3	Porcine 4	Human 1	Human 2	Human 3	Human 4	Human 4	Human 5
Transduction Method	n.a.	A	B	C	n.a.	C	n.a.	C	n.a.	C
Selection	No	Yes			No	Yes	No	Yes	No	Yes
Cryo-preservation	Yes									

6.1.2 Isolation of human MSCs

Aspirates the bone marrow were collected from volunteers in accordance to the regulatory demands. A physician performed the aspiration under standard clinical and aseptic conditions. Volunteers received a short-time anaesthesia and the needle was brought into the *iliac crest* aspirating a bone-marrow volume of 75-100 mL by several punctures. The marrow was transported in sterile containers to the laboratory.

The cultivation started in less than 24 h after extraction. The bone marrows of the human donors were seeded without any previous purification or manipulation steps. Therefore, a cell stack system was used and the bone marrow was suspended in $>150 \mu\text{L}/\text{cm}^2$ Bio-1 medium, cultured under 5% CO_2 , 37°C temperature and more than 90% humidity. New adhesion after trypsinization takes minutes to hours. Because of that, the bone marrow and medium containing supernatant was completely changed with a delay of at least 48 h to allow enough time for adherence, but not later than 96^h to assure a sufficient nutrition. These colonies could be observed and were split by trypsinization and EDTA within 14 days, counted (see 6.2.4) with a *Neubauer Zählkammer*, and seeded again.

6.1.3 Isolation of porcine MSCs

Bone marrow was isolated from the femur and tibia of both hind legs of a three months old male MGH miniature pig. Prior to isolation, the equipment was disinfected with 80% ethanol. The epiphyses of the bones were opened with a saw and bone marrow was flushed with 25 mL of pre-warmed Hank`s salt solution supplemented with 1000 U/mL heparin. Several 25 mL samples of aspirate were layered over 25 mL lymphocyte separation medium (LSM-1077) and centrifuged at 1000 \times g for 20 min with slow acceleration and deceleration. The mononuclear cell fraction was collected from the interphase, transferred to another centrifuge tube and washed with 35 mL Hank`s salt solution. After centrifugation at 600 \times g for 10 min, the cell pellet was suspended in porcine MSC culture medium (Advanced DMEM, 2mM GlutaMAX®, 1x NEAA, 10% FCS, 5 ng/mL FGF-2, 0.1 mM 2-mercaptoethanol) supplemented with 100 $\mu\text{g}/\text{mL}$ Penicillin/Streptomycin and 100 $\mu\text{g}/\text{mL}$ Amphotericin B, plated into five 150 cm^2 flasks and incubated at 37°C with 5% CO_2 in humidified atmosphere. After 24 h, cells were washed twice with PBS and medium replaced to remove all non-adherent cells (e.g. hematopoietic cells).

For the first three days medium was supplemented with antibiotics and antimycotics and changed daily. After three days half of the cells were cultured without antibiotics and

antimycotics, the rest of the cells after five days. Seven days after isolation, cells were split (1:3 or 1:5 depending on confluence; passage 1) using Accutase® and cultured in MSC medium without antibiotics and antimycotics for a further three days and then cryopreserved.

The isolation of the porcine MSCs was performed by personnel of the *Lehrstuhl für Biotechnologie der Nutztiere* of the *Technische Universität München*.

6.2 *In Vitro* Cultivation

6.2.1 General

All working steps with open flasks and tubes were performed under sterile conditions. A laminar flow working bench was used to handle all cell culture experiments. All cells were cultured under 5% CO₂, humidity of more than 90% and 37±1 °C conditions. Necessary equipment was disinfected properly with ethanol. Plastic or other consumable materials were sterilized before usage (see 5.1).

6.2.2 Thawing of cells

Cryopreservation vials were taken out of the vapor phase of liquid nitrogen and brought into a water bath (37°C) for at least two min until no ice crystals could be seen anymore. After proper disinfection, the vials were transferred into the laminar flow of a working bench. The tube was opened, re-suspended and diluted with the cultivation media for at least 10:1 in a 50 mL tube before given into a cell culture flask. A sufficient dilution of the DMSO was necessary to mitigate possible cell proliferation inhibitions by DMSO (see 6.4.2). The next working day, the cells attached completely and the whole media was change to delete the DMSO.

6.2.3 Standard *in vitro* cultivation and detachment of cells

Half of the medium was changed every two to four days of a cell culture flask depending on the confluency. If the cells were nearly 70-90% confluent, they were detached from the plastic surface by using an EDTA and trypsin containing solution. After a washing step with PBS, the suspension was given into the flask. The cell culture flask was then put into the incubator for three to ten min, if the cells have not detached meanwhile. Then, at least the same amount of medium was added to stop the trypsination process. The cell suspension was aspirated and given into an appropriate tube (1.0 mL – 50 mL tube). The culture flask was additionally washed with PBS to assure a quantitative transfer of all cells in to the tube. After a centrifugation of 5 min with 300 g, the supernatant was deleted and the cell pellet was suspended in PBS. After cell count determination (see 6.2.4), the cells were seeded into a medium containing cell culture flask with a determined ratio of cells/cm² depending on the type of cell between 500 to 5000 cells/cm².

Table 2: Description of the cultivation media. Bio-1 was used for human MSCs. This media does not contain FBS but platelet lysate that is based on a patent, referenced in 4.1. All other media, also for porcine MSCs, had FBS as an ingredient. The recipe for the porcine MSCs cultivation media is based on personal communication with the working group of *Prof. Angelika Schnieke* of the *Technische Universität München* leading the “Chair of Livestock Biotechnology”.

Cells	Cultivation Media	
Porcine MSCs	88% Advanced DMEM 10% FBS	
Porcine Cell Lines	1% Non-Essential Amino Acids 1% Glutamax	
Human MSCs	100% Bio-1 (see Abbreviations: 3)	Bio-M: 87% DMEM 10% FBS 2.5% HEPES
Human Cell Lines	89% DMEM 10% FBS 1% Glutamax	

6.2.4 Cell count determination

The cells are suspended in an appropriate amount of PBS after detachment and washing (see 6.2.3.). After distribution of the cells by several slight inversions of the tube, 50 μ L of the suspension was taken and given into 50 μ L trypan blue. 10 μ L of this suspension was given into a *Neubauer Zählkammer*, counted and the cell concentration per mL calculated. Based on this calculation, new cell seeding were performed. Where needed, the cell count determination was performed more than once to facilitate a higher assurance and less variance of the result.

6.2.5 Isolation of single cell line clone (after transduction with a GFP gene)

If an isolation of a population by a selection agent (e.g. puromycin) could not be performed, a single cell seeding was pipetted to generate a new population out of one cell. The cells were detached (see 6.2.3) and washed. The cell suspension was counted with a *Neubauer Zählkammer* (see 6.2.4) and seeded into at least one 96-well plate with a cell density of 0.1 cells/well (theoretically calculated value). It was statistically assumed that in every tenth well one cell clone would exist. This single cell proliferated to a colony, which was detached and seeded (see 6.2.3 and 6.2.4) into a new flask as soon as the colony was detectable by microscopy. If a second colony or no colony was detected in a well, the cells of this well were discarded. An appropriate population was expanded until a sufficient amount of cells was available to measure for e.g. GFP by flow cytometry. Based on this measurement, the

desired cell clone was chosen, expanded and cryopreserved (see 6.2.3) for further experiments.

6.2.6 Calculation of the population doubling time

The doubling time of a cell population was calculated based on following formula:

$$\text{Population Doubling Time [h]} = \frac{\text{days from P0 to cryo} * 24}{\left(\frac{\text{Log}_{10} \left(\frac{\text{cell count}_{\text{cryo}}}{\text{cell count}_{\text{P0}}} \right)}{\text{Log}_{10} (2)} \right)}$$

6.3 Insertion of Genes

Cells were transduced with SIN-gamma retroviral vectors to tag them (e.g. GFP) or express functional genes (e.g. HSV-TK). The HSV-TK vector backbone (see Figure 1) and producer cell line based on the work of an external working group [277]. Both, the self-produced and externally manufactured vector supernatant were stored at -80 °C. To thaw the viral solution, the tubes were thawed at 37 °C in a water bath until no more small ice crystals were visible. Then the tubes were put under the laminar flow of a working bench. As soon as no more ice crystals could be observed, the solutions were mixed gently with a micropipette.

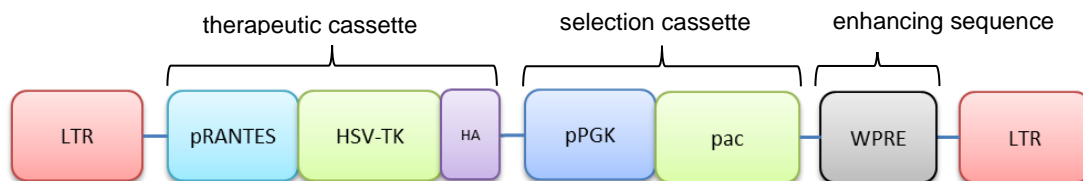


Figure 1: Here, a schematic description of the therapeutic cassette pEMTAR.bi-RANTES.tk including the selection gene is shown. The LTR sequences were part of the viral system facilitating an insertion of the gene, which was embedded between both LTR sequences. The HSV-TK gene was under the control of an inducible promoter, called RANTES. This RANTES promoter generally is inducible with pro-inflammatory cytokines e.g. TNF α and IFN γ . The HA-tag was attached to the kinase, which allowed a detection with accordant antibodies for measurement through flow cytometry. The enzyme PAC deactivated the cytotoxin puromycin by acetylation. This enzyme was expressed continuously because it was under the control of a constitutive promoter (pPGK) allowing a selection by puromycin during cultivation. The WPRE sequence enhanced the stability of the transcribed transgene increasing protein expression [278].

Since the viral vector load and the cell count were known, a ratio of 3 (three viral vector particles / one cell: MOI = 3) was chosen. For the production of all batches a ratio of three viral vectors to one cell was chosen to maintain comparable transduction conditions. The cell lines were transduced with a higher viral load per cell to facilitate an easy recognition while measured by flow cytometry. Following transduction methods were performed:

6.3.1 Transduction by direct seeding (Method A)

This virus solution was mixed with 0.01% PLL with a 100:1 ratio (99 parts virus solution and 1 part PLL solution). The cells were added to the virus / PLL solution and mixed gently to

generate a homogenous suspension. If the suspension volume for seeding was less than $125 \mu\text{L}/\text{cm}^2$, PBS was added to ensure a sufficient distribution of the volume over the whole culture flasks surface. The seeding density was determined to result in a confluence of 20-30%.

6.3.2 Transduction on PLL plates (Method B)

A solution of PLL 0.01% is given into 6-well plates and centrifuged for 30 min at 4°C and $2000\times g$. Afterwards, the supernatant was deleted and the plates were washed with PBS. The PLL adhered at the plastic and these molecules charged the plastic surface positive. The negative charged virus particles attached at the surface and interacted with the cell surface. The seeding density was determined to result in a confluence of 20-30%.

6.3.3 Transduction in suspension (Method C)

This virus solution was mixed with 0.01% PLL before a defined amount of cells was added. Over three hours, this transduction mix was inverted every 15 min to assure a good distribution of the cell-vector mix. Afterwards, the mix was diluted with the appropriate serum containing culture medium and seeded into the culture flasks. The seeding density was determined to result in a confluence of 20-30%.

6.4 Selection, Expansion and Cryopreservation of Cells

6.4.1 Selection

Cells transduced with the pEMTAR.bi-RANTES.tk vector were selected using puromycin not earlier than 48 h after transduction. Half of the medium was deleted and medium with a concentration of 6 µg/mL was added, resulting in a final concentration of 3 µg/mL. Two days later, half of the medium was deleted and fresh medium with 3 µg/mL puromycin was added again to continue the selection process. Not earlier than five days after the start of the selection, the whole medium was changed to delete dead cells, cell debris and remaining puromycin. Afterwards, the cells were cultured in a standard medium to allow proliferation of the selected population as described before (see 6.2).

6.4.2 Expansion and cryopreservation

The expansion procedure after selection was carried out in accordance to 6.2 until the desired cell count was reached. The following detachment was performed as described before (see 6.2.3). After washing, the cell count was determined and the cells were suspended in a concentration of between 5 to 10×10⁶ cells/mL in the accordant cryopreservation medium (see Table 3).

Table 3: Description of the cryopreservation media used for different types of cells [279]. 10% DMSO was used for all cell types to reduce the amount of crystallization during the freezing process. Hydroxyethyl starch served as the cryoprotective supplemental protecting the cell surface [280].

Cells	Cryopreservation Media
Porcine MSCs	45% hydroxyethyl starch 45% porcine serum 10% dimethyl sulfoxide
Human MSCs	45% hydroxyethyl starch 45% human albumin 10% dimethyl sulfoxide
Cell Lines	90% fetal bovine serum 10% dimethyl sulfoxide

Aliquots of 1.5 mL were pipetted and transferred into the freezing containers (“Mr. Frosty”). Then, the freezing containers were put into a freezer with a temperature of minus 80°C. These containers controlled the temperature reduction in a time dependent manner lowering the temperature by one degree Celsius per minute. As a consequence, the temperature reduction from room temperature (about +20 °C) to -80 °C lasted 100 min. Afterwards, the vials were transferred into the vapor phase of liquid nitrogen tanks at -196°C.

6.5 Differentiation into Osteocytes and Adipocytes and Staining

Commercial differentiation media compiled for human MSCs (see 5.1) were used for porcine and human MSCs following the manufacturer instructions. In short, the cells were seeded into 12-well plates and cultured under standard conditions (see 6.2) until 100% confluence. Then, the medium was deleted and the differentiation medium was added. The differentiation itself took 14 to 21 days. Half of the medium was changed every 2-3 days. At the end, the supernatant was deleted; the culture flasks were washed with PBS twice. Then, the staining was as described in 6.5.1 and 6.5.2. Accordant controls cultivated using a standard medium were stained, too.

6.5.1 Staining of osteocytes and analysis

The staining of osteocytes was done utilizing a fixation with a neutral buffered 10% formalin solution at room temperature. After an incubation time of 30-45 min, the formalin supernatant was deleted and the wells were washed twice with deionized water. A freshly prepared alizarin red solution (2.0 g/mL) was given into the wells for 30-45 min. Afterwards, the cells were washed again with deionized water for two times. PBS was added to assure that the preparation does not run dry. A microscopic analysis was performed and representative photos were taken of sections of $\sim 750 \mu\text{m} \times 1000 \mu\text{m}$.

6.5.2 Staining of adipocytes and analysis

To stain adipocytes, the cells were fixed with a neutral buffered 10% formalin solution for 30-45 min at room temperature. Then, the formalin was deleted and the cells were washed with non-sterile water two times. An additional fixation was done with 60% isopropanol for 3 -5 min at room temperature. A freshly prepared Red Oil solution was added and incubated for 5 - 10 min at room temperature. After washing with PBS twice, *Mayer's* Hematoxylin Solution was given into the wells for 1 - 5 min at room temperature and the wells were washed with non-sterile water twice. PBS was added to assure that the preparation does not run dry. A microscopic analysis was performed and representative photos were taken. All adipogenic cells were counted in three representative sections of $\sim 750 \mu\text{m} \times 1000 \mu\text{m}$.

6.6 Measurements by Flow Cytometry

6.6.1 Identification of surface markers

MSCs have a determined set of proteins, which are presented on their surface. These can be identified by accurate staining and flow cytometry measurements. For this, the cells were detached as described before (see 6.2), washed twice with PBS and counted (see 6.2.4). Multiple 100 μ L PBS aliquots with a cell concentration of 1×10^6 - 2×10^6 cells/mL were generated as needed. The accordant antibody was added to the cell suspension and mixed. After an incubation time of 20 min at room temperature, the cells were washed with PBS two times again. Then, the cells were measured. If needed, accurate compensation was performed. At least 10,000 events were measured per analysis. Isotype controls for each antibody and fluorophore were used to set appropriate gates for the measurement.

The antibodies listed in Table 4 were used for porcine MSCs. The antibodies listed in Table 5 were used for human MSCs.

Table 4: The staining of porcine MSCs for flow cytometry measurement was performed with the following fluorophore-conjugated antibodies and 7-AAD. All stainings were performed as single stains to reduce compensational work. All antibodies were generated from murine cell lines as declared by the manufacturer.

Mix	Antigen	Dye	Isotype	Volume [μ L]	Company
1 (Isotype Control)	N/A	7-AAD	N/A	15	Beckman-Coulter
		APC	IgG1	20	BD Bioscience
		FITC	IgG1	20	Beckman-Coulter
		PE	IgG1	20	Beckman-Coulter
		PE	IgG2a	20	BD Bioscience
2	CD45	FITC	IgG1	10	AbD Serotec
3	CD90	APC	IgG1	10	BD Bioscience
4	CD29	PE	IgG1	20	Abcam
5	CD44	APC	IgG1	10	Novus Biologicals
6	CD105	PE	IgG2a	20	Novus Biologicals
7	HLA-DR	PE	IgG2a	10	Novus Biologicals

Table 5: The staining of human MSCs for flow cytometry measurement was performed with the following fluorophore-conjugated antibodies and 7-AAD. The stainings were done by multiple stainings per tube, so called master mixes. All antibodies were generated from murine cell lines. Accurate compensation was done as needed.

Mix	Antigen	Dye	Isotype	Volume [μ L]	Company
1 (Isotype Control)	N/A	FITC	IgG1	22	Beckman-Coulter
		PE	IgG1	22	
		PE	IgG2a	22	
		PE	IgG3	11	
		ECD	IgG1	11	
		PC7	IgG1	11	
2	CD90	FITC	IgG1	22	BD Pharmingen
	CD73	PE	IgG1	22	
	CD34	PC7	IgG1	11	
3	CD235a	FITC	IgG1	22	Beckman-Coulter
	CD105	PE	IgG3	22	
	CD45	ECD	IgG1	11	
4	CD3	FITC	IgG1	22	
	CD14	PE	IgG2a	22	
	CD19	PC7	IgG1	11	
5	CD41	FITC	IgG1	22	
	CD61	PC7	IgG1	11	
6	N/A	7-AAD	N/A	20	
7	HLA-DR	ECD	IgG1	11	

6.6.2 Intracellular staining of the HA-tag

The insertion of the suicide gene HSV-TK was performed under controlled conditions as described before (see 6.3). The rate of transduced cells per population was quantified by HA-tag staining and measurement by flow cytometry. TNF α and IFN γ were added in a final concentration of 3 ng/mL each that induced the RANTES promoter and increased the HSV-TK expression. Not earlier than 48 $^{\circ}$ h after the transduction or completion of the selection (see 6.4), the cells were detached (see 6.2) and the cell count was determined (see 6.2.4). After washing twice with PBS, cells were fixed with Cytofix/Cytoperm $^{\circ}$ for 20-30 min at +4 C. Afterwards, the cells were washed twice with Perm/Wash Buffer $^{\circ}$ to enhance the permeability of the membrane for intracellular staining. While being protected from light, the antibodies were added and incubated for 30 min at +4 $^{\circ}$ C. Then, the cells were washed twice with PBS and suspended in FACS buffer before they were measured by flow cytometry.

The same assay was performed make sure whether the puromycin selection was completed or not.

Table 6: The staining of the HA-tag for flow cytometry measurement was performed with the following fluorophore-conjugated antibodies. The antibody was generated from a murine cell line as declared by the manufacturer.

Mix	Antigen	Dye	Isotype	Volume [μ L]	Company
1 (Isotype Control)	N/A	PE	IgG1	11	Beckman-Coulter
2	HA	PE	IgG1	11	Miltenyi

6.6.3 Differentiation of apoptotic and dead cells in a single or several cell populations

To determine the amount of apoptotic and dead cells in a population, all adherent and non-adherent cells were saved for preparation. First, the supernatant was transferred into a tube to save all non-adherent cells. In a next step, the adherent cells were detached following 6.2.3 and transferred into the same tube. 7-AAD was added and – protected from light - incubated for 10 min at room temperature. Then, the cells were centrifuged at 600 g for 5 min, the supernatant was deleted and the cell pellet was suspended in a 200 μ L Annexin-V binding buffer® (Ca^{2+} enriched saline, isotonic buffer). This Ca^{2+} enriched buffer mediated a proper binding of Annexin-V to phosphatidylserine. 5 μ L of Annexin-V were added to the suspension and incubated for 10 min at room temperature, protected from light. 400 μ L binding buffer were added to this solution (for dilution only) and directly measured by flow cytometry. Since 7-AAD and PE-Cy7 have an overlap in their emission spectrums, accurate compensation was performed to avoid false-positive signals.

Table 7: The staining of apoptotic and dead cells was performed utilizing Annexin-V and the dye 7-AAD. These markers / dyes allow a distinction of apoptotic and necrotic cells. Mediated by Ca^{2+} , Annexin-V binds phosphatidylserine on the cell's surface if presented. Apoptotic cells can not be stained with 7-AAD since these cells still have an intact lipid bilayer.

Mix	Target molecule/structure	Agent	Dye	Volume [μ L]	Company
1	Phosphatidylserine	Ca^{2+} enhanced Annexin-V	PE-Cy7	5	eBioscience
	<i>Intercalation into double-stranded DNA</i>	7-AAD		20	Miltenyi

The morphological alterations of cells undergoing apoptosis were also considered in the gating strategy. Due to condensation effects, the MSCs appeared smaller and more granular resulting in a population shift in the FS/SS scatter. Accurate settings were evaluated and the gating strategy allowed a measurement of this shift (see Figure 21).

In 6.7.3, MSCs were co-cultured with cell lines, which were transduced with a GFP expressing gene according to 6.3. This GFP-tag allowed the differentiation between cell lines and MSCs during the flow cytometry measurements. This was done for all bystander killing assays.

6.7 Treatment of Cell Populations with GCV

6.7.1 Titration of cell sensitivity to GCV by using the MTT-assay

HSV-TK expressing cells are more sensitive to GCV than naïve cells. To provide proof of a functional expressed protein, the increased sensitivity was quantified by an MTT (3-(4,5-dimethylthiazol-2-yl)-2,5-diphenyltetrazolium bromide) staining assay.

MTT is a water-soluble, yellow dye (tetrazolium salt), which is converted into the purple formazan by reductive compounds of viable cells. This conversion occurs if reduction equivalents are available e.g. NADH or NADPH. These molecules are produced during glycolysis of viable cells. Formazan shows a characteristic absorption spectrum between 500 nm and 600 nm and a maximal emission at about 630 nm. Here, the absorption was measured at 570 nm.

On day 1, cells were detached and counted as described before (see 6.2.3 and 6.2.4). Then, the cells were seeded into 5 wells of a 96-well plate (0.32 cm² per well) in accordance to Table 10. The cell lines HT1080 and K67 were seeded with a cell density of 7500 cells/cm². On day 2, the pro-inflammatory cytokines TNF α and IFN γ were given into the media in a concentration of 3ng/ μ L each. GCV was added in a serial dilution as shown in Table 8. On day 3 and 4, half of the medium was changed and GCV was added to the medium to maintain the desired concentration.

Table 8: GCV was given into a serial dilution and added to the media to quantify the GCV sensitivity. All cells were treated following the same GCV dilutions.

Dilution Step	GCV concentration [μ M]
A (Negative Control)	0
B	0.001
C	0.01
D	0.1
E	0.5
F	5
G	50
H	200
I	2000
J (Positive Control)	16000

Table 9: Each cell line and each batch of MSCs was measured for GCV sensitivity in a 96-well plate. Five parallel cultures were generated to take the assay variance into account. The accordant GCV concentrations are listed in Table 8. A staining control (st ctrl) without any cells was performed to consider staining artefacts. PBS was given in the outer rows and columns to reduce evaporation effects.

PBS	PBS	PBS	PBS	PBS	PBS	PBS	PBS	PBS	PBS	PBS	PBS
PBS	A 1	B 1	C 1	D 1	E 1	F 1	G 1	H 1	I 1	J 1	PBS
PBS	A 2	B 2	C 2	D 2	E 2	F 2	G 2	H 2	I 2	J 2	PBS
PBS	A 3	B 3	C 3	D 3	E 3	F 3	G 3	H 3	I 3	J 3	PBS
PBS	A 4	B 4	C 4	D 4	E 4	F 4	G 4	H 4	I 4	J 4	PBS
PBS	A 5	B 5	C 5	D 5	E 5	F 5	G 5	H 5	I 5	J 5	PBS
PBS	St ctrl	PBS									
PBS	PBS	PBS	PBS	PBS	PBS	PBS	PBS	PBS	PBS	PBS	PBS

On day 5, the controls were checked to show that no more adherent cells in column “J” were visible (positive control) and that attached cells were visible in column “A” (negative control) (see Table 9). The staining was performed in accordance to the kit’s manufacturer’s instructions, adding 15 μ L of MTT-containing dye solution and 100 μ L cultivation media after the deletion of the supernatant. After 4 h of incubation, the “stop solution” was given into the wells and the solution was thoroughly mixed by pipetting up and down. The measurement was performed by photometric absorption at 570 nm in reference to the absorption at 650 nm. An additional staining control was performed to exclude any artificial staining errors. The mean absorption value of column “J” was used for normalization: 0% viable cells. Column “A” was used to normalize to 100% viable cells. The EC50 value was calculated using the Graph Pad Prism® software.

6.7.2 Mono-cultivation: characterization of apoptosis under the treatment with GCV

Activated GCV leads to the apoptosis of a cell. To characterize both species in their apoptotic pathway, all human and porcine batches of MSCs were seeded, treated with GCV and measured by flow cytometry (see 6.7.3 for flow cytometry measurements).

On day 1, the cells were detached and counted as described before (see 6.2.3 and 6.2.4). The cells were seeded in 12-well plates (4 cm²) in triplicates. The confluency was less than 15-25% to assure enough plastic surface for proliferation. The used seeding densities are presented in Table 10. The amount of cells seeded per batch differed since the size of the MSCs depended on species, donor and passage. An additional visual check was done 24 h \pm 4 after seeding to assure that the confluency was not higher than 30% and that the cells

successfully adhered. HEPES was additionally given into the medium (in a final concentration of 2.5%) for a sufficient pH buffering because GCV shows alkaline attributes.

Table 10: To characterize the apoptotic pathway under the treatment with GCV, the cells were to reach a confluency of less than 25%. Because the size of a cell also depends on its origin, species and “*in vitro* age”, different cell seedings were chosen.

Species / Batch	Cells Seeded [cells/cm ²]
Human 1	1000-3000
Human 2 (HSV-TK)	
Human 3	
Human 4 (HSV-TK)	
Human 5	
Human 6 (HSV-TK)	
Porcine 1	4000-5000
Porcine 2 (HSV-TK)	
Porcine 3 (HSV-TK)	
Porcine (HSV-TK)	

On day 3, TNF α and IFN γ were added to the medium with a concentration of 3 ng/mL each to induce the expression of HSV-TK (RANTES activation). Then, GCV was added in a final concentration of 25 μ M (this concentration was on the results from 6.7.1 as shown in 7.4.3). On day 4 and 5, half of the medium was changed and GCV was added to maintain a concentration of 25 μ M. Next, the supernatant was saved; the cells were detached, counted, (see 6.2.4) stained and measured in accordance to the previously described procedure (see 6.6).

6.7.3 Co-cultivation: proof of the bystander effect

All batches were co-cultivated with the porcine (K67) and the human cell line (HT1080) to evaluate the bystander effect (see 1.6). Except for day 1, the assay was performed in exactly the same way as described in 6.7.2. The MSCs and the cell line were equally seeded into the 12-well plates. Following Table 10, half of the described cell count was used for each cell line and the accordant MSC batch. All following steps were performed as described before (see 6.7.2).

The MSCs and the cell lines were discriminated by GFP (see 6.6.3). Bio-M was used for the cultivation of human MSCs instead of Bio-1 to enable the proliferation of the cell lines. HEPES was additionally given into the medium (in a final concentration of 2.5%) for a sufficient pH buffering because GCV shows alkaline attributes.

6.8 Isolation and Quantification of DNA

6.8.1 Isolation of DNA from cells and photometric quantification

The DNA isolation was performed with a commercial kit (*Quiagen® Blood & Tissue Kit*) according to the manufacturer's instructions. In short: the cells were lysed, protein and RNA were digested, and the DNA was precipitated with ethanol. Then, the DNA was washed with an ethanol containing saline buffer before it was eluted with TRIS buffer in at least 50 μL .

If the DNA of porcine blood samples was to be isolated, an additional lysis step was performed. The 10x *RBC Lysis Buffer®* was diluted to the working concentration (1x) and 750 μL of blood were mixed with 15 mL lysis buffer to lyse erythrocytes and thrombocytes. After an incubation time of 10-15 min, a centrifugation was performed with 350 g for 5 min. Then, the supernatant was aspirated and discarded before the cells were suspended in PBS. Finally, the DNA was isolated following the protocol described above.

The whole DNA-containing solution was unspecifically quantified by photometric determination. A volume of 4 μL was sampled and given onto the photometric unit of the photometer. The absorption at 260 and 280 nm was measured. In general, an extinction of 1 at 260nm correlates to approximately 50 $\mu\text{g/mL}$ DNA. Any absorption at 280 nm represents possible protein contamination. The quotient of both extinctions indicates a high contamination if the value is <1.8 . If the quotient was less than 1.8, another precipitation, washing und elution procedure was conducted.

If the concentration of the eluted DNA was >150 ng/ μL , the solution was diluted with TRIS buffered water to ≤ 150 ng/ μL .

6.8.2 Quantification of genomic DNA or a sequence of interest by real-time PCR

To quantify a defined sequence of DNA in a sample, real-time PCR was performed thereby amplifying the targeted sequence. Single copy genes were chosen with appropriate primers to determine the amount of genomic porcine and human DNA (see Table 11).

Standards containing a determined amount of genomic DNA of a species were logarithmically diluted and amplified by real-time PCR. The measured cycle threshold (CT) values represented the quantity of amplification cycles before the fluorescent signal was detected. This fluorescent signal was generated by a probe (specific amplicon

complementary fluorescent reporter dyes) that was hydrolyzed during amplification or by double-strand-intercalating dyes (e.g. SYBR green).

This value was put into correlation to the absolute number of sequence copies before amplification by the logarithmic transition of the CT values and the known number of sequences. Following formula was used for the linear regression:

$$y = -m * x + n$$

Table 11: Single-copy genes or a defined sequence of interest allowed the quantification of DNA by specific real-time PCR. Because photometric measurements unspecifically measure the whole DNA in a sample, the defined quantification of a DNA or a sequence of interest was performed by real-time PCR [281]. To measure the insertion rate into a population, the therapeutic gene was quantified by the amplification of the transgene enhancer WPRE [278], which generally is not present in naïve cells.

Species / Origin	Pig	Human	Woodchuck hepatitis B virus
Single-Copy Gene / Sequence of Interest	Zar1	Factor VII	WPRE
Genome Weight [pg]	6.0	6.5	N/A
Primer forward	5'-ACGATGCAG CGTCTTATTCC-3'	5'-GCCAAGCAA GGCACTATCTC-3'	5'-TCATGCTAT TGCTTCCCGTA-3'
Primer reverse	5'-TCATACAGG CAAGGGGAAAG-3'	5'-GGCTGTGCC GAAGTAGATTC-3'	5'-AAAGAGACA GCAACCAGGATTT-3'
Probe	5'-AAACAAACCCAG GTTGAGGAACCCTG-3'	5'-AGGACCTCC GCCAGGGTTCA-3'	UPL Probe @ #63 (sequence not known)

The primers and probes, respectively dyes, were used in the following mixes as shown in Table 12.

Table 12: The following master mixes were used for the quantification of single copy genes or the transgene sequence WPRE. All mixes were tested with different concentration of primers and probes / dyes to optimize the amplification and the robustness of the result.

Master Mix	Species / Gene	Primer / Substance / Dilution	volume [μ L]
#1	Pig: Zar1	PCR-Grade H ₂ O	4,2
		Primer: Pig Zar1 for 300nM	0,3
		Primer: Pig Zar1 rev 300nM	0,3
		Probe Pig Zar1 200nm	0,2
		Probes Master 480 (FAM) (Roche)	10
		Sample	5
		Sum	20
#2	Human: Factor VII	PCR-grade H ₂ O	4,25
		Primer: human FVII for: [300nm]	0,3
		Primer: human FVII rev: [300nm]	0,3
		Probe human FVII [2x]	0,15
		Probes Master 480 (FAM) (Roche)	10,0
		Sample	5
		Sum	20
#3	Therapeutic Gene: HSV-TK (WPRE)	PCR-Grade H ₂ O	4,1
		Primer: WPRE for 300nM	0,3
		Primer: WPRE rev 300nM	0,3
		Probe: UPL #63 150nM (Roche)	0,3
		Probes Master 480 (FAM) (Roche)	10
		Sample	5
		Sum	20

The ratio of WPRE sequences to the amount of cells result in the vector copy number (VCN). A successful selection of population must show a VCN ≥ 1 .

6.8.3 Determination of the mean retroviral vector insertion rate of a population

The transgene HSV-TK was inserted into the MSCs by retroviral vectors carrying a WPRE sequence. To determine the mean insertion rate into a cell population, the cells were analyzed after transduction (see 6.3) and selection (see 6.4.1) by real-time PCR. After the preparation procedure as described before (see 6.8.2), the DNA-containing samples were measured by amplification with the master mixes #1 (for porcine MSCs) or #2 (for human

MSCs) and additionally with master mix #3 (WPRE sequence). Based on the standard curve, the generated CT values were used to calculate the quantity of DNA copies before amplification. The quotient of the transgene copies and the single-copy genes resulted in the mean transduction ratio: the vector copy number of a population.

6.9 *In Vivo* studies and Histopathological Staining

6.9.1 Infusion of MSCs into pigs, clinical observation and pathology

A veterinarian, a member of the *Institut für Molekulare Tierzucht und Biotechnologie der Ludwig-Maximilians-Universität München*, was responsible for the animals involved in the study. She performed all surgical interventions and observed the mini-pigs for clinical relevant symptoms. The competent regulatory authority allowed the animal trial in accordance to the *Tierschutzgesetz*.

HSV-TK expressing porcine MSCs were manufactured in accordance to the protocol described in Figure 2 and were verified for all identity criteria checked in 7.2. The batches were stored in 2 mL cryopreservation vials containing 10×10^6 cells/mL in the vapor phase of liquid nitrogen. The absence of mycoplasma and sterility was tested to assure the safety of the product.

On the day of infusion, the vials were transported from the laboratory in a dry shipper to the study site and were thawed in a 37°C water bath. The thawed cells were counted with trypan blue and prepared for infusion under aseptic conditions. The filled syringes were transported to the stables. Before the cell were infused, the animals were narcotized and a catheter was implanted into the *jugularis* vein by surgery. This catheter was used for the infusion of the cells only. The wound was stitched up and the access was thoroughly pasted at the neck with an accordant catheter expansion. In addition, an intravenous access to an ear vein was established with a short catheter for blood aspiration only (see Figure 29). This configuration of the catheters was intentionally set up to prevent a sampling of just infused cells. Before the cells could reach the ear vein, the cells had to distribute throughout the whole bloodstream and including the passaging of the lungs.

Blood samples were saved in EDTA-containing tubes at ambient temperature, which were transported to the laboratory the same day. The DNA isolation of the MNCs was performed as described before (see 6.8.1)

At the end of the in-life phase, the veterinarian necropsied the animal by previous anesthesia and following euthanasia. Veterinary Pathologists of the *Institut für Tierpathologie* of the *Ludwig-Maximilians-Universität München* performed the pathological investigation. Tissue preservation and IHC staining was performed as described in 6.9.2.

6.9.2 Immunohistochemistry (IHC) on porcine tissues

During the pathological investigation, squarish tissue samples of 3-5 mm size were generated and embedded in formalin for 3-7 days. Afterwards, the samples were fixed in paraffin. The blocks were sent to the external laboratory (*Indivumed*) for immunohistochemical analysis and were stained following the established protocol. In short, the formalin-fixed paraffin-embedded tissue (FFPE) tissue samples were sliced into 3 μm sections and mounted on positively charged glass slides. The FFPE slides were deparaffinized and immunostained with the rabbit monoclonal antibody Anti-HA (clone C29F4, Cell Signaling Technology). Positive Control runs were performed in each run as well as an accordant isotype control of the neighbored tissue slice as negative control. As second negative control, naïve porcine tissue was stained using the Anti-HA antibody to identify potential artefacts.

Afterwards, the slides were manually washed using hot water supplemented with detergent, followed by tap water and dH₂O. For dehydration, the slides were transferred to an ascending ethanol series (2x 80%, 2x 96%, 2x abs. EtOH; 1-3 min each). After dehydration, the slides were transferred to xylene (3x 2 min) and embedded in Pertex®. Finally, the stained sections were analyzed by microscopy for positively stained cells and manually counted.

6.10 Statistical Analysis of Results

For statistical analysis and plotting of graphs, the software Graph Pad Prism 7® was used. All statistical results stated in this work based on calculation of the Graph Pad Prism software.

If normal distribution was assumed, the *D'Agostino & Pearson* normality test, *Shapiro-Wilk* normality test or *Kolmogorow-Smirnow* normality test was performed. The student's paired t-test was performed, if two data sets were compared by their mean and they derived from the same population. Unpaired t-test was performed for data sets that did not derive from the same population but were compared by their mean and had the same variance. *Welch's* unequal variances t-test was performed for data sets that did not have the same variance and therefore did not derived from the same population.

An Analysis of Variance (ANOVA) was performed in a so called "one-way" or "two-way". The One-Way ANOVA (*Tukey's* or *Dunnnett's* multiple comparison test) was performed for

comparison of more than two data sets to one control and to identify if any statistical difference from any of these data sets to the control could be observed. Two-Way ANOVA (*Tukey's* or *Sidak's* multiple comparison test) compared all data sets to each other and aimed to identify any significant differences between any sets of data. Linear Regression was performed based on the normality tests that were described above.

Differences of two normal distributed data sets were described as statistical significant or not following Table 13.

Table 13: This overview summarizes the difference between data sets that were entitled as statistically significant or not. If the assumed normal distribution of two data sets differed for more than 95% from each other, the difference was assessed to be significant. If the statistical differences of the distributed values were even 99% or higher, it was described with the accordant symbol to underline this difference.

p value	described as	symbol
$p > 0.05$	Not significant	ns
$p < 0.05$ and > 0.01	Significant	*
$p < 0.01$ and > 0.001	Significant	**
$p < 0.001$ and > 0.0001	Significant	***
$p < 0.0001$ and > 0.00001	Significant	****

7 Results

7.1 Strategy and Batch Production

Testing homologous, preclinical cell therapy products requires sufficiently characterized cells from the chosen species. Therefore, good *in vitro* characterizations have to be completed before *in vivo* experiments are ethically reasonable and generate valid results allowing a translation to the human setting.

Following strategy was pursued: Bone marrow was aspirated out of the *iliac crest* from three human donors. The mini-pig's cells were taken by scraping out the marrow of both *femur* and *tibia* after necropsy of one mini-pig. The MGH mini-pig in question (Massachusetts General Hospital mini-pig) derived from an isogeneic brood animal [282]. The generated cell populations were described as "Porcine 1 (naïve)" and "Human 1, 3 and 5 (naïve)" (see Table 1). The three ISCT requirements: plastic adherence (and fibroblast-like morphology), differentiation potential and a defined set of surface proteins should be confirmed in both species. In addition, a typical characteristic of human MSCs was investigated: showing HLA-DR on the surface, especially after pro-inflammatory cytokine induction. The population doubling time was also assessed.

A suicide gene was inserted with the same SIN- γ -retroviral vector into both species' cells. Three HSV-TK expressing, porcine batches were generated ("Porcine 2, 3 and 4") as well as one HSV-TK expressing human batch from each donor ("Human 2, 4, and 6"). The transduction rate was determined as well as the mean transgene insertion rate of a puromycin-selected population. The functionality of the human-derived promoters in the porcine MSC was quantified in comparison to human MSCs. The functionality of the gene was quantified by an MTT assay evaluating the GCV sensitivity. A characterization of the apoptotic cell death was performed by flow cytometry regarding morphological and surface changes after GCV treatment. The therapeutic effect was assessed by *in vitro* co-cultivation of HSV-TK expressing MSCs with cell lines and the addition of GCV. Finally, experimental *in vivo* studies were performed. Porcine MSCs were intravenously administered to evaluate the biodistribution of the cells in the mini-pig's bloodstream and representative tissues.

Figure 2 shows the performed strategy in a flow chart.

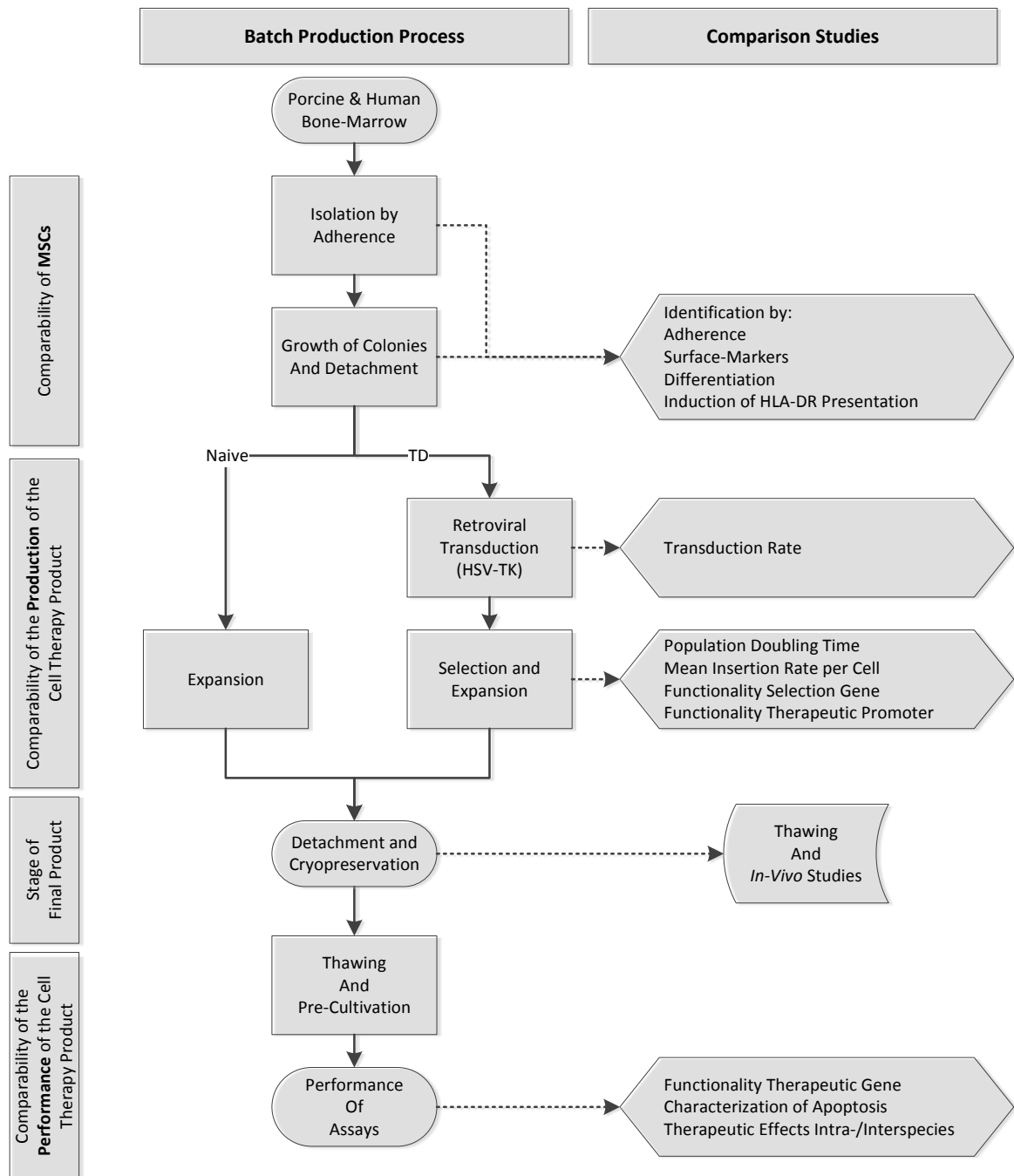


Figure 2: This flow chart presents the comparison approach of the human and the porcine-derived cell therapy products. Both species cells derived from the bone marrow and were produced in the same way. After the first detachment, the cells were split into a naïve line and into a line that was transduced with the HSV-TK vecotor. Testing was performed on several different steps of the MSC product. *In vivo* studies were performed with porcine MSCs only.

7.2 Adherent Bone-Marrow MNCs from the Pig are MSCs

7.2.1 Porcine and human MSCs were plastic adherent and showed similar morphology

The isolation process is the most critical production step in the eyes of many working groups and crucial for the amount and quality of MSCs as described before. To mitigate non-desired effects on the MSC properties, the same isolation protocol was used for all human donors. The freshly aspirated marrow was cultivated in less than 24 h. After initiating the cultivation, the culture media showed a reddish colour due to the massive presence of erythrocytes.

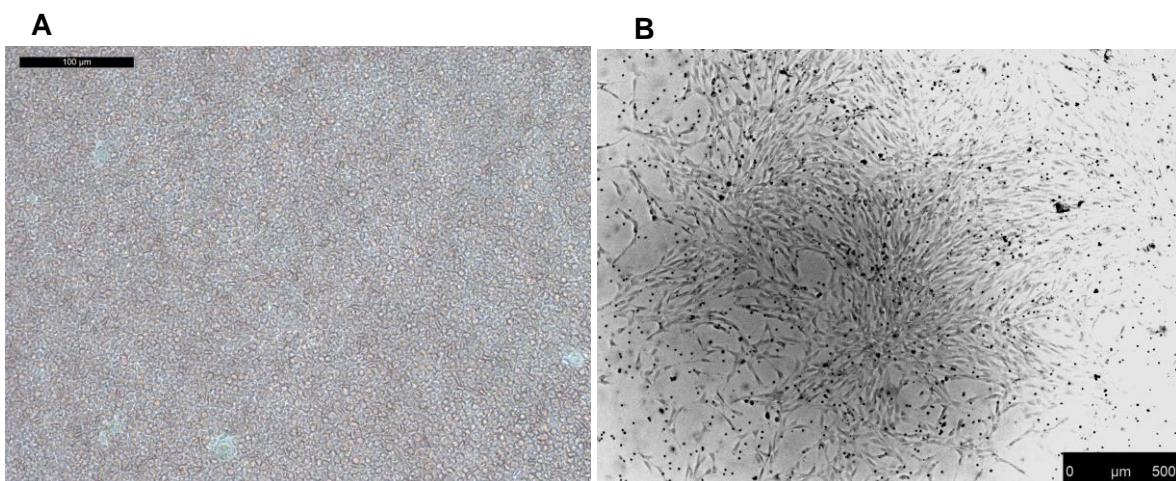


Figure 3: Before the first media change, no adherent cells were visible (A) since erythrocytes completely masked the plastic surface. The successive media changes reduced the amount of suspension cells dramatically until only adherent cells remained in the cultivation flask. Here, stromal cells (B) built up adherent colonies that showed a circular proliferation with a high cell density at the inner part. Within days, the colonies grew up until they got in touch with each other. Not later than 14 days, the cells were split and scattered for further proliferation. Scale bar: (A) 100 µm and (B) 500 µm.

In the first hours of seeding, MSCs started to adhere. The supernatant was changed every 2-4 days to assure sufficient amounts of nutrients in the media e.g. glucose. Although the erythrocytes were diluted step-by-step and finally not present in culture anymore, no obvious cell colonies could be detected by visually screening during the first week of cultivation.

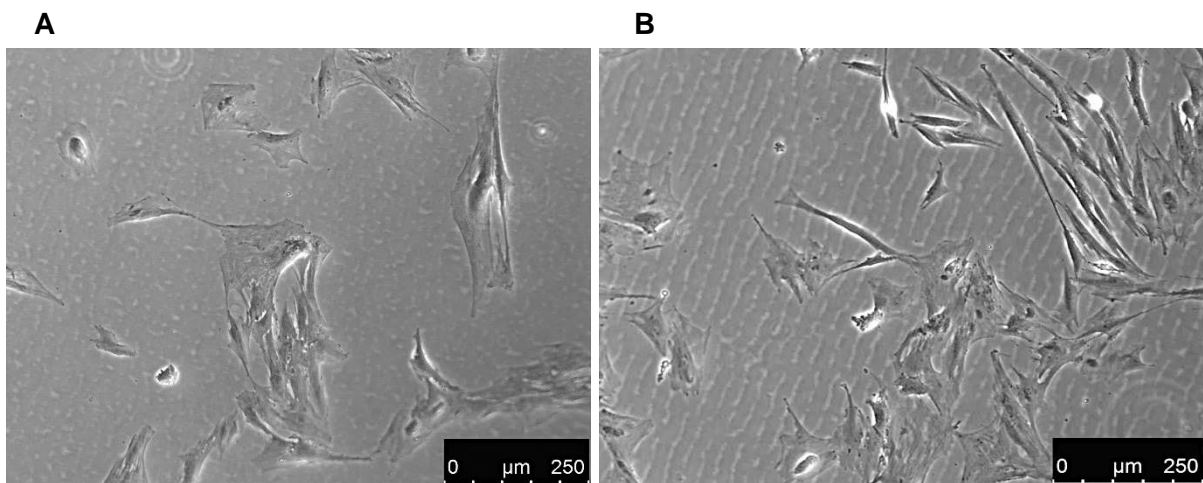


Figure 4: Porcine (A, batch: Porcine 0) and Human MSCs from donor 1 (B, batch: Human 1) in low-density seed showed fibroblast-like morphology. Microscopy showed that human MSCs tended to be larger than their porcine counterparts and were slightly more spindle-shaped. After seeding, both species showed nearly complete adherence in less than 2 h. Scale bar: 250 μm .

After 6-12 days, proliferating colonies could be observed. These colonies were typically confluent in the middle and looser at the outer edge. Not later than 14 days, the colonies were split.

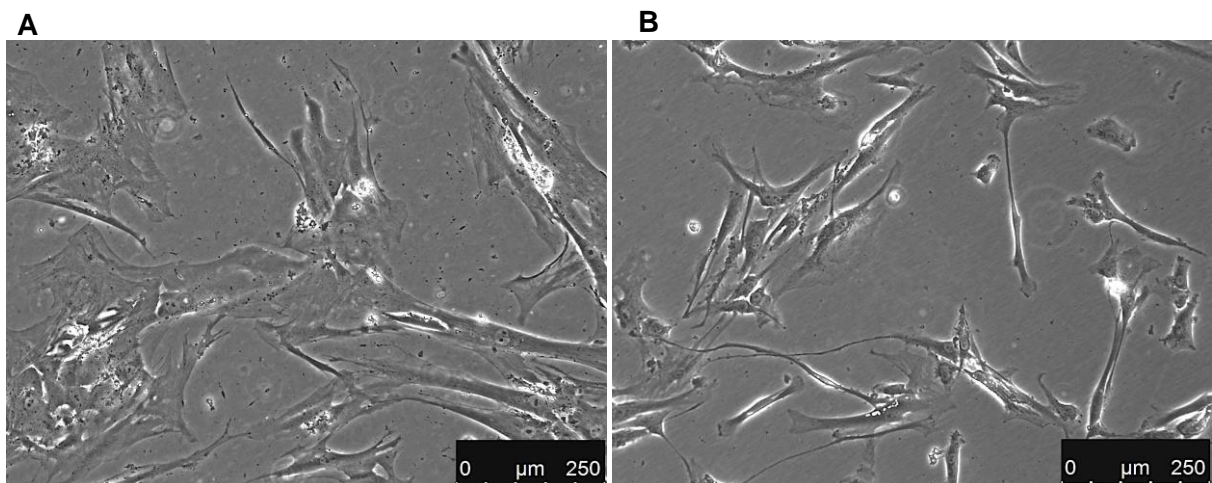


Figure 5: The human donor 2 (A, batch: Human 3) and donor 3 (B, batch: Human 5) were comparable in morphology to donor 1 and the porcine MSCs. Comparing donor 2 to the other human donors, a more flattened and enlarged size was visible. Scale bar: 250 μm .

The cells showed a fibroblast-like morphology and strong adherence to the plastic since slight movement of the culture flasks did not lead to any detachment. Partially, these cells were more flattened or showed single thin and long forms. The morphology of porcine and

human MSCs was quite comparable. All batches of both species showed good adherence and spindle-shaped morphologies, especially donor 1 and 3. Donor 2 was noticeable regarding the more flattened morphology and the relatively large and broad cells.

7.2.2 Surface markers of both species were nearly identical

A single surface marker identifying the MSC population has not been described yet. The ISCT demands a check for CD90, CD73 and CD105 and for several hematopoietic cell markers to exclude possible impurities. The isolation by adherence eliminates hematopoietic cells normally after regular media changes (as described before, see 7.2.1) since hematopoietic cells out of the marrow do not show sustained adherence during cultivation.

All batches (listed in Table 1) were stained with a panel of antibodies to check their surface profile (see 6.6). Therefore, the cells were cultivated for at least 48 h before detachment and stained with an accurate isotype control and the accordant antibody. Measurement was done by flow cytometry. If needed, accurate compensation was done.

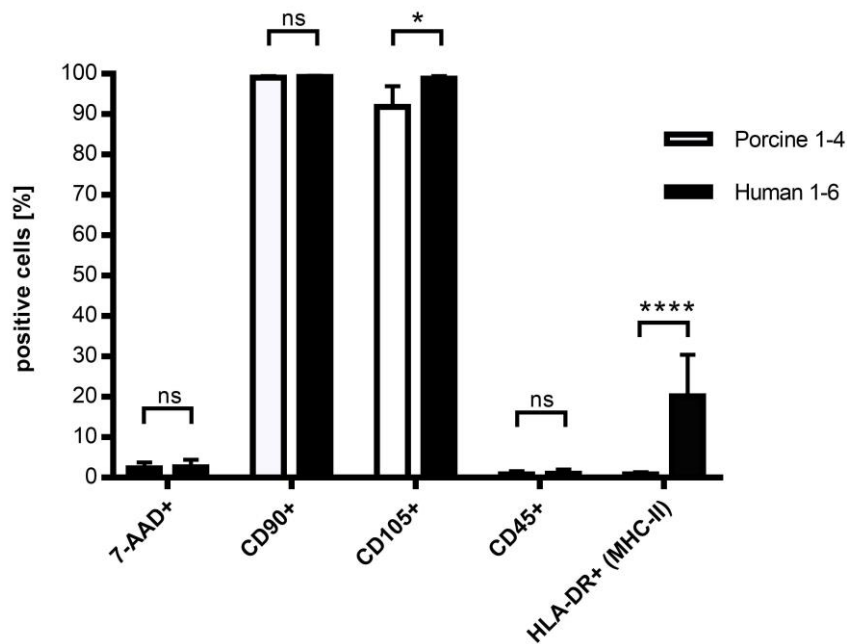


Figure 6: In general, porcine and human MSCs showed a similar set of surface markers (also viability).

The criteria of the ISCT were fulfilled. In contrast to CD90, CD105 was significantly less presented on porcine MSCs, which was further evaluated in Figure 7. CD45+, a typical haematopoietic marker, was not present on both species. HLA-DR was found on human MSCs (see Figure 8) but not on porcine MSCs. More comparison stainings could not be performed due to the lack of commercially available antibodies for porcine cells. Statistics: two-way ANOVA.

The positive markers CD90 and CD105 showed strong expression in both species in contrast to the pan-leukocyte marker CD45, which was not measurable in any species. HLA-DR could be detected on human MSCs but not on porcine MSCs. The presentation of this surface protein was quite different between the human donors (see also Figure 8) resulting in high standard deviations between the batches. Interestingly, a small sub-population of CD105 negative porcine cells showing no expression could be identified. Further negative sub-populations could not be observed for any other surface marker.

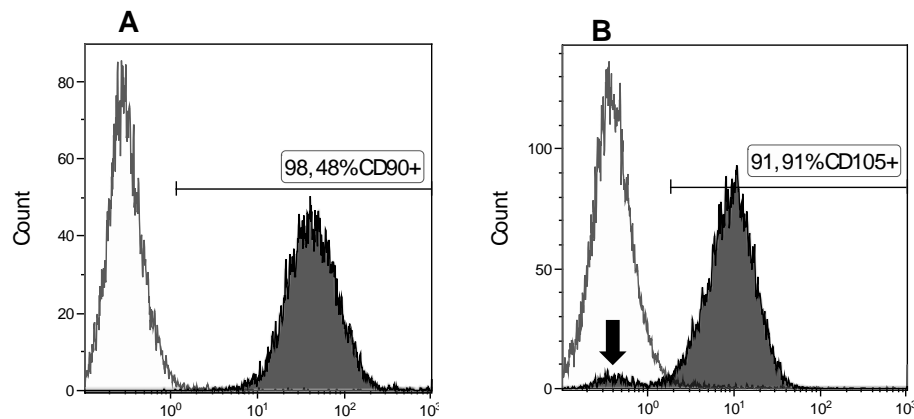


Figure 7: In contrast to other positive MSC markers like CD90 (A), a small sub-population of CD105 negative porcine MSCs (B) could be observed (see arrow). The porcine MSCs showed a single population overlapping with the isotype control. A second population of positive cells could be discriminated.

Beyond the markers that were available for both species, an additional panel of antibodies was tested (Table 14) to assure the MSC surface profile based on publications and known markers for other cell types (see 1.2 and 8.1 for more details).

Table 14: Here, a detailed list of all measured, present and absent marker of both species is shown (as well as viability in the measured populations). For porcine cells, the variety of commercially available antibodies was very low in contrast to human MSCs. Most of the markers were described before (see 1.2). Hematopoietic markers e.g. CD45 and CD34 were absent for both species (CD34 could only be measured for human MSCs). Statistics: With the exception of batch Porcine 1, all groups are described by their mean value and standard deviation.

Viability / Surface Marker	Porcine 1 [%]	Porcine 2-4 (HSV-TK) [%]	Human 1,3,5 [%]	Human 2,4,6 (HSV-TK) [%]
Dead Cells	2,1	2.4±1.8	3.2±2.1	2.5±1.5
CD44+	98.0	99.6±0.4	N/A	N/A
CD90+	98.5	99.2±0.3	99.1±0.5	99.1±0.1
CD105+	91.9	91.7±6.3	99.0±0.2	98.6±0.9
CD29+	98.5	99.3±0.1	N/A	N/A
CD45+	1.9	0.4±0.5	0.5±0.5	1.5±1.3
CD34+	N/A	N/A	0.3±0.3	1.6±2.8
HLA-DR+ (MHC II)	0.2	1.0±0.4	24.5±9.6	20.1±10.3
CD73+	N/A	N/A	98.8±0.4	98.8±0.7
CD235a+			1.0±0.7	0,3±0.4
CD3+			0.5±0.4	0.1±0.1
CD14+			0.3±0.3	1.2±2.1
CD19+			1.0±0.9	0.4±0.4
CD41+			5.9±5.0	1.4±0.7
CD61+			95.8±4.7	96.4±3.2

7.2.3 HLA-DR presentation on human MSCs was inducible – not in porcine MSCs

Although the ISCT suggests that MSCs are HLA-DR negative, several publications demonstrated the inducible HLA-DR presentation on MSCs (see 1.3). This presentation can be induced by addition of pro-inflammatory cytokines and was investigated in addition to the ISCT criteria.

All porcine and human batches were tested for HLA-DR presentation on their cell surface with or without stimulation. Cells were seeded in confluence of 10-20% and stimulated with IFN γ and TNF α . HLA-DR presentation was measured by flow cytometry.

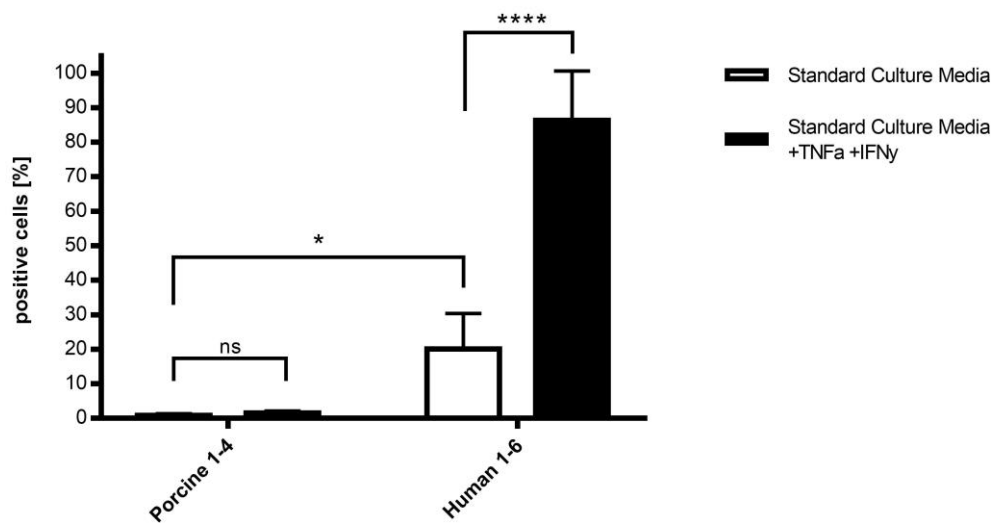


Figure 8: The presence of TNF α and IFN γ induced no up-regulation of HLA-DR on porcine MSCs in contrast to human MSCs. MSCs of both species were cultivated w/wo pro-inflammatory cytokines and stained for HLA-DR. The naïve and genetically modified batches were grouped. Porcine MSCs did not show any HLA-DR presentation on their surface whether stimulated or not. Human MSCs increased HLA-DR presentation under stimulation significantly. Statistics: two-way ANOVA.

Figure 8 shows that it was possible to identify HLA-DR on human MSCs in contrast to porcine MSCs. All batches of human MSCs showed a HLA-DR presentation whether without stimulation (20%) or significantly increased with stimulation (86%). Porcine MSCs did not show any reaction.

7.2.4 Porcine MSCs differentiated with human stimulation media

The third ISCT criterion is the successful proof of the differentiation potential of the cells. It is well-described that MSCs are able to build up lipid vacuoles or to enrich calcium as indicators for an adipogenic or osteogenic differentiation (see 1.1).

The differentiation of the porcine MSCs was conducted with the same protocol that was used for human MSCs. Over 14-21 d of induction, the same stimulation media were utilized. The cells were stained for lipid, lipophilic droplets with red oil and for enrichment of calcium with alizarin red. In addition, control cells were cultured with standard media (6.5 for method description).

It was possible to differentiate porcine MSCs as well as human MSCs following the same protocol. All batches cultivated with standard media showed no differentiation. The visual

analysis showed differences in the amount of differentiated cells between the lots and species. The porcine MSCs were less sensitive than their human counterparts for adipocyte stimulation. If the porcine cells were additionally transduced, selected and hence longer expanded (Porc1-3 TD), the amount of lipophilic droplets was additionally decreased (see Table 15).

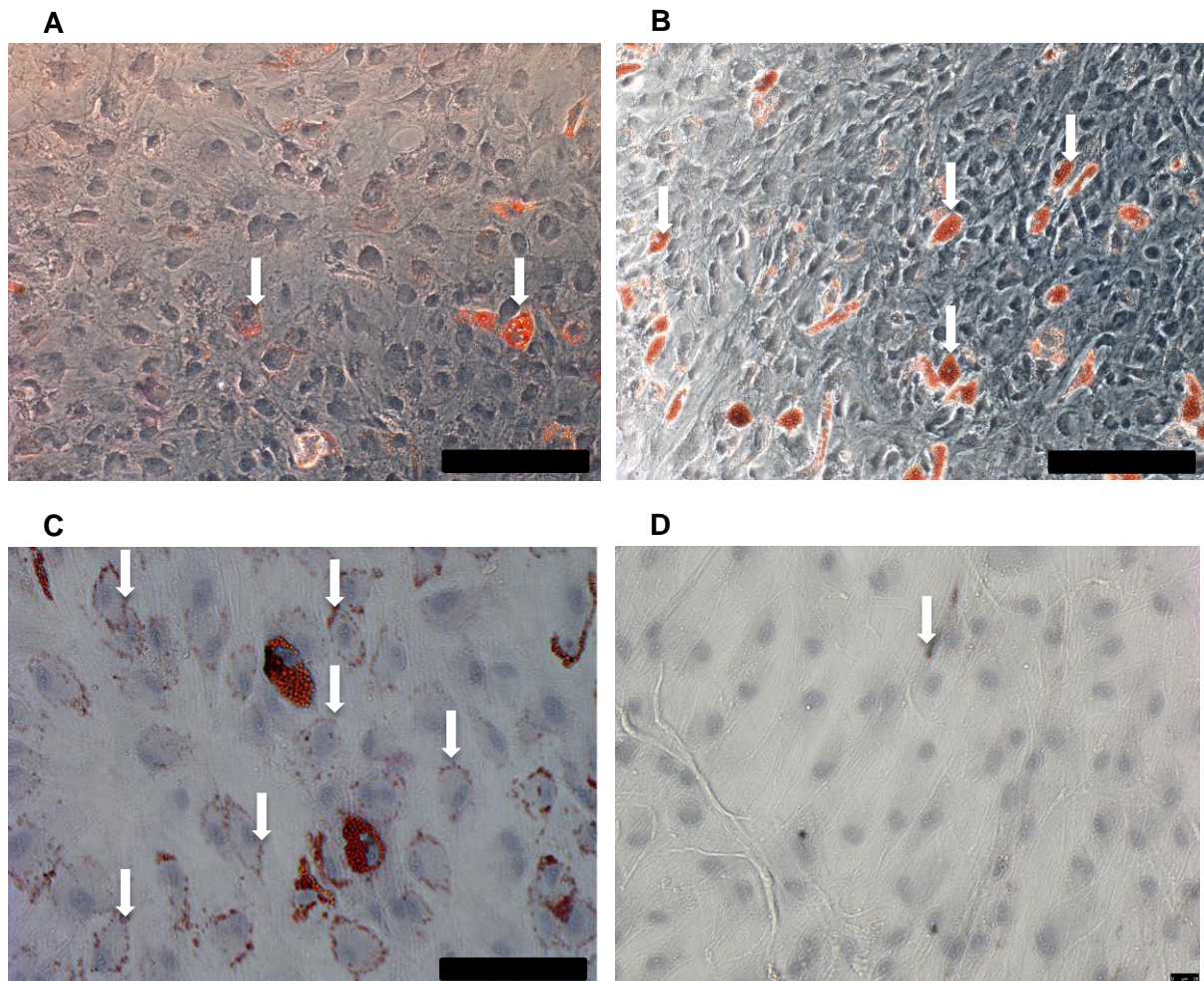


Figure 9: Both porcine (A) and human (B) MSCs showed an adipogenic lineage potential. Defined stimulation media induced the cell differentiation. After 10 d, first fat vacuoles were observed. Not earlier than 14 d after the start of differentiation, the cells were washed and stained. The reddish colour of the droplets was caused by the red oil, which was used to detect the fat vacuoles more easily. The same commercial differentiation media were used for both species (the used media were indicated for human MSCs only). The human donors generally showed more lipid vacuoles than the pig (see Table 15). The human batch 1 (C) showed a significantly higher sensitivity for differentiation because the appearance large fat vacuoles was observable. In addition, small vacuoles lined up in a row (see arrows) at the edge of nearly all cells. (D) Appropriate controls showed no red oil staining although very small vacuoles could be observed in some sections. Scale bar: 250 μm for (A,B,C) and 25 μm for (D) (all sections had the same optical magnification).

The osteogenic lineage potential was nearly identical in all species and batches and no differences could be observed. The homogeneous distribution of calcium enrichments on the cells was stained with alizarin red, which enhanced a strong color of the complexed Ca^{2+} ions.

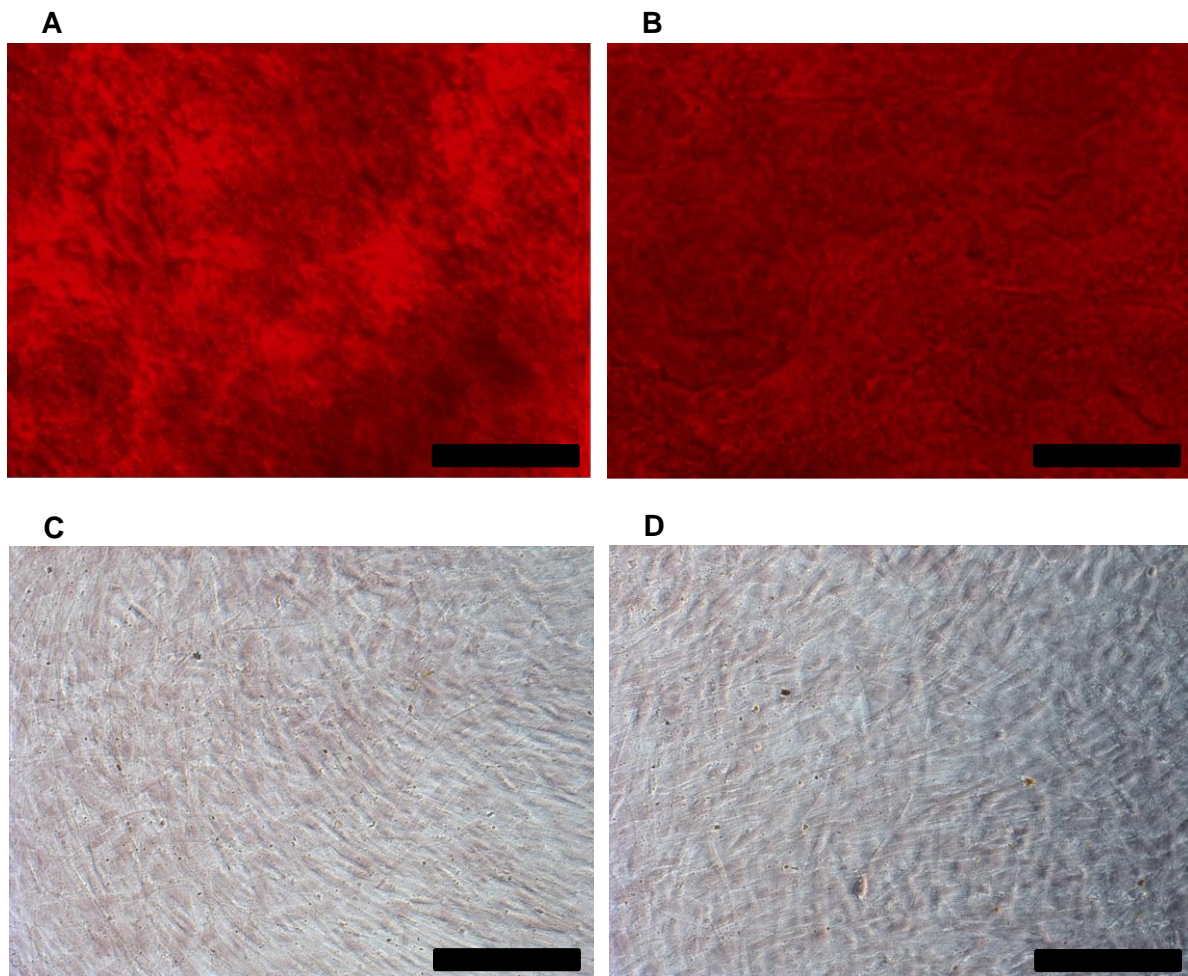


Figure 10: Both species (porcine (A), human (B)) showed strong calcium enrichment. No significant difference between the batches and species could be observed. The porcine MSCs were equivalent to the human MSCs in their osteogenic potential with the human stimulation media. (C porcine, D human) Controls for both species showed no calcium enrichment if cultivated with the accordant standard media. Scale bar: 250 μ m.

The visual rating of the differentiated cells is shown in Table 15. For adipogenic differentiation, three representative sections (approximately 750 μ m \times 1000 μ m) were chosen and the amounts of cells that showed fatty vacuoles were counted. This was performed three times for each staining.

Table 15: Overview of differentiation potential of both species. All batches were differentiated following the same protocol. After differentiation, the populations were fixed, stained and representative sections (~750 μm x 1000 μm) were counted for differentiated cells. All batches kept their differentiation potential whether transduced or not. If the cells were cultured with standard media, no signs of differentiation could be observed. The porcine cells could be differentiated following the same protocol and same differentiation media designed for human MSCs. After the induction time, porcine MSCs generally showed less adipogenic potential than human MSCs. Only donor 2 (Human 3 / 4) was as weak as the porcine MSCs. Coloration: red ≥ 25 , orange 15-25, yellow ≤ 15 .

Batch	Cultivation time before differentiation start [d]	Adipogenic Stimulation			Osteogenic Stimulation	Standard Culture Media (Control)
		#1	#2	#3		
Porcine 1	10	6	10	8	+	No differentiation.
Porcine 2 (HSV-TK)	32	7	9	6	+	
Porcine 3 (HSV-TK)	26	6	5	7	+	
Porcine 4 (HSV-TK)	37	4	7	4	+	
Human 1	13	29	32	21	+	
Human 2 (HSV-TK)	23	22	25	19	+	
Human 3	14	24	22	28	+	
Human 4 (HSV-TK)	35	21	24	18	+	
Human 5	20	24	25	21	+	
Human 6 (HSV-TK)	34	26	23	20	+	

7.2.5 Doubling time of porcine MSCs was comparable to human MSCs

Based on the cell counts after the first passage and just before cryopreservation, the population doubling time for each batch was calculated (see 6.2.6) as an additional parameter for comparison.

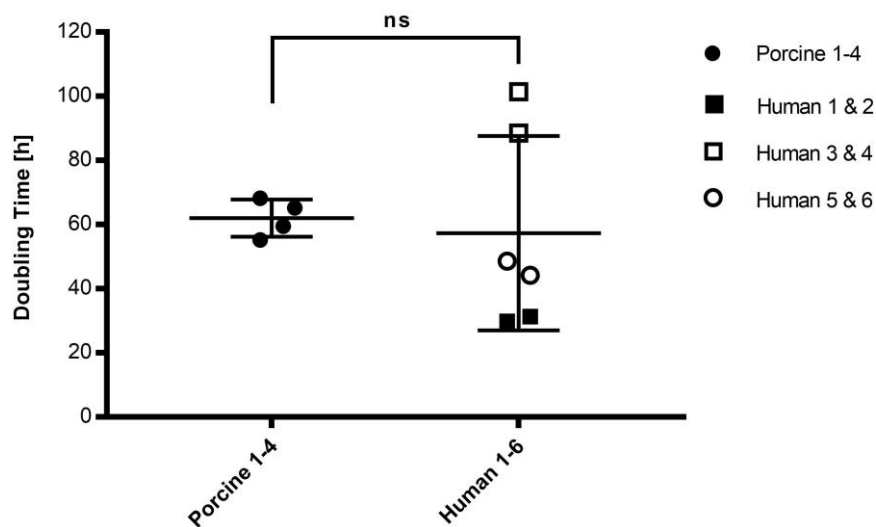


Figure 11: The mean population doubling time (PDT) of porcine and human MSCs was comparable. The mean PDT of the porcine batches was 62 h and while it was 58 h for the human batches. Obviously, a donor dependency could be observed indicating different doubling times for each donor. The porcine batches showed a similar population doubling time. Both batches of each donor showed similar population doubling times varying from 30 h to 100 h. Statistics: two-tailed, unpaired t-test.

Both species showed a mean doubling time of 60 h (mean PDT of porcine batches: 62 h and mean PDT of human batches: 58 h). But the doubling time for the human batches varied heavily from 30 h to 100 h. If both batches of each donor are depicted, a clustering can be observed. It is obvious that the time needed for the production of one batch is strongly dependent on the proliferation speed of the donor's cells.

7.3 Insertion of the Therapeutic Gene into Porcine MSCs was Controllable and Comparable to Human MSCs

A SIN- γ -retroviral vector inserted the suicide gene HSV-TK (see Figure 1 for schematic description of the inserted transgene). After transduction, the cells were selected using the also inserted transgene PAC (regulated by the constitutive promoter PGK). Then, the HSV-TK expressing population was expanded to generate the desired cell count (see 6.3).

7.3.1 Same vector / cell ratios lead to comparable transduction rates

After the first detachment of the freshly procured MSCs, the transduction process was started. For this, the SIN- γ retroviral supernatant with a determined load of viral particles was used.

Based on the titer and the cell count just before transduction, the viral supernatant was mixed with the cells suspended in a PLL containing serum-free medium and seeded into culture flasks (method A). The chosen viral particle load per cell was three (MOI = 3). The other methods B and C differed in the methodological approach (see 6.3 for detailed description).

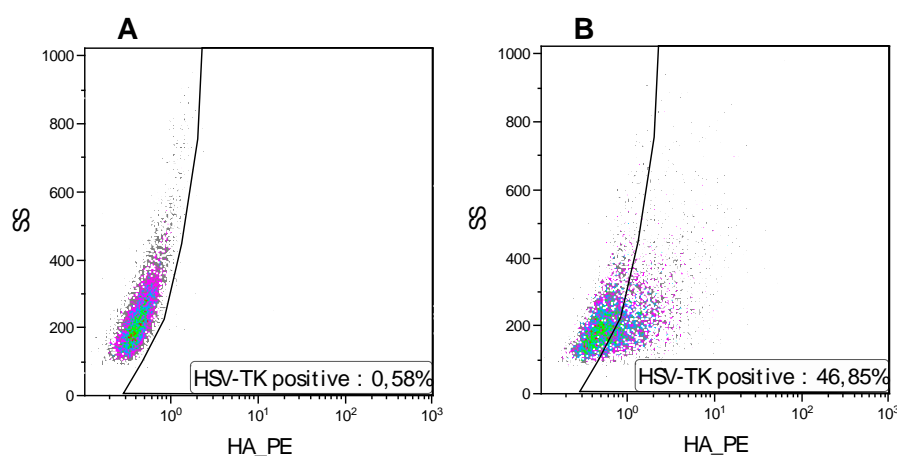


Figure 12: Successful transduction was identified by flow cytometry measuring a second population (B) in contrast to a single population of naïve cells (A). (A) Naïve cells showed a typical negative population in the SS / fluorescence plot. (B) The heterogeneous cell population of transduced and naïve cells showed a partial shift creating a diffuse second population. Isotype-controlled gating showed more than 46% cells expressing the transgene.

Pro-inflammatory cytokines stimulated the RANTES-regulated transgene cassette to increase the HSV-TK expression (see 7.4.2 for induction of RANTES in porcine environment). The heterogeneous population of naïve and transduced cells was stained with an anti-HA antibody and quantified by flow cytometry (see Table 16).

Table 16: Different transduction methods led to different transduction rates although the vector / cell ratio was equal. Method C and A showed transduction rates that obviously did not differ as much as method B. Statistics: none, descriptive only.

Transduction Rate	Porcine 4	Porcine 3	Porcine 2	Human 2	Human 4	Human 6
Viral Particle / Cell Ratio (MOI)	3					
Transduction Method	A	B	C			
Fraction of Transduced Cells [%]	5	46	3	7	11	3

Method C showed comparable results in regard to transduction rate (see Table 16) and VCN (see Figure 13 (A)). If the cells were transduced in suspension (method A), there was a slight increase from 3% to 5% in porcine MSCs. If the viral supernatant was centrifuged onto PLL containing culture flasks, there was an increase up to 42% (method B).

The vector copy number was determined by real-time PCR (see 6.8.3) after the selection of the transduced population (see Figure 13).

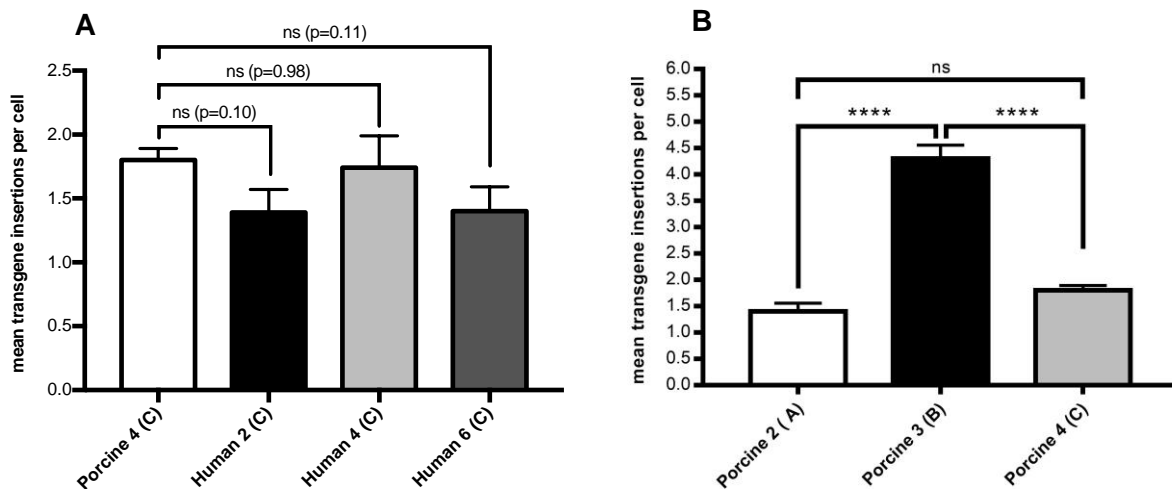


Figure 13: (A) Transducing MSCs with the same vector/cell ratio and the same method led to comparable mean transgene rates in both species. The human batches 2 and 6 had slightly reduced insertion rates, whereas Human 4 was quite similar to Porcine 4. (B) If only the method of transduction was changed (same vector / cell ratio), the insertion rate varied significantly. Method B showed the highest efficiency while method A and C did not show any statistical relevant changes. Statistics: (A) ordinary One-Way ANOVA and (B) ordinary Two-Way ANOVA.

Method C showed no significant difference for both species in all human batches (VCN = 1.4; 1.7; 1.4) and porcine batch 4 (VCN = 1.8). But method B (VCN = 4.2) differed significantly from method A (VCN = 1.4) and C (VCN = 1.7), enabling higher transduction rates although the amount of viral vector supernatant was not increased (see Figure 13 (B)).

7.4 Human-derived Promoters worked comparably in Porcine MSCs

7.4.1 Proof of functional human PGK promoters in porcine MSCs

The constitutive PGK promoter is required to work constantly and has to express the PAC resistance gene correctly for a successful selection of not-transduced cells. This system also has to be functional in the foreign porcine cell if a model system is to be applicable.

Puromycin was given into the cultivation medium obviously killing the not-transduced population (see Figure 14). After 24 to 48 h, the selection process started since the accumulation of spherical cells in the supernatant could be observed. The majority of cells was depleted from the plastic surface and only small numbers of adherent were still visible (see Figure 14). Five days later, the medium was completely changed and all non-adherent cells were depleted. Now, the remaining cells started to proliferate again in the standard medium without the selection agent puromycin and a cell growth could be observed clearly.

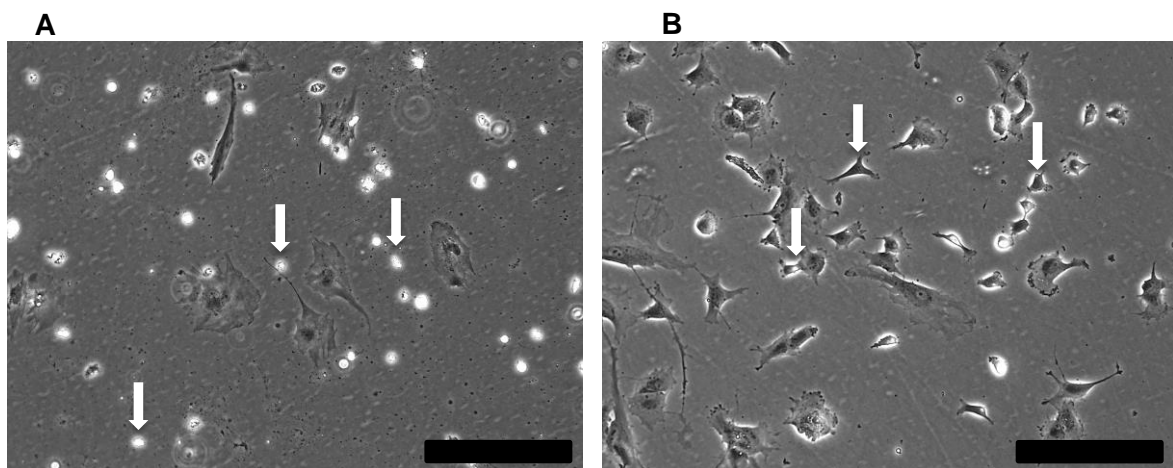


Figure 14: (A) The selection by puromycin killed most of the adherent cells visible as detached, spheric units. (B) As soon as the selection medium was depleted and a standard medium was given into the culture, the MSCs started to proliferate again, indicated by small, not flattened cells. Scale bar: 250 μ m.

Proliferating cells were identified by a small, less flattened and less fibroblast-like morphology, showing a fast increase in the number of cells in the surrounding area the following days (Figure 14 B).

The selection procedure was verified by flow cytometry as shown in Figure 15. HA-tag staining was performed and measured as described before (see 6.6.2).

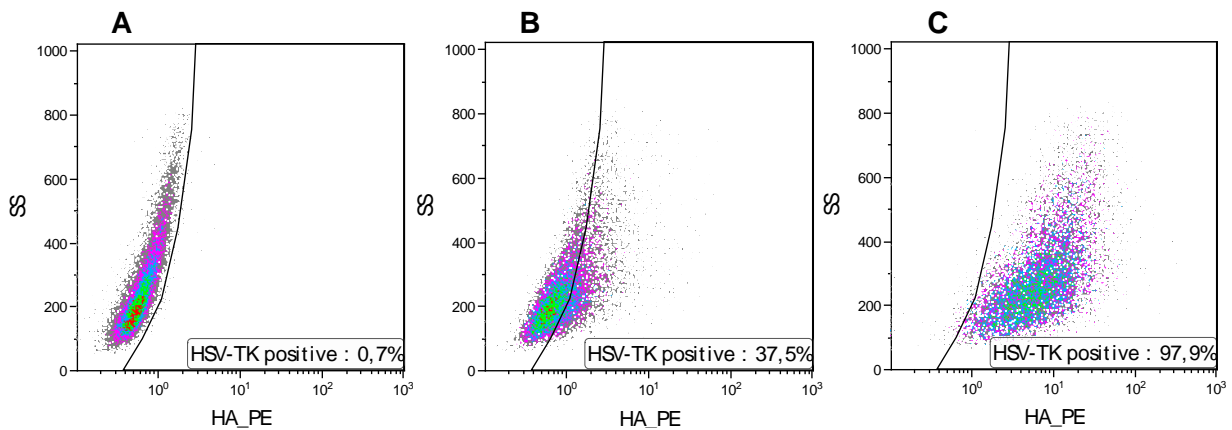


Figure 15: (A) Naïve porcine cells showed a typical population distribution in the fluorescence / SS depiction. (B) After transduction and selection without RANTES activation, background expression of the not induced promoter was detectable (37%). Here, the cells distributed on both sides of the gate. (C) If pro-inflammatory cytokines were given into the medium, a single population of porcine HSV-TK expressing cells was identified.

No second population could be observed during measurement indicating a complete selection process (see Figure 15 (C)). The corresponding control of naïve cells (A) was clearly definable in contrast to positive cells (C). Without any pro-inflammatory activation, the population drifted slightly into the positive gate and could almost not be defined against the control (B). It can be concluded that the selection was sufficiently effective and transduced cells were resistant because the PGK-regulated PAC resistance gene was successfully expressed.

7.4.2 Up-Regulation of RANTES in porcine MSCs was feasible

Since RANTES is an inducible promoter, an up-regulation in porcine MSCs should be possible. Therefore, the naïve and HSV-TK expressing batches were stained with / without a previous pro-inflammatory stimulation and measured by flow cytometry. The geometric mean of the fluorescence-emitting population was normalized to the corresponding naïve cells of the batch.

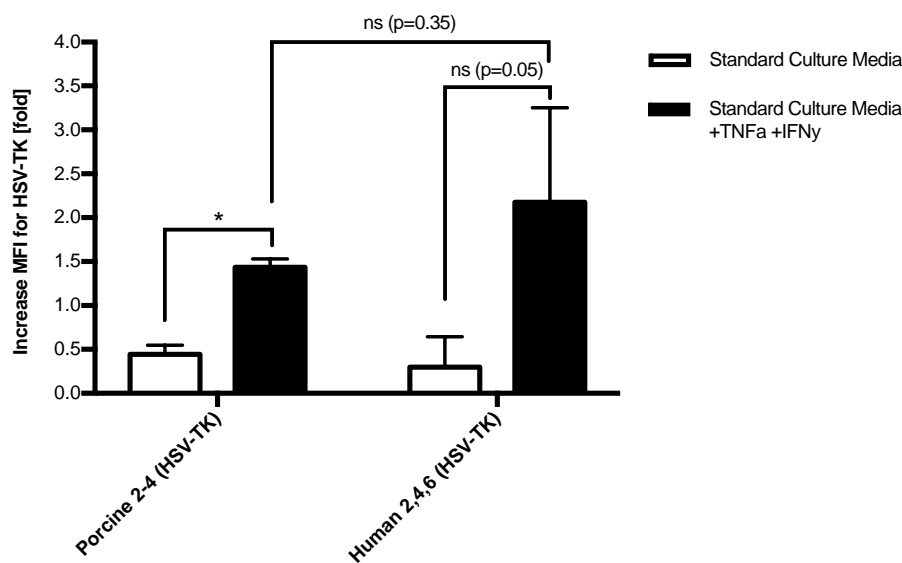


Figure 16: Stimulation of the human RANTES promoter with pro-inflammatory cytokines led to increased HSV-TK expression in both species. Although the RANTES promoter was isolated from human cells, it showed functionality in porcine MSCs. Slight background expression was detectable in both species in comparison to naïve cells as the negative control. Statistics: paired t-test for columns A/B and C/D and Welch's test (unpaired t-test, non-equal stdv) for the comparison of porcine to human batches.

Background expression without any pro-inflammatory activation could be measured for porcine MSCs (0.4-fold increased expression) as well as for human MSCs (0.3-fold increased expression). Although the RANTES promoter was isolated from human cells, it also worked in the porcine MSC with inflammatory activation (1.4 fold increased expression). The up-regulation in human MSCs (2.2 fold increased expression) was even stronger compared to porcine MSCs although it showed a larger variance.

7.4.3 Porcine HSV-TK expressing cells showed higher sensitivity to ganciclovir

GCV is a prodrug and highly activated by viral kinases. HSV-TK expressing cells should be more sensitive to GCV than naïve cells (as described before 1.6). The HSV-TK expressing

cell should become apoptotic under treatment with GCV, which then leads to cell death if the enzyme is working properly.

To determine the GCV sensitivity of naïve and HSV-TK expressing batches, the cells were seeded in 96-well plates and exposed to different, logarithmically distributed GCV concentrations. After five days, the substrate tetrazolium dye MTT (see 6.7.1) was given into the medium. The more living cells were available, the more formazan was synthesized. After a defined incubation time, photometric measurement allowed the quantification of and a comparison between the naïve and HSV-TK expressing batches. All batches and the cell lines HT1080 and K67 were quantified for their GCV sensitivity represented in the amount of absorption by formazan.

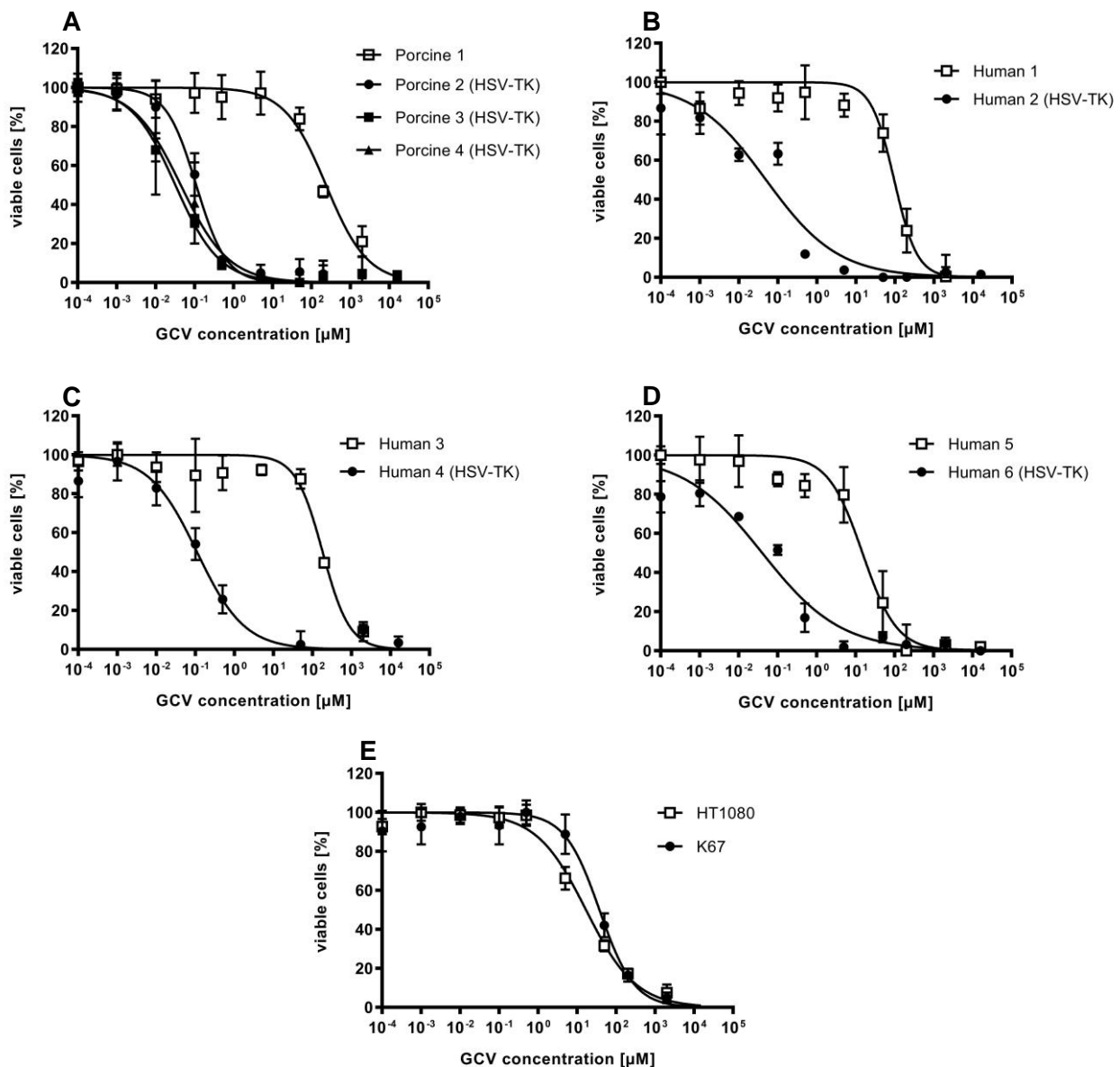


Figure 17: Porcine (A) and human MSCs (B-D) expressing HSV-TK showed a higher sensitivity to GCV than their naïve counterpart. Increasing the GCV concentration in a logarithmic scale showed an earlier effect on transduced MSCs, decreasing the amount of living cells. The cell line HT1080 and the porcine cell line K67 did show a GCV sensitivity profile (E) like naïve MSCs. Statistics: nonlinear regression (dose response inhibition), *goodness of fit* for each figure A-E: $R > 0.9$.

To determine the sensitivity, the half-maximal efficacy concentration (EC₅₀) was calculated based on the approximation for a dose response inhibition (see Figure 17). The response curves showed that HSV-TK expressing MSCs were more sensitive to GCV than their naïve counterpart and naïve cell lines. The resulting EC₅₀ values are shown in Figure 19.

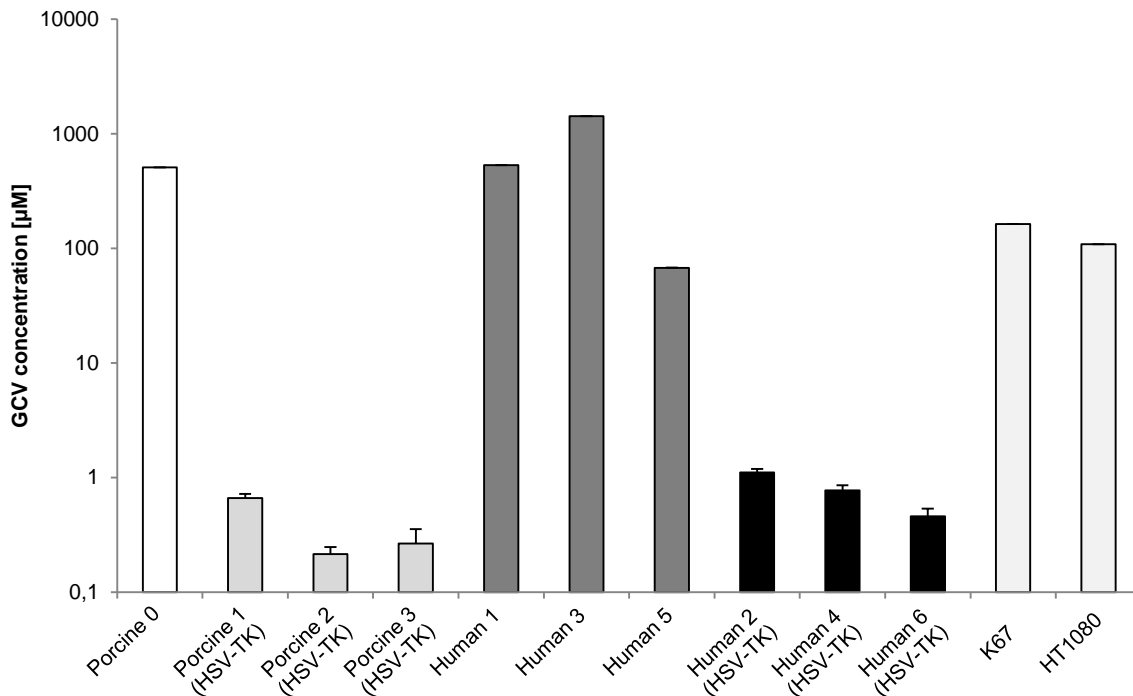


Figure 18: The EC₅₀ (half-maximal effectivity of GCV) of all non-transduced MSCs and cell lines were more than 100-fold lower than HSV-TK expressing cells. The porcine cells showed sensitivity differences of nearly 1000-fold. Statistics: standard deviation bases on the 95% confidence interval of the nonlinear regression.

The EC₅₀ value of HSV-TK expressing porcine MSCs lay between 0.2 µM and 0.7 µM, whereas the naïve batch was measured with more than 500 µM GCV, which represents a sensitivity that was 1000-fold higher. The naïve human batches showed differences in the GCV sensitivity between 67 µM and 1400 µM while the transduced batches were in the range of 0.5 µM to 1.1 µM – a more than 100-fold higher sensitivity. The cell lines were only slightly more sensitive than the naïve batches with 109 µM to 163 µM GCV.

7.5 Porcine MSCs showed the same Mode of Action under GCV Treatment

In 7.4 it was successfully shown that the insertion of the transgene was successful and quantifiable. Also, the functionality of the selection cassette PGK-PAC and the inducible RANTES promoter could be shown. In this section (7.5), the apoptosis as an effect pathway due to the treatment is to be characterized and compared between the species.

7.5.1 Activated GCV initiated the apoptotic cascade in both species in a comparable manner

As introduced before (see 1.6), there are several kinds of cell death that could end the cells' life cycles: necrosis, autophagy, mitotic catastrophe and apoptosis. In contrast to others, apoptosis is a self-regulated cell death initiated by internal (e.g. DNA damage) or external signals (e.g. FAS activation). The apoptotic death of a cell is complex and the process is characterized by different changes: morphological alteration into spherical and granular cells, detachment, appearance of phosphatidylserine (PS) on the surface and loss of the cells' integrity making it possible for dyes to get into the cell and stain the DNA (e.g. 7-AAD).

Here, the characterization of the apoptotic pathway initiated by GCV in human and porcine HSV-TK expressing MSCs was investigated. All batches were seeded and treated with pro-inflammatory cytokines on day two and GCV on day two, three and four. GCV was added in a concentration of 25 μM . This value was chosen based on the results generated in 7.4.3. The highest sensitivity to GCV showed the batch Human 5 with an EC50 value 64 μM . Therefore, the chosen concentration was less than half the EC50 value of Human 5.

On day five, the cells were harvested and stained with Annexin-V as apoptotic marker as well as 7-AAD as dead marker. The cells were counted and analyzed regarding morphological and membrane surface changes through flow cytometry.

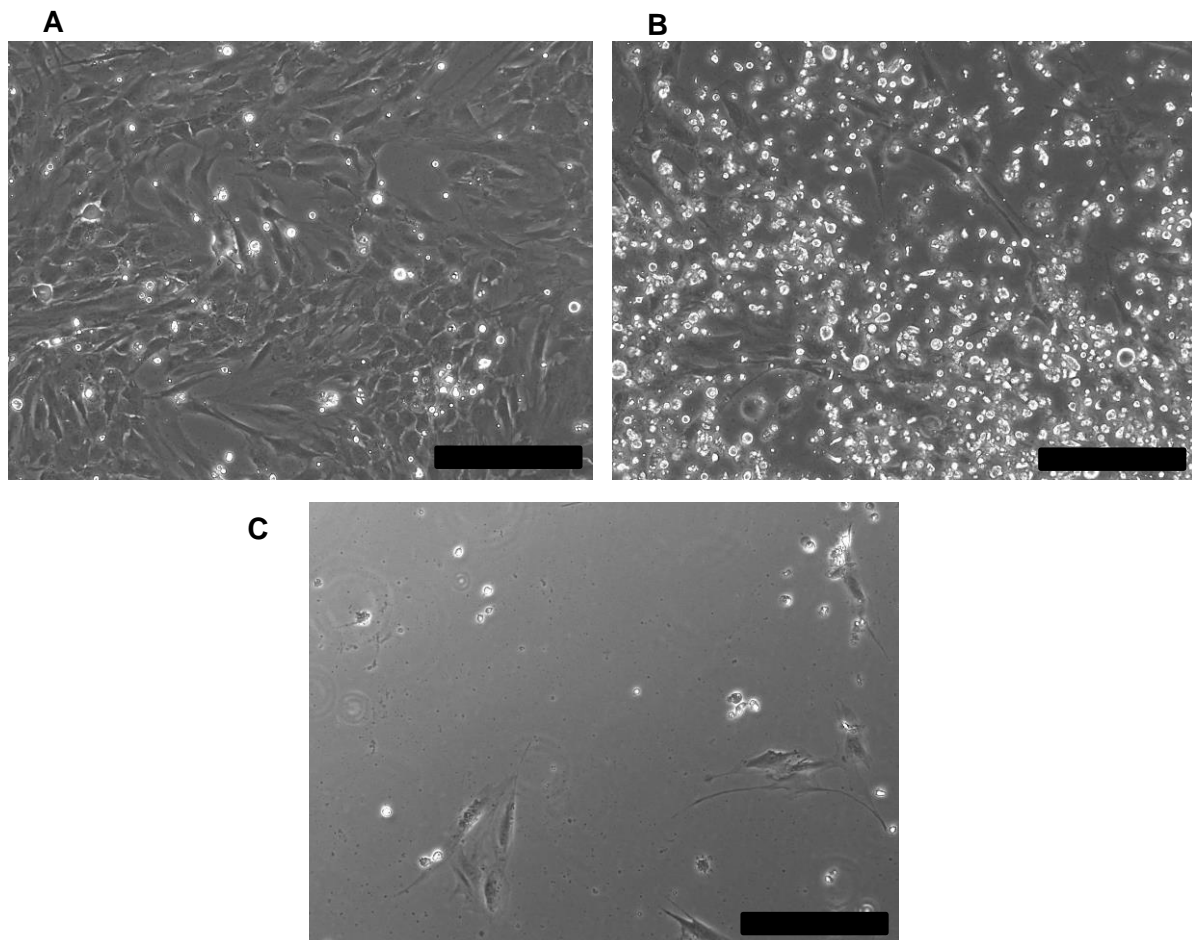


Figure 19: (A) Naïve porcine MSCs did not react with massive apoptosis if GCV was added to the medium. The naïve cells showed good adherence and only occasional deachment was visible although GCV was present. (B) The treatment of HSV-TK expressing MSCs with GCV led to a massive accumulation of cells and cell debris in the supernatant, which could be seen on day five. (C) Depleting the medium only occasionally showed adherent cells. Scale bar: 250 μm .

Throughout the treatment, the visual analysis showed no effects on naïve MSCs because only single cells were in the supernatant. In contrast, the majority of HSV-TK expressing cells detached already one day after the start of the treatment. A massive congregation of cells and cell debris could be observed, which accumulated in the supernatant. Depleting these cells by changing the cultivation medium showed that nearly no adherent cells were on the surface. Some cells still attached to the plastic although they partially showed signs of apoptosis due to their spherical morphology.

To determine the inhibitory effects of the pro-inflammatory cytokines and GCV, cell counts were performed after five days of cultivation and three days of treatment. The treated naïve

and HSV-TK expressing cells were compared to their non-treated controls considering the proliferation capacity over five days. The cell count differences between standard cultured cells and treated cells were calculated and are shown in Figure 20.

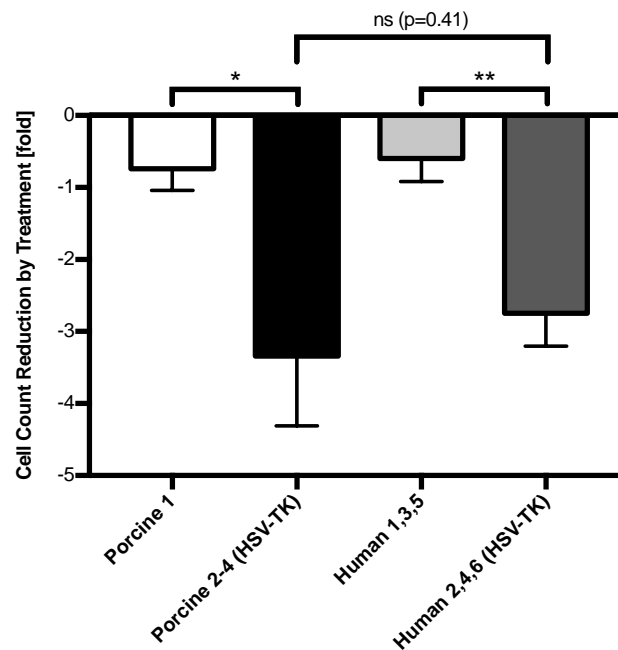


Figure 20: The treatment (pro-inflammatory cytokines + GCV) of HSV-TK expressing cells showed significant reduction in cell proliferation in contrast to also treated naïve cells. All groups were additionally cultivated without treatment as negative control. At the end of the assay, the cell counts of the treated groups were normalized to the negative control and the reduction was calculated. Both species showed a comparable percentage of killed cells during treatment for HSV-TK expressing and naïve cells. Statistics: paired t-test for columns Porcine 1 / Porcine 2-4 (HSV-TK) and Human 1,3,5 / Human 2,4,6 (HSV-TK) and Welch's test (unpaired t-test, non-equal stdv) for the comparison of porcine to human batches.

The cell count reduction of porcine (-3.34 fold) and human (-2.75) HSV-TK expressing MSCs did not differ significantly and was therefore comparable. In both species, the reduction of HSV-TK expressing cells is significantly higher than their naïve counterpart (porcine: -0.74 and human: -0.6). The alterations by apoptosis are characterized by a reduction of the cell's size, a change of its surface profile and a loss of the cell's integrity. As shown in Figure 19, the death of cells corresponded with a small and spherical morphology and the loss of adherence to the plastic surface. To give a clear proof of an apoptotic pathway for porcine MSCs, the cells were analyzed through flow cytometry. For this, all batches were seeded, cultured and treated with GCV as described before (see 6.7.2). On day five, the supernatant and the cells were harvested, stained with Annexin-V and 7-AAD and measured by flow cytometry.

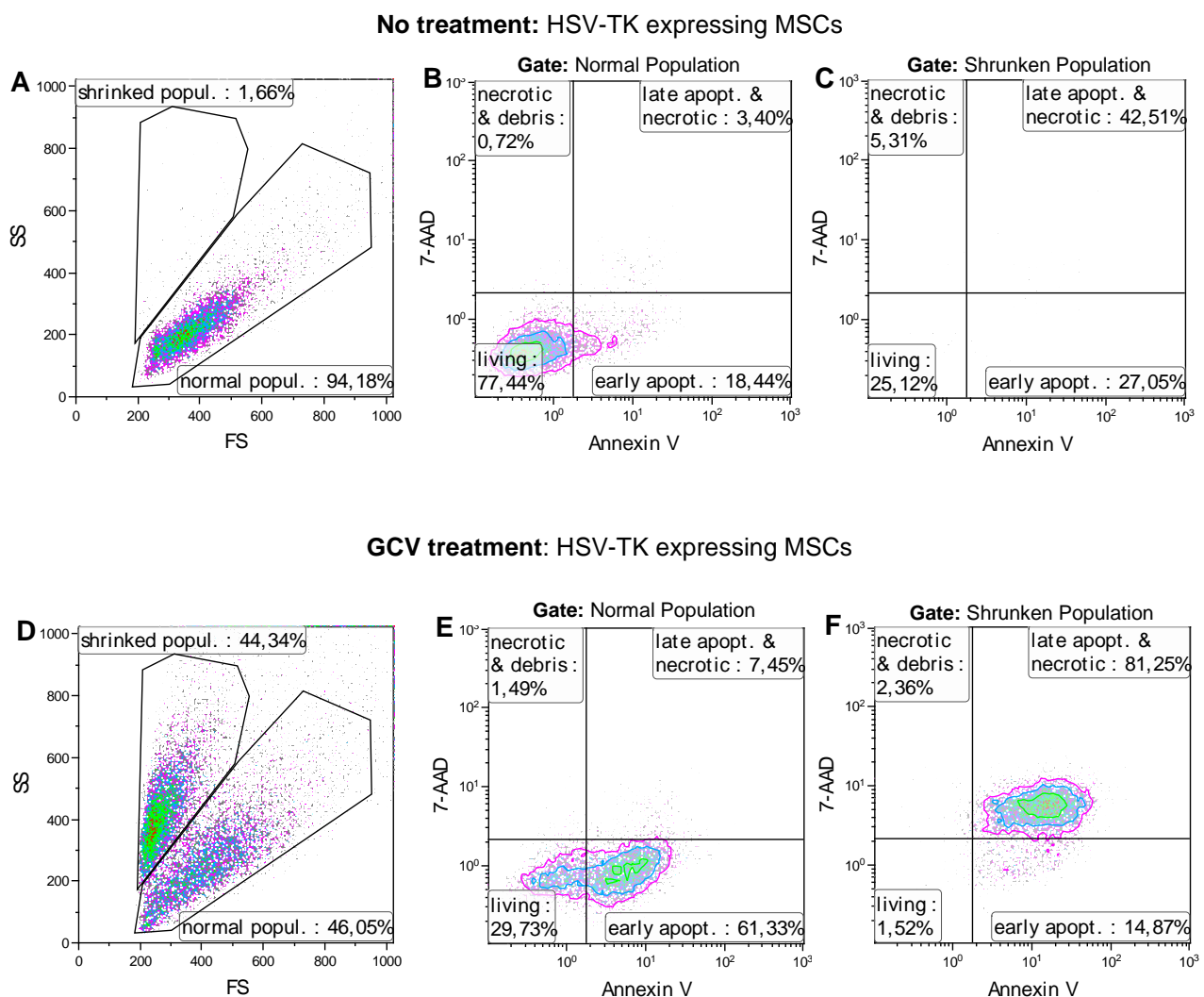


Figure 21: GCV-treated, HSV-TK expressing porcine MSCs in contrast to non-treated MSCs: Morphological changes correlated with different stages of apoptosis. (A) Non-treated MSCs were characterized by one population in the FS / SS plot. (B) If this population was stained for 7-AAD and Annexin-V, a slight drift to Annexin-V positive cells was observable. Very small amounts of cells were 7-AAD positive indicating dead cells. (C) Since no further populations were visible, the gating showed no cells. (D) Treatment of HSV-TK expressing cells generated a second, smaller but more granular population in the FS / SS plot. (E) Staining with 7-AAD and Annexin-V for cells gated on the “normal population” showed mainly Annexin-V positive cells and a smaller Annexin-V and 7-AAD negative population indicating living cells. 7-AAD cells were increased if compared to the amount of 7-AAD in (B). (F) Gating on the smaller and more granular population (here “shrunken population”) showed that nearly all cells were 7-AAD and Annexin-V positive. A smaller sub-population was Annexin-V positive only.

Figure 21 shows that morphological changes correlated with different stages of apoptosis. One population in the FS / SS plot, a small amount of Annexin-V positive and a very small amount of 7-AAD cells characterized non-treated MSCs. If these HSV-TK expressing cells

were treated with GCV after promoter induction, a significant change in the morphology could be seen. The cells started to become smaller and showed more granularity. These shrunken cells were positive for Annexin-V and 7-AAD, which is typical for late-apoptotic cells. In contrast to necrosis, a population with Annexin-V positive and 7-AAD negative cells indicated an apoptotic pathway.

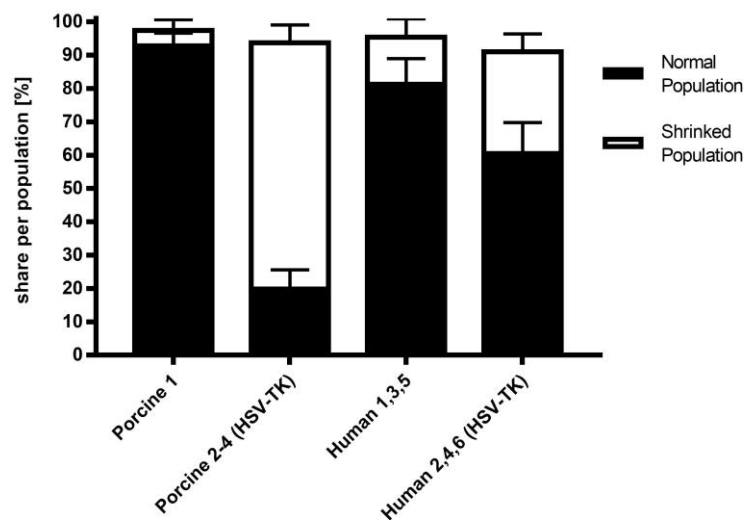


Figure 22: Porcine and human HSV-TK expressing MSCs became smaller and more granular if they were treated with pro-inflammatory cytokines and GCV. In this figure, the distributions of the cells in the FS / SS are summarized for all batches after treatment following the gating strategy of Figure 21. Naïve cells of both species primarily showed a normal morphology in the FS / SS with more than 80% in the “normal population” gate in spite of the treatment. HSV-TK expressing MSCs showed a change to more granular and smaller cells. Human HSV-TK MSCs showed about 30% of shrunken cells but porcine HSV-TK MSCs showed up to 70% of shrunken cells. Statistics: two-way ANOVA; following comparisons did not show a significant difference: Porcine 1 and Human 1,3,5 for normal and shrunken population ($p=0.34$ and $p=0.56$); Human 1,3,5 and Human 2,4,6 for shrunken population ($p=0.05$). All other comparisons did show a significant difference ($p<0.05$).

Figure 22 describes the drift in the morphology induced by GCV treatment for all batches. 93% of porcine and 82% of human naïve cells showed no change in morphology despite of the treatment. The amount of shrunken cells was 5% for porcine and 14% for human naïve cells. If the treated cells expressed HSV-TK, the percentage in the “shrunken population” gate increased: human MSCs showed 31%, porcine MSCs even 74% of shrunken cells.

Besides cell count reduction and morphological change, the surface profile changed during apoptosis. These observations were quantified for Annexin-V and for 7-AAD in Figure 23.

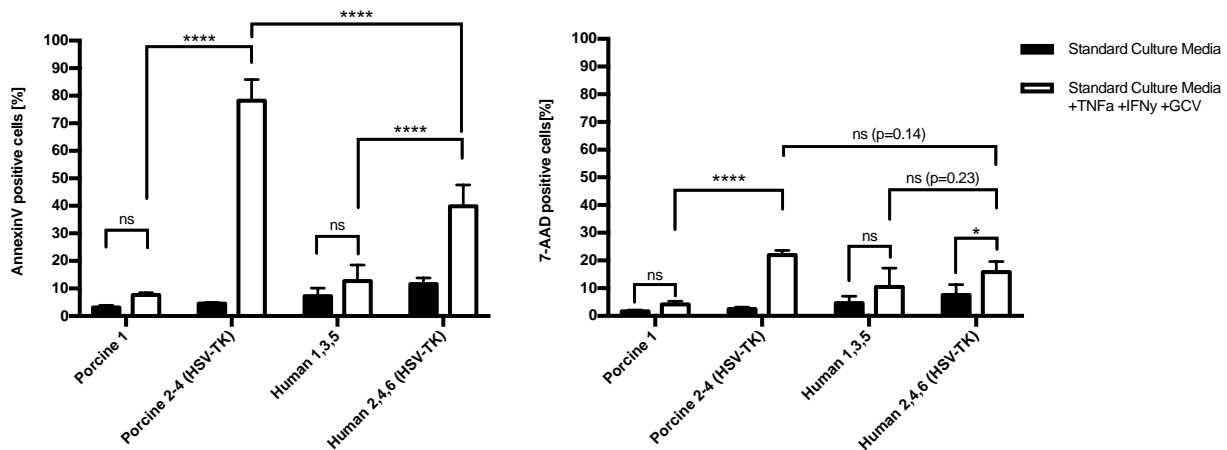


Figure 23: (A) Annexin-V stains phosphatidylserine as apoptotic marker and was significantly higher presented on HSV-TK expressing MSCs under treatment. All naïve and HSV-TK expressing batches were cultured with or without treatment on day three, four and five. On day five, the cells were detached and stained with Annexin-V. In contrast to naïve cells under treatment, the increase in Annexin-V for all HSV-TK expressing batches was significant. If naïve cells were treated, they showed a trend to be more Annexin-V positive although this was not statistically significant. (B) HSV-TK expressing cells showed also a statistically significant shift to 7-AAD. All batches were treated the same way as described in section 7.5. Here, only Annexin-V positive cells were gated for 7-AAD following the described gating strategy (see Figure 21). This increase was statistically significant only in porcine cells. Human MSCs expressing HSV-TK showed the tendency to be more 7-AAD positive, which cannot be confirmed statistically ($p=0.23$). Statistics: two-way ANOVA.

All batches were cultured in standard media and compared to cultivation in standard media with treatment (see Figure 23). There were no significant differences between treated or non-treated naïve cells in both species. If HSV-TK MSCs were treated, a significant up-regulation of phosphatidylserine could be detected. Non-treated HSV-TK MSCs served as control.

The amount of 7-AAD as well as Annexin-V positive cells increased under treatment. Porcine HSV-TK expressing MSCs differed significantly from the corresponding control of naïve cells showing more dead cells than under standard treatment. Human HSV-TK expressing MSCs did not show a significant increase ($p=0.23$).

7.5.2 Population doubling time correlated with the efficacy of HSV-TK induced cell death

It was examined whether the population doubling time correlated with the amount of killed cells or not. Therefore, the same protocol as described before (see 6.7.2) was used and the proliferation during the assay was calculated based on two cell counts: at the beginning and the end of the assay. The amount of killed cells was normalized to the amount of living cells in the corresponding control culture without any treatment. The normalization was necessary to facilitate a comparison because all batches had highly varying population doubling times. Figure 24 shows that a correlation between the proliferation speed and the amount of killed cells was probable ($R^2=0.92$).

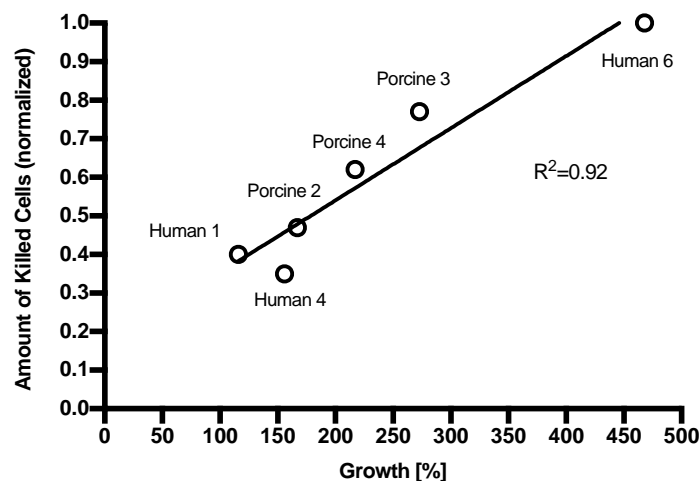


Figure 24: The growth speed of a population correlated with the reduction of cells due to GCV-initiated apoptosis. All HSV-TK expressing batches were counted before seeding and after cultivation in the standard medium (after harvest). This growth is described by percentage in the horizontal axis. All HSV-TK expressing batches were treated over five days. The amount of killed cells of each batch was normalized to the seeded cells cultivated in the standard medium. Irrespective of the species, the killing efficacy correlated with the growing speed of a population. Statistics: linear regression, $R^2=0.92$.

7.6 Proof of a Therapeutic Effect *in vitro* for Porcine MSCs

The most important aim of providing a valid model system is furnishing proof of a comparable potency. The therapeutic effect - the bystander killing with activated GCV - must initiate the apoptosis in MSCs as well as in the target tumor cells in both species.

7.6.1 Inter species killing: porcine and human HSV-TK MSCs killed human cell line (HT1080) and porcine cell line (K67)

The most critical parameter in this suicide gene system is the killing of the target cells. The intended bystander killing was realized *in vitro* by co-cultivation of HSV-TK MSCs and the target cell line following the protocol as described in 6.7.3. In short, cells were seeded equally and treated with pro-inflammatory cytokines and GCV. After detachment, the cells were counted in accordance to 6.2.4. All cells were stained with Annexin-V and 7-AAD and measured by flow cytometry. The GFP expression of the cell lines allowed discrimination between the cell lines and MSCs during flow cytometry.

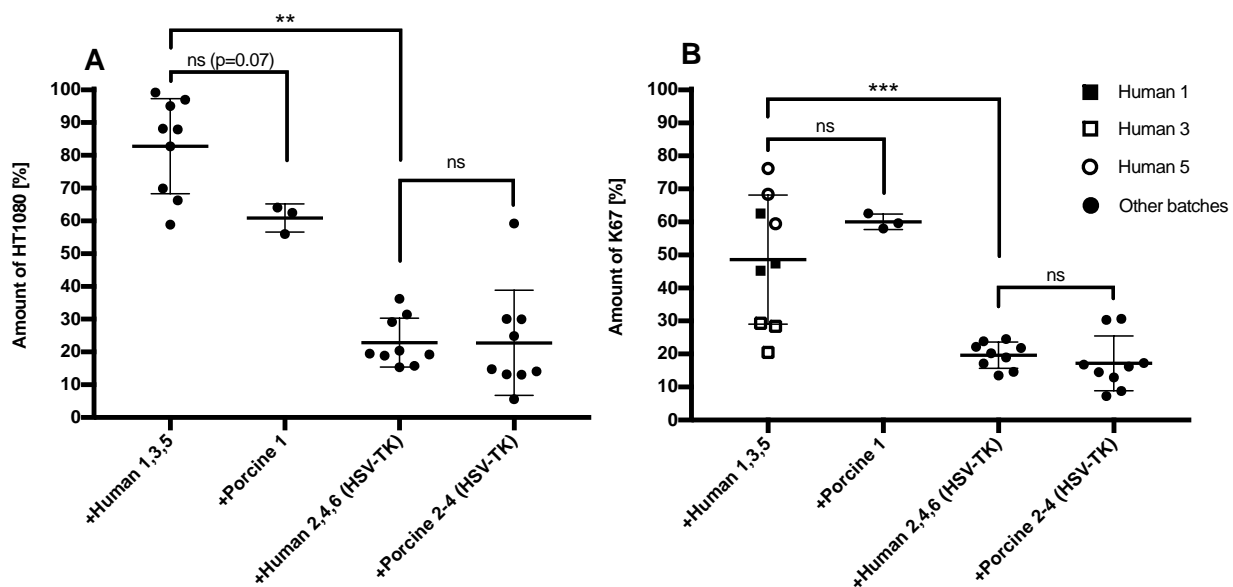


Figure 25: Porcine and human HSV-TK MSCs reduced the amount of the porcine and the human cell line during co-cultivation and treatment. (A) If HT1080 were co-cultivated with naïve cells, no significant shifts could be observed between porcine and human cells. But there were less HT1080 cells present in the population if cultivated with porcine cells. The killing of HT1080 cells by both species was comparable. (B) K67, the porcine cell line, was killed by both species with the same efficacy. In contrast to naïve porcine MSCs, the naïve human cells also showed anti-proliferating effects: the batch Human 5 and, partially, Human 1 showed an inhibition of the proliferation since less than 50% K67 cells were left after treatment although no HSV-TK expressing cells were present. This effect was species-specific as no similar observations could be made if co-cultivated with naïve porcine MSCs. Statistics: ordinary one-way ANOVA for each graph, referring to first column in graph A and to second column in graph B.

HSV-TK expressing MSCs of both species killed the human HT1080 and the porcine cell line K67 in a comparable manner (see Figure 25). Human and porcine naïve cells did not show a significant difference in the amount of HT1080 cells during co-cultivation. Batches that expressed HSV-TK killed significantly more cells than their naïve counterparts. Here, both species showed the same mean of 22% remaining cells of the cell line HT1080.

The amount of K67 cells was highly varying if co-cultured with naïve human cells. Measured values ranged from 21% to 76%. In presence of porcine naïve cells, the percentage of K67 was 59%. This effect was annihilated if HSV-TK expressing MSCs were present. Then, the percentage share of K67 was reduced to less than 20% for both species. Here, porcine HSV-TK MSCs were able to kill the human and porcine cell line HT1080 and K67 in a comparable manner during co-cultivation.

7.6.2 Both species induced the apoptotic cascade in co-cultivated cell lines

The Killing of cells is the main goal of a suicide gene system. If the cytostatic agent induced cell death in the neighboring cells, an apoptotic pathway should be traceable. Therefore, the cells' apoptotic reaction as described in 7.5.1 was examined.

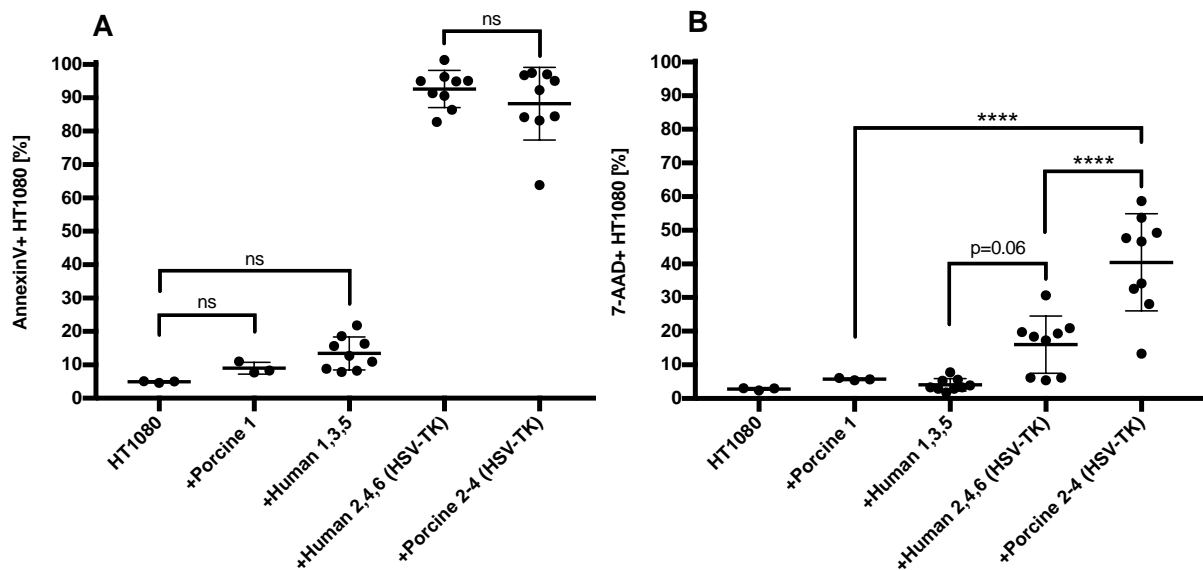


Figure 26: MSCs of both species induced the apoptotic cascade in HT1080 as shown by a simultaneous increase of Annexin-V and 7-AAD. (A) Naïve porcine or human MSCs did not induce any significant increase of Annexin-V or 7-AAD in HT1080 cells. HT1080 cells in mono-cultivation served as control. HSV-TK expressing human and porcine MSCs raised the mean percentage of Annexin-V positive HT1080 to 93% respectively 88%. (B) Also, the amount of 7-AAD positive cells increased in the presence of HSV-TK expressing MSCs. Human HSV-TK expressing MSCs did not induce a statistically significant increase ($p=0.06$). Porcine HSV-TK expressing MSCs caused an accumulation of 7-AAD positive cells of 40%. Statistics: two-way ANOVA.

Following the five day protocol as described before (see 6.7.3), all batches were co-cultivated with each cell line.

The presence of HSV-TK MSCs of both species caused a high increase of Annexin-V positive cells in contrast to naïve cells (see Figure 26). If naïve cells were co-cultivated, less than 15% of all HT1080 cells were positive for Annexin-V. The bystander effect induced more than 85% of all cells to be positive for Annexin-V. The same observations were also true for 7-AAD. Although the human batches 2, 4 and 6 did not increase the amount of 7-AAD positive cells significantly ($p=0.06$), the porcine batches 2-4 were able to raise 7-AAD

positive HT1080 to 40%. This was significant in contrast to porcine naïve cells. HT1080 showed an apoptotic character if treated while HSV-TK expressing MSCs were present.

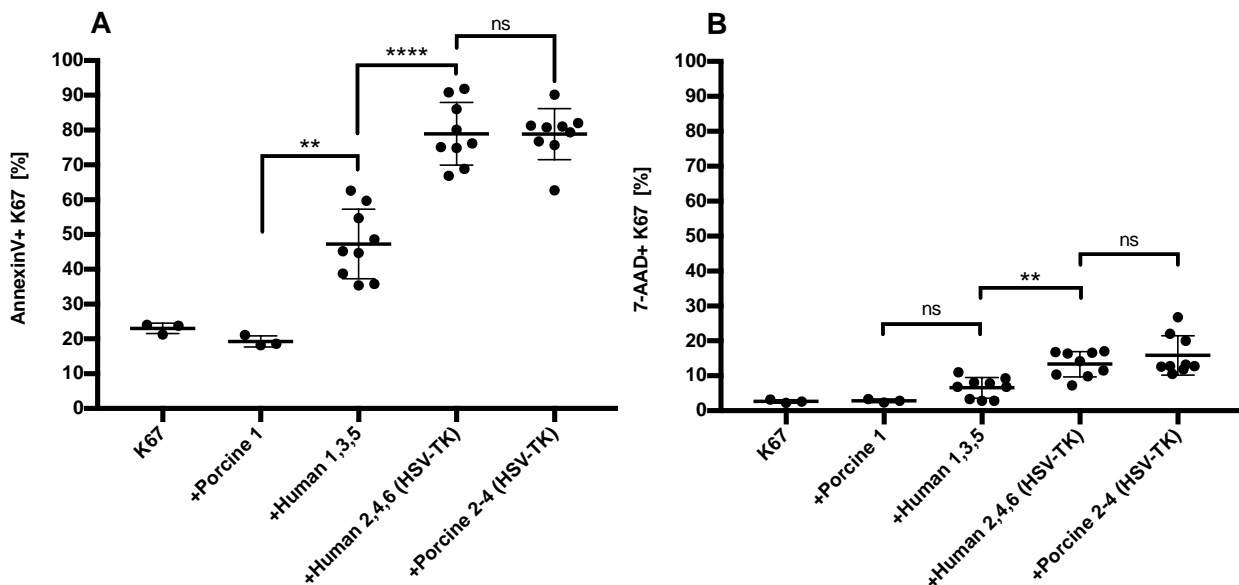


Figure 27: As well as HT1080, K67 cells were killed by in an apoptotic mode of action by both species. (A) Annexin-V was significantly increased for HSV-TK expressing, porcine and human MSCs. But also naïve human MSCs showed an increase of Annexin-V positive K67 cells in contrast to naïve porcine MSCs. This effect differed significantly from HSV-TK expressing human MSCs. (B) 7-AAD was increased, too, although it was overall lower than observed for HT1080. Statistics: two-way ANOVA.

In the case of K67 (see Figure 27), the results differed from those with HT1080 co-cultivation (see Figure 26). Basically, the target cell line in mono-cultivation or co-cultured with porcine naïve cells showed about 20% of Annexin-V positive K67 if GCV was added. Human naïve cells raised this percentage share significantly to 47%. If the treatment was done while HSV-TK expressing cells were present, the Annexin-V positive percentage share was additionally increased to 79% for both species.

These results could not be observed for 7-AAD on a statistical basis. Here, human naïve cells did not induce a significant increase from mono-cultivation K67 (3% 7-AAD positive) to K67 co-cultivated with human naïve cells (7% 7-AAD positive). A relevant increase could be observed if HSV-TK expressing MSCs were present: the human batches 2, 4 and 6 showed 13% and the porcine batches 2-4 16% of 7-AAD positive cells. As well as HT1080, the porcine cell line K67 showed the same mode of action following the apoptotic cascade.

7.7 Experimental *in vivo* Studies: Biodistribution of intravenously infused MSCs in the Mini-Pig

The systematic *in vitro* comparison of porcine and human MSCs was used to allow an *in vivo* approach to assess the biodistribution of the cells in the mini-pig. After administration of a determined amount of cells, blood and tissue samples were collected. The DNA of peripheral MNCs were isolated and analyzed by real-time PCR. Furthermore, an immunohistochemically analysis of representative tissues should be done.

7.7.1 Freshly thawed MSCs were stable for 90 min in the cryopreservation medium

All used batches for the *in vivo* studies were cryopreserved after having been produced successfully as described before (see Figure 2). Before the cells were administered, they had to be thawed, counted, formulated and filled into the syringe under aseptic conditions. Afterwards, the cells were transported to the pigs and infused. This preparation needed time and the thawed cells were exposed to the DMSO-containing cryopreservation medium at ambient temperature. Due to the DMSO in the medium and the lack of nutrition and plastic adherence, the cells became impaired over time. The procedure described here is also relevant for a setting in clinical trials with human cell-based products.

To assure that most of the administered cells were functional, a kinetic considering possible impairment was performed. For this, one vial of each batch was thawed, counted and left in the accordant cryopreservation medium at ambient temperature (see Table 3). Every 30 min, a defined amount of cells was sampled and seeded with an equal confluence of $20\pm 10\%$. The latest seed-out was performed 180 min after thawing. After four days, all batches were harvested and counted (see Figure 28). This approach was chosen to simulate the protocol of thawing and preparing the MSCs for infusion at the study site.

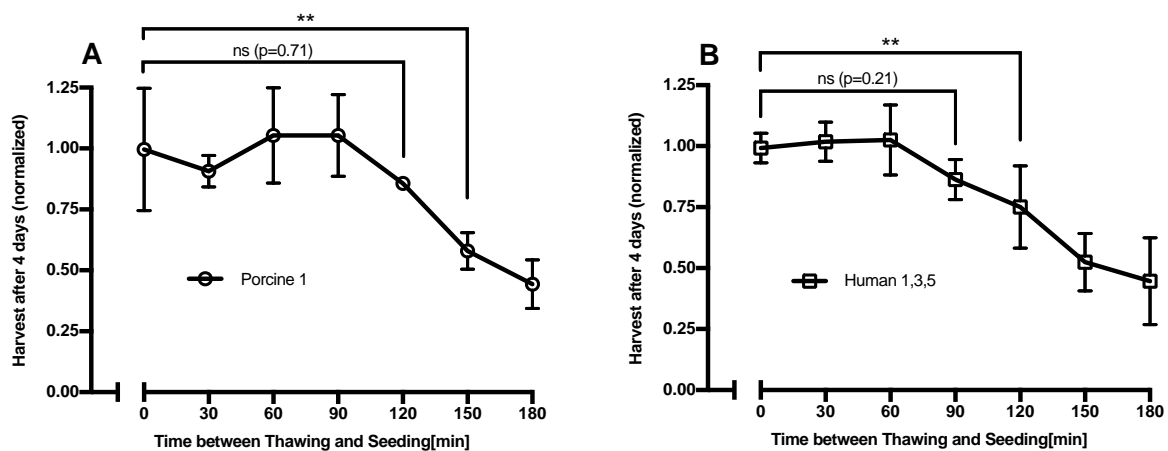


Figure 28: Porcine MSCs (A) and Human MSCs (B) showed no significant reduction in proliferation if they stayed in the cryopreservation medium for 120 min (A) or respectively 90 min (B) after thawing. On day one, one vial of each batch was thawed and left for 180 min in the cryopreservation medium. A defined amount of cells was sowed out in triplicates every 30 min. After four days, all wells were harvested and counted. (A) Porcine MSCs showed a significantly reduced amount of cells, if the cells were left for 150 min. Human MSCs already showed a significant difference after 120 min in contrast to the same amount of cells, which were sowed out immediately after thawing. Statistics: one-way ANOVA (all data were compared to point in time 0 min).

Porcine MSCs did not show any impairment if they were left in the medium for 90 min. After 120 min, a slight trend could be observed although it was not statistically significant ($p=0.71$). After 150 min the harvest differed from the harvest at 0 min which indicated impairment. The harvest at 180 min confirmed the previous result. Human MSCs seemed to be more sensitive to the lack of nutrition, adherence and the exposure to DMSO. After 90 min, the cell yield became lower ($p=0.21$) and differed significantly after 120 min. Following harvests confirmed this impairment with even lower yields.

During the *in vivo* studies, all infusions were performed in less than 90 min (animal #1: 62 min and animal #2: 51 min).

7.7.2 Intravenously infused MSCs were detectable in the peripheral blood stream

The aim of the *in vivo* studies was to perform a protocol in accordance to ethical and scientific demands. Therefore, the protocol was designed in close collaboration with the responsible veterinarian. Due to the limited stability of the cells (see Figure 28), the narcotization and surgery of the animal were performed simultaneously with the preparation of the cells.

Table 17: This table shows all relevant facts about the pigs and the cells used for the biodistribution study. Two clinically healthy mini-pigs were chosen for the study. Two intravenous catheters were implanted into each pig to separately inject the cells into the jugularis vein and aspirate blood samples from the ear vein (see Figure 29). After positive results were generated in the first animal (see Figure 30), the amount of blood samples was increased and the second animal's life-time was expanded to five days. After three, respectively five days, the pigs were euthanized and necropsied at the *Institut für Tierpathologie der Ludwig-Maximilians-Universität München*.

Animal	Gender	Weight [kg]	Infused Cells	Quality check	Amount of cells Injected [$\times 10^6$]	Dosage: MSCs /kg Bodyweight [$\times 10^6$ / kg]	Day of necropsy after Cell Infusion [d]
#1	male	82	HSV-TK expressing, isogenetic, porcine MSCs	fulfilling ISCT criteria (see 7.2)	422	5,1	3
#2		58			343	5,9	5

All cells were infused in less than 90 min after thawing. The infusion lasted one to three min and the catheter was washed with PBS to reduce cell residues in the tube. All details are listed in Table 17.

Immediately after the completion of the infusion, the first blood sample was taken followed by sequential aspirations in the first hour. The next aspiration was performed 6 h after the infusion.



Figure 29: (A) Blood samples were aspirated through a peripheral venous catheter, which was implanted into an ear vein (see arrow). (B) The cells were infused into the jugularis vein by a catheter that was fixed at the nape to reduce possible damage by the pigs' movement after waking up. (C) A sleep-inducing drug was injected to allow the correct placement of the intravenous access and to reduce the stress for the animal. The sleeping agent's activity lasted for about two to four hours until the pigs woke up again. This immobilization allowed for a simplified blood sampling during the first hour of infusion. From day two on, the blood sample counts were deliberately low. Otherwise, the stress for the animals would have been too high. On day three, respectively five, the animals were euthanized in the *Institut für Tierpathologie der Ludwig-Maximilians-Universität München* and pathologically examined.

The blood was directly aspirated into vacutainers, stored at room temperature and brought back to the laboratory on the same day. The isolation of DNA was performed in accordance to the isolation protocol of blood samples, in short: lysis of thrombo- and erythrocytes with a hypotonic buffer, centrifugation of mononuclear cells and the start of DNA isolation with accordant solutions (following protocols 6.8). The eluted DNA was solved in TRIS-buffered water. Samples of these DNA-containing solutions were amplified by real-time PCR.

The resulting CT-value was regressed to a defined amount of DNA copies (considering a standard curve). This number of copies correlated with an extrapolated value of MSCs per mL blood. This extrapolation considered the following aspects: blood sample size, real-time PCR sample size and DNA loss due to the isolation and washing procedure. Also, the real-time PCR method had a specified sensitivity resulting in a defined detection limit of approximately 5-10 copies. The amounts of cells identified in the blood of both pigs are described in Figure 30 and Figure 31.

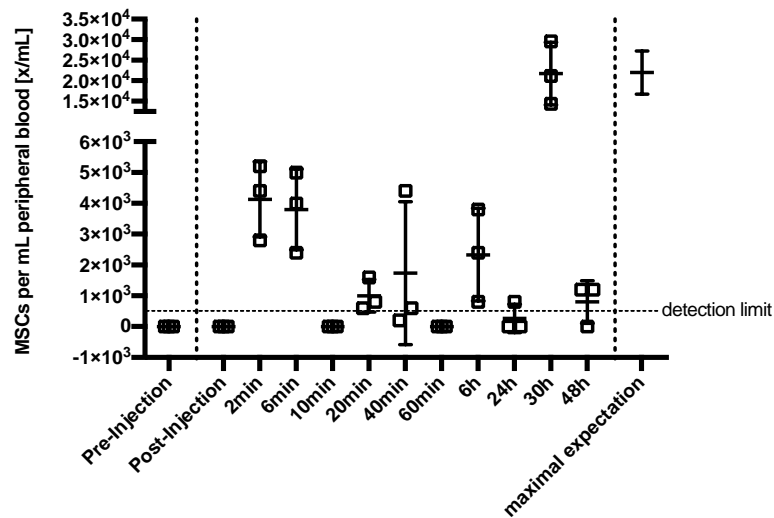


Figure 30; Pig 1: Intravenously administered cells could be detected in the peripheral blood stream by accurate isolation and quantification through real-time PCR. Pig 1 received a dosage of 5.1×10^6 MSCs / kg bodyweight. Blood samples were aspirated at different points in time before and after injection. The detection limit of the method was 450 MSCs per mL due to the preparation of the sample for measurement. Assuming an even distribution of all cells in the blood stream, the maximal expectation would be about 22,000 MSCs per mL blood (supposing 6% blood volume / bodyweight). MSCs could be identified at 2 min and 6 min after infusion. In the following minutes to hours, infrequent signals could be detected. In the end, a strong signal could be identified after 30 h. Statistics: none, descriptive only; three analysis (each consisting of five measurement) are depicted.

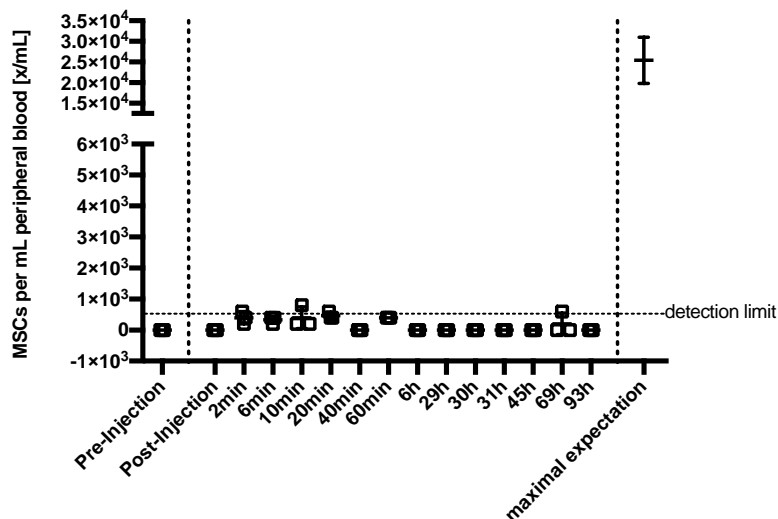


Figure 31, Pig 2: In contrast to pig 1, no significant consistent signals could be detected in the peripheral blood. Pig 2 received a dosage of 5.9×10^6 MSCs / bodyweight. Although the dosage was increased, only signals next or under the detection limit were identified. At no point in time the measured signals were higher than the detection limit. Statistics: none, descriptive only; three analysis (each consisting of five measurement) are depicted.

Immediately before and after infusion, no signals were detected in pig 1. After 2 min, MSCs could be identified. This signal was confirmed at 6 min, 20 min and 6 h, although there were less MSCs present in the sample. 30 h after infusion, a single strong signal could be identified which was not confirmed at 48 h.

In contrast to these results, no consistent signals above the detection limit could be detected in pig 2 although the dosage per kg bodyweight for this pig was increased. As a consequence of the results from pig 1, it was possible to manage more blood sample points in collaboration with the veterinarian at around 30 h: at 29 h and at 31 h. Also the life-time of the animal was expanded from three days to five days to see if the MSC presence from pig 1 at 30 h would occur to a later point in time in pig 2. No signals could be detected on day 3, 4 or 5.

7.7.3 Pathological report showed pneumonia in pig 2

On day three, respectively day five, the animals were narcotized in the stable and brought to the *Institut für Tierpathologie der Ludwig-Maximilians-Universität München*. In the institute of veterinarian pathology, the last blood sample was taken before the pigs were put down to sleep. The weight of the pigs was measured and the dissection was performed.

Table 18: At the end of the life-time, both animals were necropsied for histo-pathological examination.

The main anatomical and histological findings and the final pathological expertise are described in the table. Pig 1 showed a pericarditis and pig 2 showed a high-grade pneumonia and a chronic gastritis. During the study, no clinical observations by the responsible veterinarian (member of the *Institut für Molekulare Tierzucht und Biotechnologie der Ludwig-Maximilians-Universität München*) were noticeable. The pathological and histological assessment was performed by members of the *Institut für Tierpathologie der Ludwig-Maximilians-Universität München*.

Mini-Pig	Clinical Observation	Anatomical / Pathological Observations	Histological Findings	Final Pathological Expertise
#1	No clinical observations	-well-fed -calcification of the aorta -Pericarditis	- heart: Pericarditis - lung: weak binding of the bronchus-associated lymphoid tissue (BALT); light lympho-cellular infiltration -spleen: multi-focal proof of eosinophilic granulocytes -lymph nodes: slight hyperplasia -liver: no findings	-Fibrotic Epi- and Pericarditis

Mini-Pig	Clinical Observation	Anatomical / Pathological Observations	Histological Findings	Final Pathological Expertise
#2	No clinical observations	-well-fed	-lung: moderate, interstitial pneumonia with high-grade activation of BALT -stomach: high-grade, chronic follicular gastritis -lymph nodes: moderate hyperplasia -liver: slight lympho-cellular infiltrations -kidneys: slight lympho-cellular infiltrations	-Interstitial Pneumonia -Chronic Gastritis

Besides the observations during the dissection, tissue samples were fixed in formalin and embedded in paraffin. A pathologist analyzed these sections. A confirmed pericarditis was identified in pig 1 as well as slight inflammatory findings regarding lymph nodes, spleen and lung. Pig 2 showed an interstitial pneumonia and also a chronic gastritis. This inflammatory process is also reflected in the hyperplasia of the lymph nodes.

7.7.4 Immunohistochemically analysis showed MSCs in lung and spleen

The generated tissue samples of lung, liver and spleen were analyzed by immunohistochemically staining. The workup and the staining of the tissues are described in 6.9.2. In short, the FFPE tissue blocks were sliced into several sections, deparaffinized, stained with an Anti-HA antibody or an appropriate isotype control and fixed before microscopy. The sections were visually analyzed and the brownish-red stained cells (HA-tag positive) MSCs were counted.

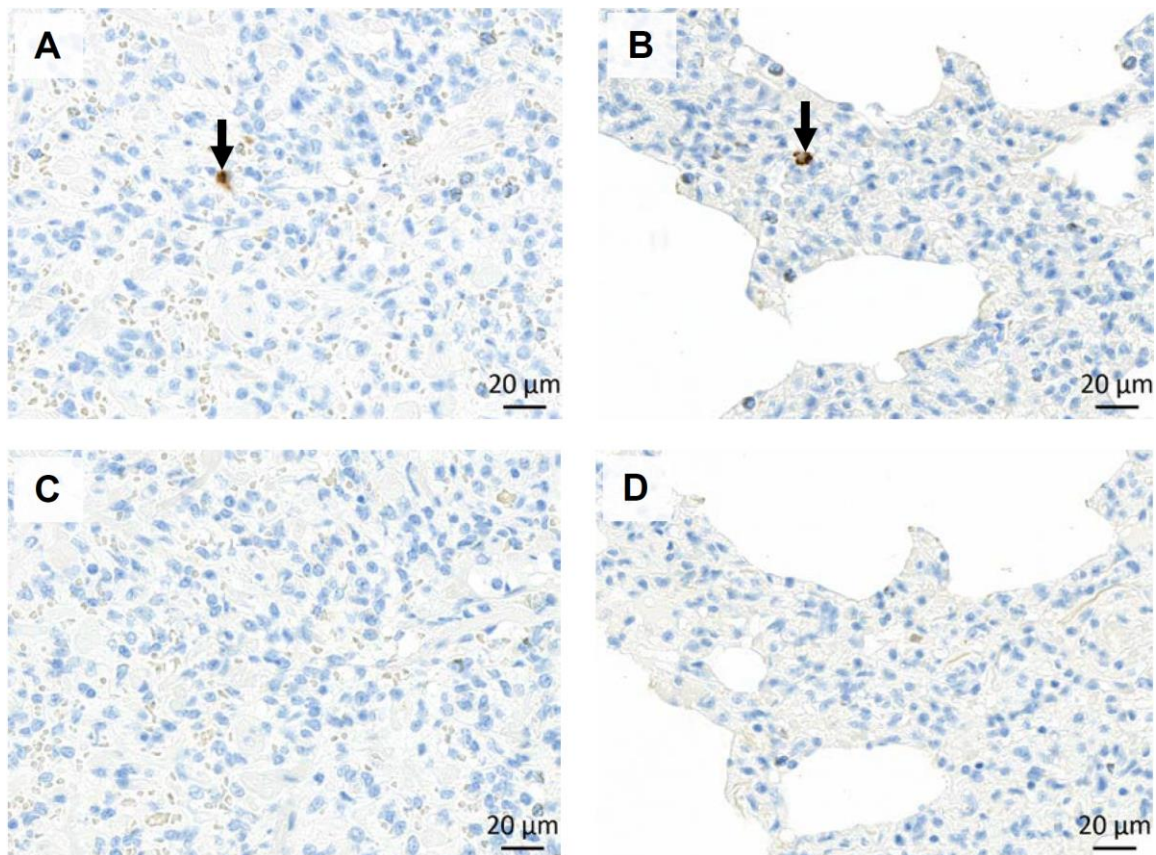


Figure 32: Anti HA-tag immunohistochemistry detected HSV-TK expressing MSCs in spleen (A; animal 1) and lung (B, animal 2); identifiable by a brownish colour (see arrow). Lung, spleen and liver of both animals were sent into an external laboratory for immunohistochemical examination. Several histo-pathological sections were analyzed to detect any MSCs in the tissues in question (see Table 19). In addition, three tissue samples of a mini-pig that received no MSCs were sent as control, too. As a second negative control, all stainings were compared to an appropriate antibody isotype (C, D).

The recognition of MSCs was simple due to the brownish-red colour. Appropriate isotype control from directly neighboured slices showed no MSCs as well as no artefact staining proven by MSC-free tissue sections.

Table 19: The immunohistochemical analysis of lung, spleen and liver showed MSCs in both animals.

Several sections were analyzed before MSC-positive slices were identified. The number of sections represents the count which was positive for MSCs. Pig 1 showed MSCs in lung and spleen. Pig 2 showed MSCs in the lung only.

Animal	Lung		Spleen		Liver	
	MSCs in total	Number of Sections	MSCs in total	Number of Sections	MSCs in total	Number of Sections
Pig 1	4	2	1	1	0	1
Pig 2	4	2	0	1	0	2
Pig 3 (Control, no MSCs infused)	0	1	0	1	0	1

In Table 19, the number of MSCs identified by histological staining is shown. The amount of MSCs in the tissue was relatively small because in two sections of pig 1 four HA-tag positive cells could be identified. In two sections of pig 2, four MSCs were identified. Additionally in pig 1, one MSC was identified in the spleen. In all other sections, no MSCs could be found. Figure 32 shows the detection of MSCs in the tissue. The appropriate isotype control of the directly neighboured slice is shown, too.

8 Discussion

8.1 The Identity of Humans' and Pigs' MSCs – Comparing Apples and Oranges?

The current ISCT approach is not sufficient to determine a defined MSC sub-population with the same properties in one population [33]. Secondly, the differences between the tissues from which MSCs are isolated and varying cultivation protocols complicate the comparability of MSCs generated in different laboratories, or companies [283]. Adding a new species to this field – the pig – further increases complexity. Nevertheless, the need for large animal models is high since pharmacokinetic and pharmacodynamic questions have to be answered to satisfy regulatory [204, 230, 275] and scientific demands [211-213, 220]. For that reason, the general approach of this work was to generate as few differences as possible between both species while setting up the methods and assays for the isolation, the manufacturing of the MSC batches and the evaluation of their therapeutic efficacy *in vitro* (see Figure 2). This was supposed to have the best comparability testing of both species regarding the cell therapy product.

The isolation procedure from the marrow only differed regarding the method of withdrawal and the aspirated volume. The *iliac crest* of the human donors was punctuated while the pigs' *femur* and *tibia* were scraped out directly after narcotization. The marrow volume procured from each human donor was not larger than 100 mL. The pig's marrow volume was not determined as the whole bone marrow was scraped out. Obviously, a higher volume of marrow increases the probability of more progenitor cells being cultivated, in turn leading to a higher cell count. Since the volumes of cultivated marrow were different, a comparison at this point could not yet be made. Although the amount of marrow was not the focus of this work, this objective can be critical for the cell count of a finalized cell drug product as marrow aspiration is still a challenge [284, 285].

Both marrows were cultivated in 2D culture flasks with serum containing media. The media differed because the patented Bio-1 (containing human plasma and platelet lysate) was used for human MSCs, while for porcine MSCs on the other hand, a medium containing fetal bovine serum was used. Even though both isolations were conducted from bone

marrow and cultivated in the same manner, the different sera (platelet lysate / FCS) might have a possible impact [286, 287]. As described before, the immunological properties and proliferation speed of MSCs are highly affected by present cytokines [31, 40]. That is why the population-doubling time was hardly comparable due to the fact that the MSCs were cultured in different media (see Figure 11). Also the fact that the marrow of the pigs was taken after they were narcotized may have an influence on the cell quality since the cessation of oxygen supply may have a negative impact. Thus, well-founded statements about the comparability of the population-doubling speed can't be made easily. Nevertheless, it was possible to observe that batches of the same donor had a comparable population-doubling time while the doubling times of batches procured from different donors seemed to vary Figure 11. Whether this was caused by different used Bio-1 media batches, different properties of the donated cells or the quality of the aspirated marrow can't be determined. As different Bio-1 batches were used at different stages of the cultivation process for all donor cells, it is likely that this effect is a result of the donors' cell biology or the marrow quality. Moreover, the aspiration technique of the physician can also lead to significant variations in the amount of progenitor cells available for seed-out [288].

The microscopy observations (as shown in Figure 3, Figure 4 and Figure 5) confirmed the expectations of adherent, fibroblast-like cells as MSCs [5]. This could be shown for both species without significant differences in a subjective visual evaluation. However, the batches Human 3 and 4 that were derived from one donor showed a more flattened morphology. This conspicuous size and altered form correlated with a low population-doubling time (see Figure 11) – an observation already described in other publications regarding senescence and ageing [289, 290]. Following this correlation, proliferating cells are easily recognized as small, more granular cells, as shown in Figure 14 B.

Currently, isolating MSC by adherence is the standard procedure because no sole marker has been identified yet [31-33], which could be used for cell sorting. The insufficient set of surface markers and the ability of the MSCs to show adipogenic or osteogenic properties, which are also common in other cell types, weaken the importance of the ISCT approach (see chapters 1.1 and 1.2 for a more detailed explanation). Nevertheless, the ISCT demands currently are the best practice to identify MSCs in donor tissue. That is why the identification of the porcine adherent cells as MSCs was done in the same manner as it is described for human MSCs. The same set of antibodies carrying defined fluorophores was used for the identification of MSC markers on porcine and human MSCs (see Figure 6).

Due to commercial limitations, the choice of antibodies available for staining porcine MSCs was relatively small. Anyways, it was possible to obtain relevant antibodies for the determination of CD45, CD105 or CD90. Since CD45 is a pan-leukocyte marker, no hematopoietic markers were expected in the adherent culture. This could be confirmed for both species. Small percentages of positive cells could be observed as a byproduct of the flow cytometry method. The presence of non-adherent cells (e.g. monocytes that are CD45+) was highly improbable after several trypsin detachments and medium changes. It can be concluded that no other cells than MSCs were cultivated for both species.

Although the whole population of porcine cells was positive for the described marker, a sub-population did not show CD105. This phenomenon has already been described for murine MSCs [263], but, to my best knowledge, not for porcine MSCs (no publications were found). Murine, CD105 negative MSCs show functional changes regarding their immunoregulatory properties [263]. Immunological properties were not in the focus of this work, so further investigation could correlate this partially absent marker on porcine MSCs with immunoregulatory changes. However, this drift in the surface profile also confirms the heterogeneity of porcine MSCs *ex vivo*. Comparing the extent of this phenomenon with murine MSCs, porcine MSCs (8% negative for CD105, see Figure 7) seem to be more similar to humans, since this drift is stronger in murine MSCs (30-40% negative for CD105, [263]). The lack of CD105 could potentially indicate other cell functions that were not in the focus of this work. It could also be argued, that this was only caused by the *ex vivo* cultivation and is not inherent in *in vivo* porcine MSCs in the light of the fact that *ex vivo* cultivation can highly affect MSC populations [32, 35].

Others of the expressed markers tested for MSCs are described in the relevant publications (porcine MSCs: CD29, CD44: [231, 233, 251] and human MSCs: CD73, CD235a [3, 5, 46]). Other available markers were tested to assure the absence of those on MSCs. They were provided in Table 14 for information only. Although these confirmed the established surface profile, CD61 was also found on human MSCs. This is a typical thrombocytes marker in combination with CD41. But, CD41 could not be shown on MSCs. In addition, thrombocytes are quite small with 2–3 μm and would be apparent in the FS/SS during flow cytometry as an extra population. This could not be confirmed. In addition, microscopy showed no further cells (see Figure 4 and Figure 5), eliminating the possibility of any thrombocytes being present.

HLA-DR (MHC-II complex) is expressed in antigen-presenting cells like macrophages, dendritic cells or B-lymphocytes. MSCs are described to be HLA-DR negative [5]. Pro-inflammatory cytokines like IFN- γ on the other hand may induce a HLA-DR presentation (see Figure 8 and [64]. This can also be initiated by a high cell density (see 1.3 and [63]). Although confluence of more than 80% was mitigated during the assay run, it cannot be excluded that this parameter potentially had an influence on the results due to partial confluence. On porcine MSCs, no HLA-DR could be identified, whether stimulated with IFN- γ or not. As a positive control, porcine blood was stained successfully with the anti HLA-DR antibody proving its functionality (data not shown). Interestingly, in contrast to murine [63] or canine MSCs [62], the absence of MHC-II complexes seems to apply for porcine MSCs. HLA-DR presence on human MSCs showed high variances (see Figure 8). As potential reasons for this, it is very likely that the donor variety and confluence could have impacted the outcome. The total absence of HLA-DR on porcine MSCs is interesting and a significant difference between human and porcine MSCs.

The differentiation of porcine and human MSCs into adipogenic and osteogenic cells could be proven (Figure 9 and Figure 10). A numeral comparison based on visual sections was performed (see Table 15). Interestingly, a differentiation medium that was formulated for human MSCs also showed a successful differentiation in porcine cells. In contrast, commercial companies often offer extra murine differentiation media. It was not further investigated during the course of this work if murine media are able to induce any differentiation in porcine MSCs. Despite the same strength of differentiation into the osteogenic lineage for both species (see Figure 10), adipogenic cells were quite different (see Figure 9). Comparisons are hard to make, for the reason that the medium was not designed for porcine MSCs – otherwise, another medium would not allow any comparisons to human MSCs. The fact that porcine MSCs also showed an adipogenic differentiation potential caused by the human-conditioned medium was a good proof of comparability at this point. An improvement of the differentiation potential due to better differentiation media would surely result in more adipogenic cells but not enhance the understanding of the comparability. In the end, the ISCT criterion for adipogenic differentiation potential was fulfilled – by a medium that was designed for human MSCs.

The fundamental comparability regarding identity is difficult. The inherent heterogeneity [33] of human MSCs does not define a clear, singular identification. This lack of knowledge affects the identification of porcine MSCs, too. The insufficient description of human MSCs

renders an assessment of the porcine MSCs and their comparability more difficult. Albeit, the origin of the cells (bone marrow), the isolation procedure by adherence and the fulfilled ISCT criteria are strong arguments to define the porcine cells as MSCs. The absence of HLA-DR in accordance to the ISCT can also be confirmed for porcine MSCs. Recent publications underlined the inducibility and presence of HLA-DR on human MSCs [63], which could not be shown for porcine MSCs. As described before, this was already established for canine MSCs [62]. The sub-population of CD105 negative cells is also part of the discussion regarding the surface profile of porcine MSCs. Since the description of markers on porcine MSC is sparse [234, 291, 292], it is unclear whether other groups will confirm these findings or show diverging results. In spite of these controversies considering HLA-DR and CD105, porcine MSCs comply with all other characteristics of human MSCs.

8.2 Controllability of Gene-Modification Realizable in Porcine MSCs comparable to Human MSCs

The controllability of gene modification is highly important for the safety of a gene-modified cell therapy product. Insertional mutagenesis may induce a clonogenic proliferation that can lead to cancer [293, 294]. Therefore, the safety of gene-modification is generally based on two major factors: the choice of the inserting viral particle and the insertion rate per cell. Here, a SIN-gamma retroviral vector introduced a suicide gene into the human cell therapy product.

In contrast to murine MSCs, the same type of retroviral vector could be used for human and porcine MSCs because the used GALV (gibbon ape leukemia virus) can infect human, simian but also porcine and other mammalian cells [295]. Murine MSCs normally are resistant to GALV-carried infections [296]. If the infection of murine cells had been in the focus of this work, the production of another viral supernatant would have been necessary (e.g. MLV envelope (murine leukemia virus) [297]). From a regulatory point of view, a critical raw material would have been changed potentially altering the product properties. Here, comparison studies would be necessary to give proof of the comparability. From a scientific point of view, the determination of the viral supernatant titer would be different. Both would have complicated any meaningful comparisons.

For these reasons, using porcine MSCs instead of murine MSCs can be advantageous, because it opens the possibility of employing the same retroviral vector, thereby reducing the differences to the human cell therapy product. Considering GMP production, this is clearly a very strong argument from an economical, scientific and regulatory perspective for all preclinical and following clinical studies. The development of only one gene delivery system saves costs as well as being no potential cause for differences in the scientific results in the preclinical phase *in vitro* and *in vivo*. Finally, the transfer of preclinical results onto clinical study design is easier.

In this work, porcine MSCs were transduced with the same virus particle / cell ratio as human MSCs. The successful transduction was proven and quantified by flow cytometry and real-time PCR. The transduction rate determination by flow cytometry took the whole population into account. The resulting single values cannot be compared on a statistical basis (see Table 16) but they represent strong values due to their methodological approach

on a single-cell-based analysis evaluating a whole cell population. The porcine batch 2 was transduced in the same manner as the human batches 2,4 and 6 showing transduction rates in the range of 3 to 11%. This is consistent with the real-time PCR measurements. Here, the values did not show any significant differences between the species after transduction for this method – still, slight drifts with p values <0.2 suggest that there could be differences (see Figure 13 and Table 13).

The transduction process itself is influenced by many variables. Although the same batch of vector supernatant was used, all cell transductions were performed on different days after isolation from the tissue due to the expansion procedure. The thawing of the supernatant, cell counting and cell preparation, timing, the mixing of the supernatant with the cells and the seeding are many work steps that had impact on the transduction efficiency. In addition, a SIN-gamma retroviral vector only infects dividing cells. The fact that the cell division rate, respectively population-doubling time in all batches highly varied (see Figure 11) led to additional variances. Confirming these reservations, the mean insertion rate and the transduction efficacy were highest for batch Human 4, although the population-doubling time was the slowest during the whole production. It stands to reason that the whole transduction approach is more important than the single aspect of a cell division rate. Method optimization to increase transduction efficiency is an ongoing challenge in the field of cell-based gene therapy [298-300]. This argument is supported by the fact that method B showed the highest transduction efficiency even though the MOI stayed the same. The methods were basically the same but were manipulated during the joining of viral supernatant and cells. Method A, the method with the lowest transduction efficacy (3%), was the simple dispersing of cells and virus. If the viral supernatant was centrifuged on PLL-containing plates and the cells were seeded into these wells (method B), the percentage of transduced cells multiplied (46%). This was accomplished despite using the same virus / cell ratio. These results show that the way through which virus and cells are joined affects the transduction efficiency more than the numerical virus / cell ratio.

The results also show that the porcine MSCs are comparable to human MSCs regarding their transduction efficiency. Using the same retroviral supernatant simplifies many questions. The fact that the change of the method and not a change of the species showed significant differences might help to establish robust transduction processes – also when utilizing porcine MSCs as model cells.

8.3 Functionality of Human-Derived Promoter and Therapeutic Gene in Porcine MSCs

Tissue-specific promoters are attractive for cell-based gene therapy (see detailed in chapter 1.5) – here, the RANTES promoter was used as an inducible control unit [156]. If MSCs home to the site of the tumor stroma, present pro-inflammatory cytokines activate the promoter. The translation of the prodrug would then take place next to the cancer cells. This approach reduces systemic toxic effects of cytostatic agents because these drugs are only locally activated. The also inserted PGK promoter served as a constitutive promoter expressing the puromycin resistance gene (for transgene cassette see Figure 1 and Figure 33).

Due to the fact that the PGK promoter is constitutive, no effects related to different MSC species had to be expected [155]. This assumption was confirmed by the observations made in this work. As shown in Figure 14 and Figure 15, the selection of transgene-expressing cells was successfully proving a functional PGK cassette in MSCs of both species. The absence of any second population in the flow cytometry measurements affirmed the full selection of non-transduced cells.

To compare the *in vitro* efficacy of the therapeutic gene (see 7.6), a functionality of the RANTES promoter in the porcine cell had to be demonstrated before, as shown in Figure 16. Although the results are quite clear showing an increase of expression after induction, a high variance of the human batches could be observed. This variance could be a result of the varying cell morphology regarding size and granularity (as shown in Figure 4 and Figure 5) during flow cytometry measurement. The cells` morphology depends on the donor as well as different “*in vitro* ages” of the cell populations [289, 301, 302]. These effects have influence on the auto fluorescence and may lead to higher or lower emission signals [303]. In addition, the staining procedure can bring up differences because there are several washing and preparation steps necessary before measurement (see 6.6). Interestingly, the difference between induced and not induced porcine cells was statistically significant. These data did not include any donor variance since, as mentioned before, one isogeneic pig was used as the donor animal. This may underline the effect of different donors and potentially help to explain the high variance. In fact, an up-regulation of the RANTES activity could be seen and it is plausible to assume that RANTES worked correctly in both species.

HSV-TK was already used as a suicide gene for the treatment of oncological diseases with a bad prognosis (see detailed in 1.6) over 20 years ago. The presence of HSV-TK strongly increased the sensitivity to GCV as shown in Figure 17. The EC50 values were summed up in Figure 18. The cell lines K67 and HT1080 showed low sensitivities to GCV like naïve MSCs. The amount of living cells after treatment was determined by consumption of reductive elements like NADH that facilitated the chemical reaction of MTT to formazan. Dependent on the activity of glycolysis and the following citrate acid cycle, reductive elements are build up. The generated values based on the optical density values (OD values) after normalization as shown in Figure 17. During development and establishment of the assay it was observed, that the OD values for living MSCs - especially human MSCs - were lower than for cell lines and also porcine MSCs. These results suggested that differences between a well of dead cells and a well of living cells would be quite small (in the case of human MSCs). The OD values were in a range from e.g. 0.03 to 0.16 for human MSCs (Human 2) and for porcine MSCs from 0.15 to 0.81 (Porcine 3). The cell lines showed OD values from 0.02 to 2.02 e.g. HT1080. Small OD values implicate more variance in the assay since the difference between measured values is smaller. This fact is also reflected by the R-values for the goodness of fit; exemplary: Human 2: 0.94; Porcine 3: 0.99 and HT1080: 0.98. The variance for humans is higher and therefore the goodness of fit smaller. In Figure 17, these differences in the goodness of fit can also be visually recognized for e.g. the human naïve cells. The half-effective GCV concentrations are depicted in Figure 18. This figure visualizes the differences of the GCV sensitivity on a logarithmic scale in a descriptive manner. The variance of the assay weakens the quantitative meaningfulness although the R-values are still quite high.

Nevertheless, the increased sensitivity was substantial higher of all HSV-TK expressing MSCs, including the porcine cells. The correct expression of HSV-TK and the increased sensitivity could be clearly proven for both species.

8.4 Programmed Cell Death by GCV– Do Both Species Go the Same Way?

Apoptosis is complex - as described before, countless intrinsic as well as extrinsic pathways may lead to programmed death [191, 304, 305]. In contrast to regulated apoptosis, accidental damage can harm the cells' integrity and immediately lead to irreparable damage and cell death (necrosis). In the past few years, the differences between apoptosis, necrosis and autophagy became more and more indistinct because the pathways regulate each other by cross-talking [304, 305]. Nevertheless, the basic steps of a cell's apoptotic process are relatively well-defined. The cell shows a condensation (decrease of size and increase of granularity) and the mitochondria lose their ATP production due to a mega-channel opening. This ATP loss can be observed by phosphatidylserine (PS) presentation on the surface and ends with the cell death thereby losing all cellular structure (generation of cell debris) and generation of countless apoptotic bodies (see detailed in 1.6).

In this work, the successful killing of cells by GCV could be easily observed by microscopy (see Figure 19) as well as by trypan blue cell counting (see Figure 20). Also naïve cells showed a cell count reduction after five days. This could be confirmed for both species. The accordant assay was performed over five days and included the addition of pro-inflammatory cytokines. Especially IFN γ is well known to have antiproliferative effects on many cell types [306, 307]. In addition, GCV is also marginally translated in unmodified cells and leads to the inhibition of the cell's replication process. Finally, the seeding and harvest always include cell losses. These reasons may have caused the loss of cells despite the five days of cultivation. Therefore, the cell loss was not normalized against the seeding of the HSV-TK cells but rather against non-treated cells, which represented a more appropriate control. The observed killing was still statistically significant. Interestingly, the cell loss of HSV-TK expressing porcine and human MSCs is quite comparable indicating that the GCV affects both species in a similar strength.

The assumption of an apoptotic pathway was confirmed by flow cytometry. A protocol was developed that considered morphological aspects as well as the apoptosis and death of a cell (see Figure 21). It could be observed that both species showed a condensation and the majority of cells became granular (see Figure 22) compared to untreated cells. Both species showed statistically significant changes during treatment (except of the human shrunken population: $p=0.05$). These clear observations were made possible through the successful

staining with Annexin-V and 7-AAD. Both species showed an increase of PS presentation and loss of cell integrity (see Figure 23).

Furthermore, the results revealed a clear indication that the addition of cytokines and GCV does not lead to a considerable increase of dead naïve cells *in vitro*. Only the presence of HSV-TK and its massive translation of GCV inflicted a cell DNA damage that led to the cell death by apoptosis. Porcine MSCs correlated with the expectations made during the observation of human MSCs. It could even be said that if the changes in the cells' morphology as well as the amount of 7-AAD positive cells are compared in detail, porcine MSCs represented the apoptotic characteristics more clearly.

It is difficult to find out why these changes are more distinct in porcine cells. The five-day cultivation protocol that was used for all apoptosis characterization assays included a flow cytometry measurement on day five. Although apoptosis is an ongoing process, the measurement assesses the cell population status at a singular point of time only. It is conceivable that the chosen timeframe did not show the peak of apoptosis in the human cell population [187, 189, 303]. For this reason, the possibility that this "peak of apoptosis" was later or earlier and was missed in this assay setup exists. It is also thinkable that the results would have shifted if the flow cytometry measurement had been done on day four or six. Since the accordant clinical trial [81] was designed to have a treatment with GCV on days three, four and five after MSC infusion on day one, it made sense to evaluate the cell killing on day five.

Of course the cells of both species were treated following the same protocol to allow valid comparisons. However, one parameter had to be considered and was adapted: the seeded cell density. As shown before (see Figure 11, Figure 4 and Figure 5) the cell size highly varied throughout the species and donors. An equal seeding of all batches and species would not have considered the resulting confluency. Especially for the batches Human 3 and 4, the whole plastic surface would have been covered with cells if the same amount of cells as for Porcine 1-4 had been seeded. This was actually observed during development of the assay. The assumption that the GCV killing efficacy is dependent on cell's replication speed and therefore on the growth of a population was strongly indicated (see Figure 24). If no surface is available for growth, no replication will happen and no apoptosis will occur after GCV incorporation. This is why the cell density after seeding and not the cell count was constant throughout the assays. This makes comparisons between the species and

batches more meaningful although the correct setup of the assay was more complex. Counting cells is more easily than a visual assessment on the confluency from a methodological point of view.

The observed correlation of the growth of a population and its killing rate (see Figure 24) makes sense in regard to the mode of action of GCV. Any correlation between VCN and killing efficacy could not be made within the scope of this work although there are publications that mention an increased efficacy with higher VCN for the HSV-TK system [308]. This publication clearly shows that more HSV-TK leads to more activated GCV and therefore to more killing efficacy. But potential “growth effects” are not addressed. Furthermore, it is unclear which effects the chosen promoter might have had. Higher expression rates by e.g. viral constitutive promoters (or other [155]) may negate the necessity of further gene copies. Here, an enzyme kinetic of the expressed gene would help to understand the amount of enzymes necessary to allow a sufficient translation of GCV. A single increase of the copy number per cell is apparently only one parameter of many. In general, the presented results confirm the apoptosis as a reaction on present and activated GCV. MSCs of both species show the same behavior under GCV treatment and the killing rate of a population correlates with its proliferation speed (see Figure 24).

As described before, the therapeutic approach of the suicide gene HSV-TK is based on the bystander effect (see detailed in 1.6). Although it was not in the focus of this work, latest publications raise the questions to what extent gap junctions or other biological systems are responsible for the transport of cytostatic agents like GCV between cells. Extracellular vesicles e.g. exosomes seem to play an important role in inter-cellular communication as well as in the transport of agents, proteins or other substances [309-311]. However, while establishing the assay it could be observed that a killing effect on the target cell lines was nonexistent if the cells were seeded in low confluence of less than 10% resulting in nearly no cell-cell contacts. Confluences of 10-25% were chosen to assure sufficient empty surface for cell proliferation as well as cell-cell connections.

A human and a porcine cell line were examined to find out whether neighbored HSV-TK expressing MSCs from both species kill the cell lines or not. The already described “five-day protocol” was used to maintain consistency with previously performed assays and with the clinical trial design. The cell lines could be differentiated from the MSCs by their GFP expression (see 6.7.3). Figure 25 clearly demonstrates that the cell count of both cell lines

was reduced significantly by HSV-TK expressing batches of both species. A transport of the activated GCV to the target cell line was facilitated independent of the species because the effect did not differ between porcine and human MSCs underlining the comparability.

One interesting observation occurred in column one of Figure 25 (B). The resulting cell count of the K67 cell line highly varied and was lower than expected although the naïve human cells were used as control for the HSV-TK expressing human MSCs. This was observed for the combination of human naïve MSCs and the porcine cell line K67. Overall, there were fewer cells than observed in the other control (see second column of Figure 25 (B)). Depending on the donor, the resulting cell counts grouped around a lower or higher level. This is why the donor-separated depiction was only chosen here. This anti-proliferative effect of the human naïve MSCs was negated as soon as HSV-TK expressing MSCs were present.

Obviously, human naïve MSCs inhibited the proliferation of the cell line. It could be excluded that this happened due to a limitation of space. Microscopy rather showed cells in the supernatant and enough surface space for expansion. The possibility of the medium itself being the cause can also be disregarded because all cells were growing well in the used media. It can be assumed that the MSCs secreted cytokines that had an anti-proliferative effect on the K67 cell line. MSCs are known to secrete a large panel of trophic factors and immunological active cytokines [312-314] and thus can show anti-proliferative effects on tumor cell lines [315, 316]. These cytokines could have had anti-proliferative effects on the K67 cell line. Because the cell line was originally generated from an MSC which was isolated from a *Pietrain Landrasse* pig [276], it is open for discussion if this cell line is even more sensitive to cytokines or not [317]. Whether soluble factors are responsible for the inhibition of the proliferation or not was not proven within the scope of this work. However, it can be assumed that the secreted cytokines of the human MSCs were responsible for the reduction.

Figure 26 and Figure 27 show the successful induction of apoptosis in the target cell lines HT1080 and K67 by co-cultivated porcine and human HSV-TK expressing MSCs. In Figure 26 (A), HT1080 cells showed a very large increase of PS presentation if HSV-TK expressing MSC of both species were co-cultivated. Interestingly, a slight increase of Annexin-V positive cells could be seen if naïve human MSCs were co-cultured – an observation that wasn't true for naïve porcine cells. It could potentially indicate the anti-

proliferating effects of the naïve human MSCs that were observed before (see Figure 25 (B)), although this increase was not statistically significant. The amount of 7-AAD positive HT1080 cells was generally lower than the amount of Annexin-V positive HT1080 cells. This was in accordance to earlier observations made for apoptotic MSCs (see Figure 23), which suggests that the cell lines also underwent GCV-induced apoptosis.

The anti-proliferative effects of naïve human MSCs on the cell line K67 (see Figure 25) could be confirmed as shown in Figure 27 (A). Annexin-V positive K67 are not only significantly increased if co-cultured with HSV-TK expressing MSCs of both species, but the amount of apoptotic cells was also significantly increased by naïve human MSCs. This result confirms the assumed effects on the cell count: naïve human MSCs have an anti-proliferating effect on the cell line K67. The 7-AAD staining of K67 generally showed lower percentages. The increase of 7-AAD positive cells however was comparable for porcine and human HSV-TK MSCs on a low level and therefore shows the successful induction of apoptosis in K67.

The low 7-AAD values could compromise the usefulness of performing a staining to determine the dead cells. It could be presumed that more 7-AAD dead cells were detected because a suicide gene system was used. The fact that the cells undergo apoptosis and lose all cellular structure in the end makes it hard to identify these cells in the flow cytometry. Here, the manual cell count has more significance because only the remaining cells are taken into account and the cell number reduction can be calculated. As described before, the measurement by flow cytometry was only a single point of time measurement on one day. This “snippet” on day five was probably too late to capture more apoptotic HT1080 cells. It is thinkable that most of the cells died before the flow cytometry measurement. Furthermore, it can be assumed that the secretion of soluble factors enhanced the apoptotic process and possibly reduced the time before the cells’ integrity was lost. Finally, it can be said that the remaining amount of HT1080 was comparable between porcine and human MSCs whether expressing HSV-TK or not (see Figure 25).

The characterization of the GCV-induced apoptosis is important to generate an understanding to what extent the suicide of the neighbored cell lines is induced in a comparable manner. A model cell should fulfill the expectations to show comparable effects. Here, the suitability of porcine MSCs as apoptosis-inducing bystander cell could be shown clearly. The observed additional effects of naïve human MSCs on the K67 cell line have to

be considered separately. Similar observations for porcine MSCs were not made and can raise questions on the different secretome of porcine and human MSCs. The result that HSV-TK expressing MSCs of both species showed the same efficacy *in vitro* and induced apoptosis in a similar manner is a strong argument for porcine MSCs as a model cell in apoptosis-inducing approaches.

8.5 Infusion of MSCs into Mini-Pigs indicate Lung-Passage Dependent Delay

All batches used for the *in vivo* studies were stored and transported in the vapor phase of liquid nitrogen. Before infusion, the cells were thawed, pooled, counted, filled into the syringe for administration and transported from the laboratory to the stables. During the whole preparation time, the cells were in suspension in the DMSO-containing medium (see Table 3), which could have had a negative impact on the cells' biological functionality because MSCs pursue adherence and DMSO is a surface-active agent [318, 319]. In general, it is important to know whether functional and living cells or impaired cells are infused in *in vivo* studies. Here, it was unclear how long they would survive in the cryopreservation medium after thawing without a significant reduction of their functional activity. This risk of a methodological error due to non-functional cells should be mitigated. A growth kinetics assay (Figure 28) indicated possible impairments as described before (see 7.7.1). A significant decrease of proliferation was not shown for porcine MSCs until 150 min. All infusions were performed in less than 90 min hence no impact was expected.

The human MSCs were compared with the porcine MSCs and obviously showed an earlier decrease of the proliferation capacity than their porcine counterpart. A significant reduction in the proliferation capacities after 120 min was observable. Furthermore, a decreased functionality was indicated after 90 min although the differences were not statistically significant ($p=0.21$). It could not be clearly concluded if this observation was only related to the species or caused by other factors. Negative post-thaw effects can be caused by several parameters. First, the cryopreservation medium differed between human and porcine cells. Both media used 45% hydroxyethyl starch solution and 10% DMSO. For porcine MSCs, porcine serum and for human MSCs, a defined human albumin solution was used. In contrast to pure albumin, sera are a very heterogeneous and in general a more nutritious composition. It is quite likely that this medium could have enhanced the cell viability because more nutritional ingredients were available. Secondly, a thawing and seeding protocol naturally includes potential variabilities. The cryopreservation vial with the MSCs was put into the 37°C water bath and thawed until no more ice crystals could be seen. This can result in slightly varying thawing times. The following re-suspension may also lead to potential cell damage because the surface-active DMSO may strengthen the effect of shear forces. Finally, the status of the cells before cryopreservation is sure to

influence the result which is influenced by the last medium change before cryopreservation, confluency, the *in vitro* age of the population, passage etc. This is why – on the one hand - the generated results were a good indication for the subsequent *in vivo* studies but on the other hand it is highly probable that other working groups or companies come to other conclusions due to their specific cell therapy product and their chosen cryopreservation procedures [279]. Considering the effects of DMSO, a single publication of Mock *et al.* implicated even better results for porcine MSCs after thawing if the DMSO concentration is reduced to 5% [320]. This was taken into consideration during this work because a further change in the cryopreservation medium would have reduced the value of the comparison studies additionally. Appropriate cryopreservation and thawing is a critical topic in the field of the clinical application of MSCs [133, 319, 321]. Special attention was paid to the usage of identical equipment and medium, due to the many possibilities of influencing the results of the growth kinetics assay without intention.

In contrast to mice or other rodents, the manipulation of a large animal model to allow e.g. the aspiration of a blood sample is difficult to be put into practice. The development of an ethically acceptable and scientifically reasonable *in vivo* testing protocol in collaboration with the responsible veterinarian was a major challenge. For blood sampling, a permanent catheter was necessary because a kinetic of the cells in the bloodstream had to be measured. The fast blood coagulation of the pigs' blood and knowledge of the tendency to shy behavior (based on expertise and experience of the responsible veterinarian) of the 50 to 100 kg heavy mini-pigs impeded stress-free treatment. It was decided to reduce the stress of the animals and to narcotize them for two to three hours. During the sleeping phase, the catheters were implanted as described before (see 6.9.1 and 7.7.2) to allow the blood sample collection for the planned kinetics. Most of the samples were taken during the first hour of the pigs' sleep (see Figure 30 Figure 31). The number of the following blood samplings was minimized to reduce the stressful procedure for the animal as far as possible because the pigs were awake.

The choice of an appropriate method to detect the cells in a tissue or blood sample is continuously discussed by different working groups [89-93]. Here, three arguments led to the choice of real-time PCR as the tracking method for this work. Firstly, an already well-characterized protocol was established to determine the vector copy number of a transduced porcine cell population. Secondly, real-time PCR has a very high sensitivity and specificity in general allowing the detection of single DNA sequences. Thirdly, this approach

did not need any alterations of the cell product itself. As described before (see 1.4), other tracking methods needs major alterations of the cell e.g. transduction with a marker gene (like GFP or luciferase), an iron particles loading or a marking with radioactive substances. The use of magnetic resonance or X-ray imaging would have allowed full *in vivo* studies but would also have increased the costs. Additionally, both methods were not available on-site.

A disadvantage of the real-time PCR method is that a differentiation between viable and dead cells is not possible because only DNA sequences are measured. Furthermore, the blood sample volume for DNA isolation was limited to 750 μL and the real-time PCR measurements could be performed with only 5 μL of the isolated DNA solution containing not more than 100 $\mu\text{g}/\mu\text{L}$ of DNA. This methodical limitation made it necessary to perform multiple analyses consisting of five measurements each (see Figure 30 and Figure 31).

During the planning of the *in vivo* studies, it was assumed that signals around the detection limit of the method would occur. Spiking experiments with transduced cells in porcine blood revealed that at least five copies per reaction well were necessary to generate a valid result. This value was extrapolated to 1mL of blood and the calculation showed that at least 450 MSCs in one sample were necessary to be detected by real-time PCR. The loss during preparation of the sample, isolation of the DNA as well as the very sample size used per reaction well (5 μL) required this number of cells.

Figure 30 shows the recovered MSCs in the blood per mL in the first animal and Figure 31 in the second animal. From a "conventional" pharmacokinetics point of view, intravenous bolus injections of small chemicals are distributed throughout the whole bloodstream after a few seconds. Here, the intravenously infused MSCs could not be found in the blood stream directly after infusion. It was already described in detail why the fact that the cells were not immediately available in the peripheral blood makes sense (see 1.4). A delayed distribution is to be expected because the sizes of the infused agents (small molecule vs. cell) obviously differed significantly.

In pig 1, a relatively strong signal could be identified in after 2 min. This signal became weaker, but it was – relatively - consistent the next few hours. After 36 h, an extra-ordinary recovery was observed. This result was next to the maximum of MSCs that was to be expected if an even distribution throughout the bloodstream was assumed. Afterwards, the signals became as weak as before and were next to the detection limit.

The special pharmacokinetics of MSCs – a delay in the systemic distribution - is an often described phenomenon. MSCs are temporarily located in the lung's vascular system before they enter the peripheral bloodstream. Here, the results generated in this work are exactly in accordance with the publications that discuss the biodistribution of MSCs in most rodents and humans [85, 88, 94, 99, 100, 105, 106]. It is open for discussion whether the high signal after 36 h was also caused by MSCs that were locally enriched at the catheter or not. The fact that the following measurement after 48 h did not show any MSCs anymore weakens this potential assumption. Furthermore three single analyses consisting of five measurements were performed for each sample to increase the reliability of the results. After 48 h, the last blood sample was taken and the animal was necropsied. Tissue samples were frozen on dry ice as well as put into formalin for further analyses. The protocol was intentionally designed to have a 48 h in-life phase after the intravenous infusion to increase the probability of detecting MSCs in the saved tissues, which is going to be discussed later in this chapter. If the tissue samples had been taken to a later point of time, it could have been assumed that the MSCs wouldn't be identifiable anymore in the prominent tissues e.g. the lung.

Based on the proven feasibility of the protocol and the positive results of pig 1, the study design of the second pig was extended to potentially allow more insight into the pharmacokinetics. Two additional samples were added around the 36 h point of time and the in-life phase was prolonged for two days. For this study, unexpected results were generated observing nearly no MSCs in the blood (see Figure 31). Minor signals next to the detection limits probable indicated MSCs in the bloodstream. However, there was no result that showed all signals above the detection limit. Several investigations were performed to find causes for this possible methodological error. But spiking experiments confirmed the validity of the method showing that the transgene DNA could be recovered in the samples of pig 2. It had to be concluded that if MSCs were present, there were less than 450 cells per mL blood because all samples were practically negative. The following report of a veterinarian of the *Institut für Tierpathologie der Ludwig-Maximilians-Universität München* identified a distinct pulmonary infection in contrast to the first animal (see Table 18). This may explain that the amount of MSCs available in the bloodstream undercut the detection limit because MSCs are well known to remain in pro-inflammatory tissue environment [87, 91, 93, 322]. These inflammatory processes could have additionally caused an increased retention in the lung.

To further confirm the results of the in-house real-time PCR measurements, histological slices were sent to an external laboratory for immunohistochemical staining. The expectations of finding several MSCs in one tissue slice were low because only pieces of a few grams of the apex of the lung were sent. The whole lung of one mini-pig in the study had a weight of ca. 500 g.

The procured pieces were cut into smaller slices. To prevent false-positive results, the tissue of a third “MSC-free” mini-pig was treated the same way. A second control with antibody isotypes was performed on the directly neighbored slices to identify staining artifacts in the tissue (see Figure 32). Table 19 summarizes the results. Both pigs that received intravenous infusion showed cells positive for HA-tag staining in the lung. The prevalence of MSCs to accumulate in the lung could be confirmed in both pigs although the identified amount of MSCs ultimately was low. Other tissues were negative except for the spleen of animal 1 because a single signal could be identified. The recovery of MSCs in the spleen was already published as described before (see detailed in 1.4) and is therefore not in conflict with the results of this work.

Altogether the results generated in the mini-pigs are in accordance to publications on MSCs’ biodistribution. However, only two pigs were used in these studies. A low number of animals naturally accompanies large animal studies. In general, the generation time large of animals and their small number of offspring limits these studies in contrast to studies using rodents. In addition, isogenic MGH mini-pigs were part of the study and therefore previous nuclear transfers had to be performed, which naturally have a failure rate and challenges the planning. Even though there were just two animals, the results of both animals fulfilled the expectations of MSCs pharmacokinetics and are not in conflict with published results. Finally, the feasibility of the mini-pig as a useful and beneficial model animal for assessments of the biodistribution of MSCs could be shown.

8.6 Conclusions and Outlook

The aim of this work was to show that the pig and its MSCs are a useful model system for a therapeutic MSC-based product. Here, porcine HSV-TK expressing MSCs are described for the first time. To prove the validity of this model system, the cells of both species were systematically characterized comparing the identity, the controlled insertion of the suicide gene, the functional proof of the transgene cassettes and the apoptosis caused by GCV as well as the bystander killing of cell lines. The conclusions of all *in vitro* assays are summarized in the following Table 20.

Table 20: This overview concludes all *in vitro* tested parameters and the generated results within this work. For both species, all tested parameters were assessed against each other. Porcine MSCs showed to be a well-usable platform for human MSCs because they had many similarities regarding identification, production and therapeutic efficacy *in vitro*. Most of the *in vitro* generated results showed the comparability of both species.

Parameter	Human MSCs	Porcine MSCs	Comparable?	Remarks / Conclusion
Population Doubling Time (PDT)	highly varying from donor to donor, intra-donor variation low	only one donor available, batches equal	+	mean PDT similar, more pig donors helpful, batch production time probably similar
Morphology	fibroblast-like, one donor more flattened	fibroblast-like	++	typical morphology for both species
Differentiation	adipogenic and osteogenic line successful	adipogenic and osteogenic line successful, adipogenic differentiation weaker	++	same medium induces differentiation
Surface Marker	confirming ISCT suggestion, HLA-DR present and inducible	confirming ISCT suggestion, but CD105 negative sub-population and HLA-DR not present	+	two main surface marker show (partial) changes in expression, may limit meaningfulness
Gene modification	successful insertion, selection and therapeutic cassette functional	successful insertion, selection and therapeutic cassette functional	++	same retroviral vectors inserts therapeutic gene in a comparable manner with same VCN; selection feasible, RANTES inducible
GCV sensitivity / Cell Count Reduction	HSV-TK expressing cells show increased sensitivity and higher cell count decreases	HSV-TK expressing cells show increased sensitivity and higher cell count decreases	++	porcine MSCs are even more sensitive to GCV
Apoptosis	significant increase of Annexin-V and 7-AAD if HSV-TK expressing	significant increase of Annexin-V and 7-AAD if HSV-TK expressing	++	porcine MSCs show stronger apoptotic behavior

Parameter	Human MSCs	Porcine MSCs	Comparable?	Remarks / Conclusion
Bystander Killing	significant decrease of cells, also anti-proliferating effects of naïve cells	significant decrease of cells	+	human MSCs have negative proliferation effects on porcine cell line
Bystander Induction of Apoptosis	successful induction of apoptotic cascade in both cell lines	successful induction of apoptotic cascade in both cell lines	++	porcine and human MSCs can induce apoptosis in both species

The results of these assays showed that nearly all measured parameters are comparable for porcine and human MSCs. The only differences between both species occurred during the measurement of the surface markers and the bystander killing assays. It could be observed that there was a porcine MSC sub-population lacking CD105, that porcine MSCs generally do not show HLA-DR on their surface and that naïve human MSCs showed anti-proliferative effects on the porcine cell line K67. Although these results show differences between the species, they are not conflicting existing results. Previously mentioned publications underline the variability of murine MSCs in regard to CD105 [263]. The anti-proliferating effects of human MSCs [315, 316] as well as the presence of HLA-DR were already controversially discussed [62-64]. In that respect, the results observed for porcine MSCs seem to complement existing descriptions and are not in conflict with these.

The subsequent *in vivo* studies underlined the usefulness of the mini-pig. Here, it could be shown that intravenously administered MSCs were detectable in the bloodstream and that the porcine MSCs showed the “MSC-typical” pharmacokinetics profile. Although there were only two animals involved in the study, the time-dependent retention in the lungs before the cells distributed throughout the body could be clearly observed. The measurements of the second animal showed no signals above the detection limit. The identified severe pneumonia was a strong indication that MSCs potentially homed to the pro-inflammatory environment in the lung reducing the amount of MSCs in the peripheral bloodstream. The knowledge about the pharmacokinetics profile is essential for any medicinal product – also for ATMPs [76, 77]. As examined in mice before [100], the easier and faster passaging of the lung could increase the homing and the efficiency of the MSCs’ therapeutic effects. The pig and its anatomy and physiology regarding lungs size, structure and weight are more comparable to humans [209, 211, 323]. Therefore, these animals may promise more valuable insight into the biodistribution than rodents.

Nevertheless, during the early phases of the development of a potential cell product, mice or rats have a clear advantage over LAMs: lower costs, faster reproduction cycles, low dosages (fewer cells needed) and more animals per study group make statistically relevant studies easier. In addition, established immune-deficient rodents are available to test the human-based “original” product that enhances proof of concept studies. Immune-deficient LAMs are rarely found, although it was shown that e.g. SCID pigs are realizable [227].

LAMs could be more helpful in a second phase of the development after the proof of concept was shown in rodents. Then, the product may be tested under more serious and more challenging conditions simulating the clinical setting. To allow studies in LAMs, questions asking for the right dosage, potential toxic effects and appropriate treatment schemes have to be answered. These are the same questions that have to be addressed when clinical trials with humans are initiated. It is obvious that the treatment schemes and dosages of a 0.02 kg mouse are less comparable to humans than those of a 75 kg pig. The assumed dosages extrapolated from rodents to LAMs could be tested on these before humans are treated.

Another consequence is the fact that the increased dosage for LAMs requires an up-scaling of the production, which might be understood as a disadvantage at first glance. The need of higher dosages for LAMs as well as humans requires further efforts in the development of e.g. bio-reactors [324-326], as reviewed by *de Soure et al.* [327]. Because of the versatile and sensitive biology of cells, especially of MSCs, this up-scaling may have an impact on the cells biology. The earlier cell alterations can be characterized before humans are treated, the lower the risk that clinical trials fail. Thorough established potency assays may help to clarify whether new manufacturing methods have a significant impact or not [36, 41, 328, 329].

The complexity of cell therapeutics challenges all working groups and companies facing the development of an ATMP. Heterogeneous and versatile biological functions of cells meet regulatory expectations that were shaped by the classical, chemical compounds. The European Medicines Agency is still struggling to establish adequate GMP-guidelines for ATMPs and is still not in agreement about the necessary prerequisites [330]. The small number of ATMPs authorized for the market in the EU shows that (genetically modified) cells as a medicinal product are still a new therapeutic form, which is underlined by the fact

that merely three gene therapy medicinal products and three somatic cell therapy products were authorized as of the beginning of 2017 [331]).

The pig is not only interesting for toxicological testing. The increase in available disease models e.g. SCID [227], diabetes [226], neurodegenerative diseases [332] or adenomatous polyposis coli (APC) [333] resulting in cancer offers better testing of new therapeutic approaches. During this work, the treatment of pigs carrying this APC gene defect that develops intestinal tumors was evaluated. However, the successful gene defect led to multiple neoplasms. Homing MSCs would have been distributed throughout all neoplasms limiting the anti-proliferative effect of the therapy. In addition, these pigs were not mini-pigs as they were landrace pigs with a weight of approximately 200kg. The required dosage would have been much higher in contrast to 58kg and 82kg heavy mini-pigs. Further adjustment of the model's disease progress could increase the usability of these disease models. Still, the local implantation of tumor developing cells is a potential alternative.

For future cell therapeutics, the mini-pig and its MSCs represent a useful model system. The cost-intensive human MSCs may be replaced by porcine MSCs for defined development phases. The high comparability to humans, the possibility to perform toxicological testing without undesired immunological interactions and the compliance to regulatory demands [204] supports this conclusion. They can support or even lead the preclinical development of a functional MSC-based ATMP.

9 Acknowledgements

I am deeply thankful to Prof. Dr. Dr. Ralf Huss who offered me the opportunity to start in this extremely interesting and challenging field of MSCs and ATMPs. He enabled me to generate this work and to collect so much experience under his advice. His challenging questions and enthusiasm for new class of therapies infected me - that is why I am still eager to work in this field.

I also want to thank Prof. Dr. Eckhard Wolf. In the cooperation with him, Dr. Barbara Kessler and his team, I could perform the *in vivo* studies and gained a lot of experience in the field of large animal models.

I would like to thank Prof. Dr. Schnieke and her team, especially Anja Saalfrank, who supported me with their experience and with their efforts to isolate the mini-pig's MSCs after bone marrow collection.

Sincere thanks to Prof. Dr. Baethmann, Prof. Dr. Dr. Krombach and Prof. Dr. Angele for reviewing and assessing my thesis.

I have to thank the best technical assistant I could have worked with: Madeleine Roll. She trained me from the first day and shared all her knowledge: cell culture, flow cytometry, MSCs, handling bone marrow and so forth. She helped me out when the "*Doktorand*" was (again) not able to perform the simplest tasks in the lab. Thanks for your patience with me!

No one was scientifically challenging me more with tricky questions than my friend Sabine. Her scientifically thinking made my assays more robust and valid since there was no control she did not think of. She inspired me being creative to find solutions for problems that I had to face. Because of her, I repeated a lot of experiments until they were "scientifically reasonable" because "every experiment needs a positive and a negative control". She is great!

Daria alias Foschda is a friend I don't want to miss anymore. Her support, motivation and the discussions helped me in so many situations. Her enthusiasm and tenacity in solving problems is awesome. She is the best support you can have during your work.

I am very thankful to Dr. Felix Hermann who supported me with new ideas and the path forward throughout this work. He gave me advice and did not stop asking: "When do you

finish your work?" Jeremias was the colleague I worked with from day 1 and is today again a colleague of mine. Thanks for all your efforts to establish this "hell of qPCR".

I have to thank all my colleagues in the preclinical department like Nadja, Marina, Alexandra, Sabbel, Ulf, Patrick, Stephan, Birgit, Leona, and many more who contributed their part to this work. Thanks also to my colleagues in the quality management team who gave me the time I needed for finalizing this work: especially Christoph, Conny and Marc.

Thanks to my family that supported me as well as Karola - the best aunt in the world! And Lara who gave me the non-scientific support that is as much important as the work itself.

Many thanks to apceth for the financial support.

10 References

1. Friedenstein, A.J., et al., *Heterotopic of bone marrow. Analysis of precursor cells for osteogenic and hematopoietic tissues*. Transplantation, 1968. **6**(2): p. 230-47.
2. Owen, M. and A.J. Friedenstein, *Stromal stem cells: marrow-derived osteogenic precursors*. Ciba Found Symp, 1988. **136**: p. 42-60.
3. da Silva Meirelles, L., A.I. Caplan, and N.B. Nardi, *In search of the in vivo identity of mesenchymal stem cells*. Stem Cells, 2008. **26**(9): p. 2287-99.
4. Horwitz, E.M., et al., *Clarification of the nomenclature for MSC: The International Society for Cellular Therapy position statement*. Cytotherapy, 2005. **7**(5): p. 393-5.
5. Dominici, M., et al., *Minimal criteria for defining multipotent mesenchymal stromal cells. The International Society for Cellular Therapy position statement*. Cytotherapy, 2006. **8**(4): p. 315-7.
6. Ho, A.D., W. Wagner, and W. Franke, *Heterogeneity of mesenchymal stromal cell preparations*. Cytotherapy, 2008. **10**(4): p. 320-30.
7. Ankrum, J.A., J.F. Ong, and J.M. Karp, *Mesenchymal stem cells: immune evasive, not immune privileged*. Nat Biotechnol, 2014. **32**(3): p. 252-60.
8. Hoogduijn, M.J., et al., *The immunomodulatory properties of mesenchymal stem cells and their use for immunotherapy*. Int Immunopharmacol, 2010. **10**(12): p. 1496-500.
9. Tuan, R.S., G. Boland, and R. Tuli, *Adult mesenchymal stem cells and cell-based tissue engineering*. Arthritis Res Ther, 2003. **5**(1): p. 32-45.
10. Mendicino, M., et al., *MSC-based product characterization for clinical trials: an FDA perspective*. Cell Stem Cell, 2014. **14**(2): p. 141-5.
11. Mendez-Ferrer, S., et al., *Mesenchymal and haematopoietic stem cells form a unique bone marrow niche*. Nature, 2010. **466**(7308): p. 829-34.
12. Osawa, M., et al., *Long-term lymphohematopoietic reconstitution by a single CD34-low/negative hematopoietic stem cell*. Science, 1996. **273**(5272): p. 242-5.
13. Spangrude, G.J., D.M. Brooks, and D.B. Tumas, *Long-term repopulation of irradiated mice with limiting numbers of purified hematopoietic stem cells: in vivo expansion of stem cell phenotype but not function*. Blood, 1995. **85**(4): p. 1006-16.
14. Notta, F., et al., *Isolation of single human hematopoietic stem cells capable of long-term multilineage engraftment*. Science, 2011. **333**(6039): p. 218-21.
15. Friedenstein, A.J., et al., *Stromal cells responsible for transferring the microenvironment of the hemopoietic tissues. Cloning in vitro and retransplantation in vivo*. Transplantation, 1974. **17**(4): p. 331-40.
16. Newell, L.F., R.J. Deans, and R.T. Maziarz, *Adult adherent stromal cells in the management of graft-versus-host disease*. Expert Opin Biol Ther, 2014. **14**(2): p. 231-46.

17. Horwitz, E.M., et al., *Isolated allogeneic bone marrow-derived mesenchymal cells engraft and stimulate growth in children with osteogenesis imperfecta: Implications for cell therapy of bone*. Proc Natl Acad Sci U S A, 2002. **99**(13): p. 8932-7.
18. Prasad, V.K., et al., *Efficacy and safety of ex vivo cultured adult human mesenchymal stem cells (Prochymal) in pediatric patients with severe refractory acute graft-versus-host disease in a compassionate use study*. Biol Blood Marrow Transplant, 2011. **17**(4): p. 534-41.
19. Kim, N., et al., *Mesenchymal stem cells for the treatment and prevention of graft-versus-host disease: experiments and practice*. Ann Hematol, 2013. **92**(10): p. 1295-308.
20. Dalal, J., K. Gandy, and J. Domen, *Role of mesenchymal stem cell therapy in Crohn's disease*. Pediatr Res, 2012. **71**(4 Pt 2): p. 445-51.
21. Kastrinaki, M.C. and H.A. Papadaki, *Mesenchymal stromal cells in rheumatoid arthritis: biological properties and clinical applications*. Curr Stem Cell Res Ther, 2009. **4**(1): p. 61-9.
22. Farini, A., et al., *Clinical applications of mesenchymal stem cells in chronic diseases*. Stem Cells Int, 2014. **2014**: p. 306573.
23. Phinney, D.G. and L. Sensebe, *Mesenchymal stromal cells: misconceptions and evolving concepts*. Cytotherapy, 2013. **15**(2): p. 140-5.
24. Galipeau, J., *The mesenchymal stromal cells dilemma--does a negative phase III trial of random donor mesenchymal stromal cells in steroid-resistant graft-versus-host disease represent a death knell or a bump in the road?* Cytotherapy, 2013. **15**(1): p. 2-8.
25. Ankrum, J. and J.M. Karp, *Mesenchymal stem cell therapy: Two steps forward, one step back*. Trends Mol Med, 2010. **16**(5): p. 203-9.
26. Galderisi, U. and A. Giordano, *The gap between the physiological and therapeutic roles of mesenchymal stem cells*. Med Res Rev, 2014. **34**(5): p. 1100-26.
27. Owen, M., *Marrow stromal stem cells*. J Cell Sci Suppl, 1988. **10**: p. 63-76.
28. Caplan, A.I., *Mesenchymal stem cells*. J Orthop Res, 1991. **9**(5): p. 641-50.
29. Pittenger, M.F., et al., *Multilineage potential of adult human mesenchymal stem cells*. Science, 1999. **284**(5411): p. 143-7.
30. Bianco, P., et al., *The meaning, the sense and the significance: translating the science of mesenchymal stem cells into medicine*. Nat Med, 2013. **19**(1): p. 35-42.
31. Waterman, R.S., et al., *A new mesenchymal stem cell (MSC) paradigm: polarization into a pro-inflammatory MSC1 or an immunosuppressive MSC2 phenotype*. PLoS One, 2010. **5**(4): p. e10088.
32. Madrigal, M., K.S. Rao, and N.H. Riordan, *A review of therapeutic effects of mesenchymal stem cell secretions and induction of secretory modification by different culture methods*. J Transl Med, 2014. **12**(1): p. 260.
33. Rennerfeldt, D.A. and K.J. Van Vliet, *Concise Review: When Colonies Are Not Clones: Evidence and Implications of Intracolony Heterogeneity in Mesenchymal Stem Cells*. Stem Cells, 2016. **34**(5): p. 1135-41.
34. Hematti, P., *Mesenchymal stromal cells and fibroblasts: a case of mistaken identity?* Cytotherapy, 2012. **14**(5): p. 516-21.

-
35. Bara, J.J., et al., *Concise review: Bone marrow-derived mesenchymal stem cells change phenotype following in vitro culture: implications for basic research and the clinic*. Stem Cells, 2014. **32**(7): p. 1713-23.
 36. Bravery, C.A., et al., *Potency assay development for cellular therapy products: an ISCT review of the requirements and experiences in the industry*. Cytotherapy, 2013. **15**(1): p. 9-19.
 37. Carmen, J., et al., *Developing assays to address identity, potency, purity and safety: cell characterization in cell therapy process development*. Regen Med, 2012. **7**(1): p. 85-100.
 38. Li, X., et al., *Lung tumor exosomes induce a pro-inflammatory phenotype in mesenchymal stem cells via NFkappaB-TLR signaling pathway*. J Hematol Oncol, 2016. **9**: p. 42.
 39. Li, W., et al., *Mesenchymal stem cells: a double-edged sword in regulating immune responses*. Cell Death Differ, 2012. **19**(9): p. 1505-13.
 40. Gazdic, M., et al., *Mesenchymal stem cells: a friend or foe in immune-mediated diseases*. Stem Cell Rev, 2015. **11**(2): p. 280-7.
 41. Bloom, D.D., et al., *A reproducible immunopotency assay to measure mesenchymal stromal cell-mediated T-cell suppression*. Cytotherapy, 2015. **17**(2): p. 140-51.
 42. Russell, K.C., et al., *In vitro high-capacity assay to quantify the clonal heterogeneity in trilineage potential of mesenchymal stem cells reveals a complex hierarchy of lineage commitment*. Stem Cells, 2010. **28**(4): p. 788-98.
 43. Muraglia, A., R. Cancedda, and R. Quarto, *Clonal mesenchymal progenitors from human bone marrow differentiate in vitro according to a hierarchical model*. J Cell Sci, 2000. **113 (Pt 7)**: p. 1161-6.
 44. Kuroda, Y., et al., *Unique multipotent cells in adult human mesenchymal cell populations*. Proc Natl Acad Sci U S A, 2010. **107**(19): p. 8639-43.
 45. Sorrentino, A., et al., *Isolation and characterization of CD146+ multipotent mesenchymal stromal cells*. Exp Hematol, 2008. **36**(8): p. 1035-46.
 46. Lv, F.J., et al., *Concise review: the surface markers and identity of human mesenchymal stem cells*. Stem Cells, 2014. **32**(6): p. 1408-19.
 47. Battula, V.L., et al., *Prospective isolation and characterization of mesenchymal stem cells from human placenta using a frizzled-9-specific monoclonal antibody*. Differentiation, 2008. **76**(4): p. 326-36.
 48. Martinez, C., et al., *Human bone marrow mesenchymal stromal cells express the neural ganglioside GD2: a novel surface marker for the identification of MSCs*. Blood, 2007. **109**(10): p. 4245-8.
 49. Lee, R.H., et al., *The CD34-like protein PODXL and alpha6-integrin (CD49f) identify early progenitor MSCs with increased clonogenicity and migration to infarcted heart in mice*. Blood, 2009. **113**(4): p. 816-26.
 50. Chen, W.C., et al., *Cellular kinetics of perivascular MSC precursors*. Stem Cells Int, 2013. **2013**: p. 983059.
 51. Caplan, A.I., *Why are MSCs therapeutic? New data: new insight*. J Pathol, 2009. **217**(2): p. 318-24.

-
52. Haniffa, M.A., et al., *Mesenchymal stem cells: the fibroblasts' new clothes?* Haematologica, 2009. **94**(2): p. 258-63.
 53. Ishii, M., et al., *Molecular markers distinguish bone marrow mesenchymal stem cells from fibroblasts.* Biochem Biophys Res Commun, 2005. **332**(1): p. 297-303.
 54. Caplan, A.I. and D. Correa, *The MSC: an injury drugstore.* Cell Stem Cell, 2011. **9**(1): p. 11-5.
 55. da Silva Meirelles, L., et al., *MSC frequency correlates with blood vessel density in equine adipose tissue.* Tissue Eng Part A, 2009. **15**(2): p. 221-9.
 56. Crisostomo, P.R., et al., *Human mesenchymal stem cells stimulated by TNF-alpha, LPS, or hypoxia produce growth factors by an NF kappa B- but not JNK-dependent mechanism.* Am J Physiol Cell Physiol, 2008. **294**(3): p. C675-82.
 57. Rasmussen, J.G., et al., *Prolonged hypoxic culture and trypsinization increase the pro-angiogenic potential of human adipose tissue-derived stem cells.* Cytotherapy, 2011. **13**(3): p. 318-28.
 58. Berniakovich, I. and M. Giorgio, *Low oxygen tension maintains multipotency, whereas normoxia increases differentiation of mouse bone marrow stromal cells.* Int J Mol Sci, 2013. **14**(1): p. 2119-34.
 59. Roemeling-van Rhijn, M., et al., *Effects of Hypoxia on the Immunomodulatory Properties of Adipose Tissue-Derived Mesenchymal Stem cells.* Front Immunol, 2013. **4**: p. 203.
 60. Chang, C.P., et al., *Hypoxic preconditioning enhances the therapeutic potential of the secretome from cultured human mesenchymal stem cells in experimental traumatic brain injury.* Clin Sci (Lond), 2013. **124**(3): p. 165-76.
 61. Li, J.H., N. Zhang, and J.A. Wang, *Improved anti-apoptotic and anti-remodeling potency of bone marrow mesenchymal stem cells by anoxic pre-conditioning in diabetic cardiomyopathy.* J Endocrinol Invest, 2008. **31**(2): p. 103-10.
 62. Huss, R., et al., *Differentiation of canine bone marrow cells with hemopoietic characteristics from an adherent stromal cell precursor.* Proc Natl Acad Sci U S A, 1995. **92**(3): p. 748-52.
 63. Romieu-Mourez, R., et al., *Regulation of MHC class II expression and antigen processing in murine and human mesenchymal stromal cells by IFN-gamma, TGF-beta, and cell density.* J Immunol, 2007. **179**(3): p. 1549-58.
 64. Stagg, J., et al., *Interferon-gamma-stimulated marrow stromal cells: a new type of nonhematopoietic antigen-presenting cell.* Blood, 2006. **107**(6): p. 2570-7.
 65. Chan, J.L., et al., *Antigen-presenting property of mesenchymal stem cells occurs during a narrow window at low levels of interferon-gamma.* Blood, 2006. **107**(12): p. 4817-24.
 66. Ryan, J.M., et al., *Interferon-gamma does not break, but promotes the immunosuppressive capacity of adult human mesenchymal stem cells.* Clin Exp Immunol, 2007. **149**(2): p. 353-63.
 67. Noone, C., et al., *IFN-gamma stimulated human umbilical-tissue-derived cells potently suppress NK activation and resist NK-mediated cytotoxicity in vitro.* Stem Cells Dev, 2013. **22**(22): p. 3003-14.
 68. Gieseke, F., et al., *Proinflammatory stimuli induce galectin-9 in human mesenchymal stromal cells to suppress T-cell proliferation.* Eur J Immunol, 2013. **43**(10): p. 2741-9.

-
69. Le Blanc, K., et al., *Mesenchymal stem cells for treatment of steroid-resistant, severe, acute graft-versus-host disease: a phase II study*. *Lancet*, 2008. **371**(9624): p. 1579-86.
 70. Ringden, O., et al., *Mesenchymal stem cells for treatment of therapy-resistant graft-versus-host disease*. *Transplantation*, 2006. **81**(10): p. 1390-7.
 71. Haque, N., N.H. Kasim, and M.T. Rahman, *Optimization of pre-transplantation conditions to enhance the efficacy of mesenchymal stem cells*. *Int J Biol Sci*, 2015. **11**(3): p. 324-34.
 72. Lee, R.H., et al., *Intravenous hMSCs improve myocardial infarction in mice because cells embolized in lung are activated to secrete the anti-inflammatory protein TSG-6*. *Cell Stem Cell*, 2009. **5**(1): p. 54-63.
 73. Bartosh, T.J., et al., *Dynamic compaction of human mesenchymal stem/precursor cells into spheres self-activates caspase-dependent IL1 signaling to enhance secretion of modulators of inflammation and immunity (PGE2, TSG6, and STC1)*. *Stem Cells*, 2013. **31**(11): p. 2443-56.
 74. Ylostalo, J.H., et al., *Human mesenchymal stem/stromal cells cultured as spheroids are self-activated to produce prostaglandin E2 that directs stimulated macrophages into an anti-inflammatory phenotype*. *Stem Cells*, 2012. **30**(10): p. 2283-96.
 75. Lipinski, C.A., et al., *Experimental and computational approaches to estimate solubility and permeability in drug discovery and development settings*. *Adv Drug Deliv Rev*, 2001. **46**(1-3): p. 3-26.
 76. Pellegatti, M., *Preclinical in vivo ADME studies in drug development: a critical review*. *Expert Opin Drug Metab Toxicol*, 2012. **8**(2): p. 161-72.
 77. Lin, J.H., *Pharmacokinetics of biotech drugs: peptides, proteins and monoclonal antibodies*. *Curr Drug Metab*, 2009. **10**(7): p. 661-91.
 78. Ghose, A.K., V.N. Viswanadhan, and J.J. Wendoloski, *A knowledge-based approach in designing combinatorial or medicinal chemistry libraries for drug discovery. 1. A qualitative and quantitative characterization of known drug databases*. *J Comb Chem*, 1999. **1**(1): p. 55-68.
 79. Horwitz, E.M., et al., *Clinical responses to bone marrow transplantation in children with severe osteogenesis imperfecta*. *Blood*, 2001. **97**(5): p. 1227-31.
 80. Le Blanc, K., et al., *Treatment of severe acute graft-versus-host disease with third party haploidentical mesenchymal stem cells*. *Lancet*, 2004. **363**(9419): p. 1439-41.
 81. Niess, H., et al., *Treatment of advanced gastrointestinal tumors with genetically modified autologous mesenchymal stromal cells (TREAT-ME1): study protocol of a phase I/II clinical trial*. *BMC Cancer*, 2015. **15**: p. 237.
 82. Uchibori, R., et al., *Cancer gene therapy using mesenchymal stem cells*. *Int J Hematol*, 2014. **99**(4): p. 377-82.
 83. Ramdasi, S., S. Sarang, and C. Viswanathan, *Potential of Mesenchymal Stem Cell based application in Cancer*. *Int J Hematol Oncol Stem Cell Res*, 2015. **9**(2): p. 95-103.
 84. Caplan, A.I., *Adult mesenchymal stem cells for tissue engineering versus regenerative medicine*. *J Cell Physiol*, 2007. **213**(2): p. 341-7.
 85. Leibacher, J. and R. Henschler, *Biodistribution, migration and homing of systemically applied mesenchymal stem/stromal cells*. *Stem Cell Res Ther*, 2016. **7**(1): p. 7.

-
86. Karp, J.M. and G.S. Leng Teo, *Mesenchymal stem cell homing: the devil is in the details*. Cell Stem Cell, 2009. **4**(3): p. 206-16.
 87. Eseonu, O.I. and C. De Bari, *Homing of mesenchymal stem cells: mechanistic or stochastic? Implications for targeted delivery in arthritis*. Rheumatology (Oxford), 2015. **54**(2): p. 210-8.
 88. Sensebe, L. and S. Fleury-Cappellesso, *Biodistribution of mesenchymal stem/stromal cells in a preclinical setting*. Stem Cells Int, 2013. **2013**: p. 678063.
 89. Devine, S.M., et al., *Mesenchymal stem cells are capable of homing to the bone marrow of non-human primates following systemic infusion*. Exp Hematol, 2001. **29**(2): p. 244-55.
 90. Devine, S.M., et al., *Mesenchymal stem cells distribute to a wide range of tissues following systemic infusion into nonhuman primates*. Blood, 2003. **101**(8): p. 2999-3001.
 91. Gao, J., et al., *The dynamic in vivo distribution of bone marrow-derived mesenchymal stem cells after infusion*. Cells Tissues Organs, 2001. **169**(1): p. 12-20.
 92. IBarbash, I.M., et al., *Systemic delivery of bone marrow-derived mesenchymal stem cells to the infarcted myocardium: feasibility, cell migration, and body distribution*. Circulation, 2003. **108**(7): p. 863-8.
 93. Kraitchman, D.L., et al., *Dynamic imaging of allogeneic mesenchymal stem cells trafficking to myocardial infarction*. Circulation, 2005. **112**(10): p. 1451-61.
 94. Fischer, U.M., et al., *Pulmonary passage is a major obstacle for intravenous stem cell delivery: the pulmonary first-pass effect*. Stem Cells Dev, 2009. **18**(5): p. 683-92.
 95. Eggenhofer, E., et al., *Mesenchymal stem cells are short-lived and do not migrate beyond the lungs after intravenous infusion*. Front Immunol, 2012. **3**: p. 297.
 96. Furlani, D., et al., *Is the intravascular administration of mesenchymal stem cells safe? Mesenchymal stem cells and intravital microscopy*. Microvasc Res, 2009. **77**(3): p. 370-6.
 97. Downey, G.P., et al., *Retention of leukocytes in capillaries: role of cell size and deformability*. J Appl Physiol (1985), 1990. **69**(5): p. 1767-78.
 98. Deak, E., et al., *Suspension medium influences interaction of mesenchymal stromal cells with endothelium and pulmonary toxicity after transplantation in mice*. Cytotherapy, 2010. **12**(2): p. 260-4.
 99. Makela, T., et al., *Safety and biodistribution study of bone marrow-derived mesenchymal stromal cells and mononuclear cells and the impact of the administration route in an intact porcine model*. Cytotherapy, 2015. **17**(4): p. 392-402.
 100. Schrepfer, S., et al., *Stem cell transplantation: the lung barrier*. Transplant Proc, 2007. **39**(2): p. 573-6.
 101. Ruster, B., et al., *Mesenchymal stem cells display coordinated rolling and adhesion behavior on endothelial cells*. Blood, 2006. **108**(12): p. 3938-44.
 102. Wynn, R.F., et al., *A small proportion of mesenchymal stem cells strongly expresses functionally active CXCR4 receptor capable of promoting migration to bone marrow*. Blood, 2004. **104**(9): p. 2643-5.

103. Shi, M., et al., *Regulation of CXCR4 expression in human mesenchymal stem cells by cytokine treatment: role in homing efficiency in NOD/SCID mice*. *Haematologica*, 2007. **92**(7): p. 897-904.
104. Segers, V.F., et al., *Mesenchymal stem cell adhesion to cardiac microvascular endothelium: activators and mechanisms*. *Am J Physiol Heart Circ Physiol*, 2006. **290**(4): p. H1370-7.
105. Kerkela, E., et al., *Transient proteolytic modification of mesenchymal stromal cells increases lung clearance rate and targeting to injured tissue*. *Stem Cells Transl Med*, 2013. **2**(7): p. 510-20.
106. Nystedt, J., et al., *Cell surface structures influence lung clearance rate of systemically infused mesenchymal stromal cells*. *Stem Cells*, 2013. **31**(2): p. 317-26.
107. Toupet, K., et al., *Survival and biodistribution of xenogenic adipose mesenchymal stem cells is not affected by the degree of inflammation in arthritis*. *PLoS One*, 2015. **10**(1): p. e0114962.
108. Togel, F., et al., *Bioluminescence imaging to monitor the in vivo distribution of administered mesenchymal stem cells in acute kidney injury*. *Am J Physiol Renal Physiol*, 2008. **295**(1): p. F315-21.
109. Morigi, M. and P. De Coppi, *Cell therapy for kidney injury: different options and mechanisms--mesenchymal and amniotic fluid stem cells*. *Nephron Exp Nephrol*, 2014. **126**(2): p. 59.
110. Gholamrezanezhad, A., et al., *In vivo tracking of 111In-oxine labeled mesenchymal stem cells following infusion in patients with advanced cirrhosis*. *Nucl Med Biol*, 2011. **38**(7): p. 961-7.
111. Bergfeld, S.A. and Y.A. DeClerck, *Bone marrow-derived mesenchymal stem cells and the tumor microenvironment*. *Cancer Metastasis Rev*, 2010. **29**(2): p. 249-61.
112. D'Souza, N., et al., *MSC and Tumors: Homing, Differentiation, and Secretion Influence Therapeutic Potential*. *Adv Biochem Eng Biotechnol*, 2013. **130**: p. 209-66.
113. Hall, B., M. Andreeff, and F. Marini, *The participation of mesenchymal stem cells in tumor stroma formation and their application as targeted-gene delivery vehicles*. *Handb Exp Pharmacol*, 2007(180): p. 263-83.
114. Mishra, P.J., et al., *Mesenchymal stem cells: flip side of the coin*. *Cancer Res*, 2009. **69**(4): p. 1255-8.
115. Niess, H., et al., *Selective targeting of genetically engineered mesenchymal stem cells to tumor stroma microenvironments using tissue-specific suicide gene expression suppresses growth of hepatocellular carcinoma*. *Ann Surg*, 2011. **254**(5): p. 767-74; discussion 774-5.
116. Bao, Q., et al., *Mesenchymal stem cell-based tumor-targeted gene therapy in gastrointestinal cancer*. *Stem Cells Dev*, 2012. **21**(13): p. 2355-63.
117. Keung, E.Z., P.J. Nelson, and C. Conrad, *Concise review: genetically engineered stem cell therapy targeting angiogenesis and tumor stroma in gastrointestinal malignancy*. *Stem Cells*, 2013. **31**(2): p. 227-35.
118. Sun, X.Y., et al., *Mesenchymal stem cell-mediated cancer therapy: A dual-targeted strategy of personalized medicine*. *World J Stem Cells*, 2011. **3**(11): p. 96-103.
119. Schenk, S., et al., *Monocyte chemotactic protein-3 is a myocardial mesenchymal stem cell homing factor*. *Stem Cells*, 2007. **25**(1): p. 245-51.

-
120. Wu, Y. and R.C. Zhao, *The role of chemokines in mesenchymal stem cell homing to myocardium*. Stem Cell Rev, 2012. **8**(1): p. 243-50.
 121. Belema-Bedada, F., et al., *Efficient homing of multipotent adult mesenchymal stem cells depends on FROUNT-mediated clustering of CCR2*. Cell Stem Cell, 2008. **2**(6): p. 566-75.
 122. Humphreys, B.D. and J.V. Bonventre, *Mesenchymal stem cells in acute kidney injury*. Annu Rev Med, 2008. **59**: p. 311-25.
 123. Bruno, S., et al., *Mesenchymal stem cell-derived microvesicles protect against acute tubular injury*. J Am Soc Nephrol, 2009. **20**(5): p. 1053-67.
 124. Morigi, M., et al., *Mesenchymal stem cells are renotropic, helping to repair the kidney and improve function in acute renal failure*. J Am Soc Nephrol, 2004. **15**(7): p. 1794-804.
 125. Imberti, B., et al., *Insulin-like growth factor-1 sustains stem cell mediated renal repair*. J Am Soc Nephrol, 2007. **18**(11): p. 2921-8.
 126. Briquet, A., et al., *Human bone marrow, umbilical cord or liver mesenchymal stromal cells fail to improve liver function in a model of CCl4-induced liver damage in NOD/SCID/IL-2Rgamma(null) mice*. Cytotherapy, 2014. **16**(11): p. 1511-8.
 127. Simmons, P.J., et al., *Host origin of marrow stromal cells following allogeneic bone marrow transplantation*. Nature, 1987. **328**(6129): p. 429-32.
 128. Cilloni, D., et al., *Limited engraftment capacity of bone marrow-derived mesenchymal cells following T-cell-depleted hematopoietic stem cell transplantation*. Blood, 2000. **96**(10): p. 3637-43.
 129. Rieger, K., et al., *Mesenchymal stem cells remain of host origin even a long time after allogeneic peripheral blood stem cell or bone marrow transplantation*. Exp Hematol, 2005. **33**(5): p. 605-11.
 130. Rombouts, W.J. and R.E. Ploemacher, *Primary murine MSC show highly efficient homing to the bone marrow but lose homing ability following culture*. Leukemia, 2003. **17**(1): p. 160-70.
 131. Zischek, C., et al., *Targeting tumor stroma using engineered mesenchymal stem cells reduces the growth of pancreatic carcinoma*. Ann Surg, 2009. **250**(5): p. 747-53.
 132. Barbash, I.M., et al., *Systemic delivery of bone marrow-derived mesenchymal stem cells to the infarcted myocardium: feasibility, cell migration, and body distribution*. Circulation, 2003. **108**(7): p. 863-8.
 133. Chinnadurai, R., et al., *Actin cytoskeletal disruption following cryopreservation alters the biodistribution of human mesenchymal stromal cells in vivo*. Stem Cell Reports, 2014. **3**(1): p. 60-72.
 134. Francois, M., et al., *Cryopreserved mesenchymal stromal cells display impaired immunosuppressive properties as a result of heat-shock response and impaired interferon-gamma licensing*. Cytotherapy, 2012. **14**(2): p. 147-52.
 135. Moll, G., et al., *Cryopreserved or Fresh Mesenchymal Stromal Cells: Only a Matter of Taste or Key to Unleash the Full Clinical Potential of MSC Therapy?* Adv Exp Med Biol, 2016. **951**: p. 77-98.
 136. Haack-Sorensen, M. and J. Kastrup, *Cryopreservation and revival of mesenchymal stromal cells*. Methods Mol Biol, 2011. **698**: p. 161-74.

-
137. Lee, S.Y., et al., *Magnetic cryopreservation for dental pulp stem cells*. *Cells Tissues Organs*, 2012. **196**(1): p. 23-33.
138. Pravdyuk, A.I., et al., *Cryopreservation of alginate encapsulated mesenchymal stromal cells*. *Cryobiology*, 2013. **66**(3): p. 215-22.
139. Greenberg, B., et al., *Calcium upregulation by percutaneous administration of gene therapy in patients with cardiac disease (CUPID 2): a randomised, multinational, double-blind, placebo-controlled, phase 2b trial*. *Lancet*, 2016. **387**(10024): p. 1178-86.
140. Zsebo, K., et al., *Long-term effects of AAV1/SERCA2a gene transfer in patients with severe heart failure: analysis of recurrent cardiovascular events and mortality*. *Circ Res*, 2014. **114**(1): p. 101-8.
141. Gaspar, H.B., et al., *Hematopoietic stem cell gene therapy for adenosine deaminase-deficient severe combined immunodeficiency leads to long-term immunological recovery and metabolic correction*. *Sci Transl Med*, 2011. **3**(97): p. 97ra80.
142. Aiuti, A., et al., *Lentiviral hematopoietic stem cell gene therapy in patients with Wiskott-Aldrich syndrome*. *Science*, 2013. **341**(6148): p. 1233151.
143. Naldini, L., *Gene therapy returns to centre stage*. *Nature*, 2015. **526**(7573): p. 351-60.
144. ; Available from: <http://www.genetherapynet.com/viral-vectors.html>.
145. Wu, X., et al., *Transcription start regions in the human genome are favored targets for MLV integration*. *Science*, 2003. **300**(5626): p. 1749-51.
146. Wang, G.P., et al., *Analysis of lentiviral vector integration in HIV+ study subjects receiving autologous infusions of gene modified CD4+ T cells*. *Mol Ther*, 2009. **17**(5): p. 844-50.
147. Kustikova, O.S., et al., *Dose finding with retroviral vectors: correlation of retroviral vector copy numbers in single cells with gene transfer efficiency in a cell population*. *Blood*, 2003. **102**(12): p. 3934-7.
148. Modlich, U., et al., *Leukemia induction after a single retroviral vector insertion in Evi1 or Prdm16*. *Leukemia*, 2008. **22**(8): p. 1519-28.
149. Modlich, U., et al., *Leukemias following retroviral transfer of multidrug resistance 1 (MDR1) are driven by combinatorial insertional mutagenesis*. *Blood*, 2005. **105**(11): p. 4235-46.
150. Yu, S.F., et al., *Self-inactivating retroviral vectors designed for transfer of whole genes into mammalian cells*. *Proc Natl Acad Sci U S A*, 1986. **83**(10): p. 3194-8.
151. Stein, S., et al., *From bench to bedside: preclinical evaluation of a self-inactivating gammaretroviral vector for the gene therapy of X-linked chronic granulomatous disease*. *Hum Gene Ther Clin Dev*, 2013. **24**(2): p. 86-98.
152. Naldini, L., *Ex vivo gene transfer and correction for cell-based therapies*. *Nat Rev Genet*, 2011. **12**(5): p. 301-15.
153. Zarogoulidis, P., et al., *Suicide Gene Therapy for Cancer - Current Strategies*. *J Genet Syndr Gene Ther*, 2013. **4**.
154. Papadakis, E.D., et al., *Promoters and control elements: designing expression cassettes for gene therapy*. *Curr Gene Ther*, 2004. **4**(1): p. 89-113.

-
155. Qin, J.Y., et al., *Systematic comparison of constitutive promoters and the doxycycline-inducible promoter*. PLoS One, 2010. **5**(5): p. e10611.
156. Lee, A.H., J.H. Hong, and Y.S. Seo, *Tumour necrosis factor-alpha and interferon-gamma synergistically activate the RANTES promoter through nuclear factor kappaB and interferon regulatory factor 1 (IRF-1) transcription factors*. Biochem J, 2000. **350 Pt 1**: p. 131-8.
157. De Palma, M., et al., *Tumor-targeted interferon-alpha delivery by Tie2-expressing monocytes inhibits tumor growth and metastasis*. Cancer Cell, 2008. **14**(4): p. 299-311.
158. Pluta, K., et al., *Tight control of transgene expression by lentivirus vectors containing second-generation tetracycline-responsive promoters*. J Gene Med, 2005. **7**(6): p. 803-17.
159. Gossen, M. and H. Bujard, *Tight control of gene expression in mammalian cells by tetracycline-responsive promoters*. Proc Natl Acad Sci U S A, 1992. **89**(12): p. 5547-51.
160. Genin, P., et al., *Regulation of RANTES chemokine gene expression requires cooperativity between NF-kappa B and IFN-regulatory factor transcription factors*. J Immunol, 2000. **164**(10): p. 5352-61.
161. Zheng, C. and B.J. Baum, *Evaluation of promoters for use in tissue-specific gene delivery*. Methods Mol Biol, 2008. **434**: p. 205-19.
162. Cheng, Y.C., et al., *Metabolism of 9-(1,3-dihydroxy-2-propoxymethyl)guanine, a new anti-herpes virus compound, in herpes simplex virus-infected cells*. J Biol Chem, 1983. **258**(20): p. 12460-4.
163. Field, A.K., et al., *9-([2-hydroxy-1-(hydroxymethyl)ethoxy]methyl)guanine: a selective inhibitor of herpes group virus replication*. Proc Natl Acad Sci U S A, 1983. **80**(13): p. 4139-43.
164. Smee, D.F., et al., *Intracellular metabolism and enzymatic phosphorylation of 9-(1,3-dihydroxy-2-propoxymethyl)guanine and acyclovir in herpes simplex virus-infected and uninfected cells*. Biochem Pharmacol, 1985. **34**(7): p. 1049-56.
165. Biron, K.K., et al., *Metabolic activation of the nucleoside analog 9-([2-hydroxy-1-(hydroxymethyl)ethoxy]methyl)guanine in human diploid fibroblasts infected with human cytomegalovirus*. Proc Natl Acad Sci U S A, 1985. **82**(8): p. 2473-7.
166. Klatzmann, D., et al., *A phase I/II dose-escalation study of herpes simplex virus type 1 thymidine kinase "suicide" gene therapy for metastatic melanoma*. Study Group on Gene Therapy of Metastatic Melanoma. Hum Gene Ther, 1998. **9**(17): p. 2585-94.
167. Serman, D.H., et al., *Adenovirus-mediated herpes simplex virus thymidine kinase/ganciclovir gene therapy in patients with localized malignancy: results of a phase I clinical trial in malignant mesothelioma*. Hum Gene Ther, 1998. **9**(7): p. 1083-92.
168. Herman, J.R., et al., *In situ gene therapy for adenocarcinoma of the prostate: a phase I clinical trial*. Hum Gene Ther, 1999. **10**(7): p. 1239-49.
169. Sandmair, A.M., et al., *Thymidine kinase gene therapy for human malignant glioma, using replication-deficient retroviruses or adenoviruses*. Hum Gene Ther, 2000. **11**(16): p. 2197-205.
170. Rainov, N.G., *A phase III clinical evaluation of herpes simplex virus type 1 thymidine kinase and ganciclovir gene therapy as an adjuvant to surgical resection and radiation in adults with previously untreated glioblastoma multiforme*. Hum Gene Ther, 2000. **11**(17): p. 2389-401.
-

-
171. Ram, Z., et al., *Therapy of malignant brain tumors by intratumoral implantation of retroviral vector-producing cells*. Nat Med, 1997. **3**(12): p. 1354-61.
172. Amano, S., et al., *Use of genetically engineered bone marrow-derived mesenchymal stem cells for glioma gene therapy*. Int J Oncol, 2009. **35**(6): p. 1265-70.
173. Bak, X.Y., et al., *Human embryonic stem cell-derived mesenchymal stem cells as cellular delivery vehicles for prodrug gene therapy of glioblastoma*. Hum Gene Ther, 2011. **22**(11): p. 1365-77.
174. Freeman, S.M., et al., *The "bystander effect": tumor regression when a fraction of the tumor mass is genetically modified*. Cancer Res, 1993. **53**(21): p. 5274-83.
175. Bi, W.L., et al., *In vitro evidence that metabolic cooperation is responsible for the bystander effect observed with HSV tk retroviral gene therapy*. Hum Gene Ther, 1993. **4**(6): p. 725-31.
176. Hamel, W., et al., *Herpes simplex virus thymidine kinase/ganciclovir-mediated apoptotic death of bystander cells*. Cancer Res, 1996. **56**(12): p. 2697-702.
177. Elshami, A.A., et al., *Gap junctions play a role in the 'bystander effect' of the herpes simplex virus thymidine kinase/ganciclovir system in vitro*. Gene Ther, 1996. **3**(1): p. 85-92.
178. Dilber, M.S., et al., *Gap junctions promote the bystander effect of herpes simplex virus thymidine kinase in vivo*. Cancer Res, 1997. **57**(8): p. 1523-8.
179. Matuskova, M., et al., *HSV-tk expressing mesenchymal stem cells exert bystander effect on human glioblastoma cells*. Cancer Lett, 2010. **290**(1): p. 58-67.
180. Ilsley, D.D., et al., *Acyclic guanosine analogs inhibit DNA polymerases alpha, delta, and epsilon with very different potencies and have unique mechanisms of action*. Biochemistry, 1995. **34**(8): p. 2504-10.
181. Fick, J., et al., *The extent of heterocellular communication mediated by gap junctions is predictive of bystander tumor cytotoxicity in vitro*. Proc Natl Acad Sci U S A, 1995. **92**(24): p. 11071-5.
182. Tomicic, M.T., R. Thust, and B. Kaina, *Ganciclovir-induced apoptosis in HSV-1 thymidine kinase expressing cells: critical role of DNA breaks, Bcl-2 decline and caspase-9 activation*. Oncogene, 2002. **21**(14): p. 2141-53.
183. Beltinger, C., et al., *Mitochondrial amplification of death signals determines thymidine kinase/ganciclovir-triggered activation of apoptosis*. Cancer Res, 2000. **60**(12): p. 3212-7.
184. Wei, S.J., et al., *Involvement of Fas (CD95/APO-1) and Fas ligand in apoptosis induced by ganciclovir treatment of tumor cells transduced with herpes simplex virus thymidine kinase*. Gene Ther, 1999. **6**(3): p. 420-31.
185. Beltinger, C., et al., *Herpes simplex virus thymidine kinase/ganciclovir-induced apoptosis involves ligand-independent death receptor aggregation and activation of caspases*. Proc Natl Acad Sci U S A, 1999. **96**(15): p. 8699-704.
186. Darzynkiewicz, Z., et al., *Cytometry in cell necrobiology: analysis of apoptosis and accidental cell death (necrosis)*. Cytometry, 1997. **27**(1): p. 1-20.
187. Vermes, I., et al., *A novel assay for apoptosis. Flow cytometric detection of phosphatidylserine expression on early apoptotic cells using fluorescein labelled Annexin V*. J Immunol Methods, 1995. **184**(1): p. 39-51.
-

-
188. Vermes, I., C. Haanen, and C. Reutelingsperger, *Flow cytometry of apoptotic cell death*. J Immunol Methods, 2000. **243**(1-2): p. 167-90.
 189. Wlodkowic, D., et al., *Apoptosis and beyond: cytometry in studies of programmed cell death*. Methods Cell Biol, 2011. **103**: p. 55-98.
 190. Desagher, S. and J.C. Martinou, *Mitochondria as the central control point of apoptosis*. Trends Cell Biol, 2000. **10**(9): p. 369-77.
 191. Green, D.R. and G.P. Amarante-Mendes, *The point of no return: mitochondria, caspases, and the commitment to cell death*. Results Probl Cell Differ, 1998. **24**: p. 45-61.
 192. Green, D. and G. Kroemer, *The central executioners of apoptosis: caspases or mitochondria?* Trends Cell Biol, 1998. **8**(7): p. 267-71.
 193. Segawa, K. and S. Nagata, *An Apoptotic 'Eat Me' Signal: Phosphatidylserine Exposure*. Trends Cell Biol, 2015. **25**(11): p. 639-50.
 194. Verhoven, B., R.A. Schlegel, and P. Williamson, *Mechanisms of phosphatidylserine exposure, a phagocyte recognition signal, on apoptotic T lymphocytes*. J Exp Med, 1995. **182**(5): p. 1597-601.
 195. Fadok, V.A., et al., *Exposure of phosphatidylserine on the surface of apoptotic lymphocytes triggers specific recognition and removal by macrophages*. J Immunol, 1992. **148**(7): p. 2207-16.
 196. Lentz, B.R., *Exposure of platelet membrane phosphatidylserine regulates blood coagulation*. Prog Lipid Res, 2003. **42**(5): p. 423-38.
 197. Koopman, G., et al., *Annexin V for flow cytometric detection of phosphatidylserine expression on B cells undergoing apoptosis*. Blood, 1994. **84**(5): p. 1415-20.
 198. van Engeland, M., et al., *Annexin V-affinity assay: a review on an apoptosis detection system based on phosphatidylserine exposure*. Cytometry, 1998. **31**(1): p. 1-9.
 199. Lecoeur, H., L.M. de Oliveira-Pinto, and M.L. Gougeon, *Multiparametric flow cytometric analysis of biochemical and functional events associated with apoptosis and oncosis using the 7-aminoactinomycin D assay*. J Immunol Methods, 2002. **265**(1-2): p. 81-96.
 200. Lecoeur, H., et al., *Strategies for phenotyping apoptotic peripheral human lymphocytes comparing ISNT, annexin-V and 7-AAD cytofluorometric staining methods*. J Immunol Methods, 1997. **209**(2): p. 111-23.
 201. Maeno, E., et al., *Normotonic cell shrinkage because of disordered volume regulation is an early prerequisite to apoptosis*. Proc Natl Acad Sci U S A, 2000. **97**(17): p. 9487-92.
 202. Okada, Y. and E. Maeno, *Apoptosis, cell volume regulation and volume-regulatory chloride channels*. Comp Biochem Physiol A Mol Integr Physiol, 2001. **130**(3): p. 377-83.
 203. Ernest, N.J., C.W. Habela, and H. Sontheimer, *Cytoplasmic condensation is both necessary and sufficient to induce apoptotic cell death*. J Cell Sci, 2008. **121**(Pt 3): p. 290-7.
 204. *Guidance on nonclinical safety studies for the conduct of human clinical trials and marketing authorization for pharmaceuticals issued by the International Council of Harmonization: ICH M3 (2009)*.

-
205. Webster, J., et al., *Ethical implications of using the minipig in regulatory toxicology studies*. J Pharmacol Toxicol Methods, 2010. **62**(3): p. 160-6.
206. Balls, M. and D.W. Straughan, *The three Rs of Russell & Burch and the testing of biological products*. Dev Biol Stand, 1996. **86**: p. 11-8.
207. Rothschild, M.F., *The Genetics Of The Pigs*. 2nd ed. 2011: Cabi Publishing.
208. Cibelli, J., et al., *Strategies for improving animal models for regenerative medicine*. Cell Stem Cell, 2013. **12**(3): p. 271-4.
209. Ibrahim, Z., et al., *Selected physiologic compatibilities and incompatibilities between human and porcine organ systems*. Xenotransplantation, 2006. **13**(6): p. 488-99.
210. Merrifield, C.A., et al., *A metabolic system-wide characterisation of the pig: a model for human physiology*. Mol Biosyst, 2011. **7**(9): p. 2577-88.
211. Swindle, M.M., et al., *Swine as models in biomedical research and toxicology testing*. Vet Pathol, 2012. **49**(2): p. 344-56.
212. Bode, G., et al., *The utility of the minipig as an animal model in regulatory toxicology*. J Pharmacol Toxicol Methods, 2010. **62**(3): p. 196-220.
213. Forster, R., et al., *The RETHINK project on minipigs in the toxicity testing of new medicines and chemicals: conclusions and recommendations*. J Pharmacol Toxicol Methods, 2010. **62**(3): p. 236-42.
214. Helke, K.L. and M.M. Swindle, *Animal models of toxicology testing: the role of pigs*. Expert Opin Drug Metab Toxicol, 2013. **9**(2): p. 127-39.
215. Lehmann, S., et al., *Porcine xenograft for aortic, mitral and double valve replacement: long-term results of 2544 consecutive patients*. Eur J Cardiothorac Surg, 2015.
216. Ezashi, T., et al., *Derivation of induced pluripotent stem cells from pig somatic cells*. Proc Natl Acad Sci U S A, 2009. **106**(27): p. 10993-8.
217. Wu, Z., et al., *Generation of pig induced pluripotent stem cells with a drug-inducible system*. J Mol Cell Biol, 2009. **1**(1): p. 46-54.
218. Esteban, M.A., et al., *Generation of induced pluripotent stem cell lines from Tibetan miniature pig*. J Biol Chem, 2009. **284**(26): p. 17634-40.
219. Lunney, J.K., *Advances in swine biomedical model genomics*. Int J Biol Sci, 2007. **3**(3): p. 179-84.
220. Schook, L., et al., *Swine in biomedical research: creating the building blocks of animal models*. Anim Biotechnol, 2005. **16**(2): p. 183-90.
221. Klymiuk, N., et al., *First inducible transgene expression in porcine large animal models*. FASEB J, 2012. **26**(3): p. 1086-99.
222. van der Spoel, T.I., et al., *Human relevance of pre-clinical studies in stem cell therapy: systematic review and meta-analysis of large animal models of ischaemic heart disease*. Cardiovasc Res, 2011. **91**(4): p. 649-58.
223. Matsunari, H. and H. Nagashima, *Application of genetically modified and cloned pigs in translational research*. J Reprod Dev, 2009. **55**(3): p. 225-30.
-

-
224. Aigner, B., et al., *Transgenic pigs as models for translational biomedical research*. J Mol Med (Berl), 2010. **88**(7): p. 653-64.
225. Staunstrup, N.H., et al., *Development of transgenic cloned pig models of skin inflammation by DNA transposon-directed ectopic expression of human beta1 and alpha2 integrin*. PLoS One, 2012. **7**(5): p. e36658.
226. Wolf, E., et al., *Genetically engineered pig models for diabetes research*. Transgenic Res, 2014. **23**(1): p. 27-38.
227. Suzuki, S., et al., *Il2rg gene-targeted severe combined immunodeficiency pigs*. Cell Stem Cell, 2012. **10**(6): p. 753-8.
228. Rogers, C.S., et al., *Disruption of the CFTR gene produces a model of cystic fibrosis in newborn pigs*. Science, 2008. **321**(5897): p. 1837-41.
229. Prather, R.S., et al., *Genetically engineered pig models for human diseases*. Annu Rev Anim Biosci, 2013. **1**: p. 203-19.
230. Lehmann, J., R.M. Schulz, and R. Sanzenbacher, *[Strategic considerations on the design and choice of animal models for non-clinical investigations of cell-based medicinal products]*. Bundesgesundheitsblatt Gesundheitsforschung Gesundheitsschutz, 2015. **58**(11-12): p. 1215-24.
231. Moscoso, I., et al., *Differentiation "in vitro" of primary and immortalized porcine mesenchymal stem cells into cardiomyocytes for cell transplantation*. Transplant Proc, 2005. **37**(1): p. 481-2.
232. Bruckner, S., et al., *Isolation and hepatocyte differentiation of mesenchymal stem cells from porcine bone marrow--"surgical waste" as a novel MSC source*. Transplant Proc, 2013. **45**(5): p. 2056-8.
233. Comite, P., et al., *Isolation and ex vivo expansion of bone marrow-derived porcine mesenchymal stromal cells: potential for application in an experimental model of solid organ transplantation in large animals*. Transplant Proc, 2010. **42**(4): p. 1341-3.
234. Thomson, B.M., et al., *Preliminary characterization of porcine bone marrow stromal cells: skeletogenic potential, colony-forming activity, and response to dexamethasone, transforming growth factor beta, and basic fibroblast growth factor*. J Bone Miner Res, 1993. **8**(10): p. 1173-83.
235. Kumar, B.M., et al., *In vitro differentiation of mesenchymal progenitor cells derived from porcine umbilical cord blood*. Mol Cells, 2007. **24**(3): p. 343-50.
236. Kang, E.J., et al., *Transplantation of porcine umbilical cord matrix mesenchymal stem cells in a mouse model of Parkinson's disease*. J Tissue Eng Regen Med, 2013. **7**(3): p. 169-82.
237. Miernik, K. and J. Karasinski, *Porcine uterus contains a population of mesenchymal stem cells*. Reproduction, 2012. **143**(2): p. 203-9.
238. Park, B.W., et al., *Peripheral nerve regeneration using autologous porcine skin-derived mesenchymal stem cells*. J Tissue Eng Regen Med, 2012. **6**(2): p. 113-24.
239. Kang, E.J., et al., *In vitro and in vivo osteogenesis of porcine skin-derived mesenchymal stem cell-like cells with a demineralized bone and fibrin glue scaffold*. Tissue Eng Part A, 2010. **16**(3): p. 815-27.

-
240. Lermen, D., et al., *Neuro-muscular differentiation of adult porcine skin derived stem cell-like cells*. PLoS One, 2010. **5**(1): p. e8968.
241. Huang, T., et al., *Neuron-like differentiation of adipose-derived stem cells from infant piglets in vitro*. J Spinal Cord Med, 2007. **30 Suppl 1**: p. S35-40.
242. Zhu, W., et al., *Effects of xenogeneic adipose-derived stem cell transplantation on acute-on-chronic liver failure*. Hepatobiliary Pancreat Dis Int, 2013. **12**(1): p. 60-7.
243. Lee, A.Y., et al., *Comparative studies on proliferation, molecular markers and differentiation potential of mesenchymal stem cells from various tissues (adipose, bone marrow, ear skin, abdominal skin, and lung) and maintenance of multipotency during serial passages in miniature pig*. Res Vet Sci, 2015. **100**: p. 115-24.
244. Hwang, I.S., H.K. Bae, and H.T. Cheong, *Comparison of the characteristics and multipotential and in vivo cartilage formation capabilities between porcine adipose-derived stem cells and porcine skin-derived stem cell-like cells*. Am J Vet Res, 2015. **76**(9): p. 814-21.
245. Ock, S.A., et al., *Comparison of Immunomodulation Properties of Porcine Mesenchymal Stromal/Stem Cells Derived from the Bone Marrow, Adipose Tissue, and Dermal Skin Tissue*. Stem Cells Int, 2016. **2016**: p. 9581350.
246. Strioga, M., et al., *Same or not the same? Comparison of adipose tissue-derived versus bone marrow-derived mesenchymal stem and stromal cells*. Stem Cells Dev, 2012. **21**(14): p. 2724-52.
247. Kohli, N., et al., *An In Vitro Comparison of the Incorporation, Growth, and Chondrogenic Potential of Human Bone Marrow versus Adipose Tissue Mesenchymal Stem Cells in Clinically Relevant Cell Scaffolds Used for Cartilage Repair*. Cartilage, 2015. **6**(4): p. 252-63.
248. Liao, H.T. and C.T. Chen, *Osteogenic potential: Comparison between bone marrow and adipose-derived mesenchymal stem cells*. World J Stem Cells, 2014. **6**(3): p. 288-95.
249. Bruckner, S., et al., *A fat option for the pig: hepatocytic differentiated mesenchymal stem cells for translational research*. Exp Cell Res, 2014. **321**(2): p. 267-75.
250. Ringe, J., et al., *Porcine mesenchymal stem cells. Induction of distinct mesenchymal cell lineages*. Cell Tissue Res, 2002. **307**(3): p. 321-7.
251. Noort, W.A., et al., *Human versus porcine mesenchymal stromal cells: phenotype, differentiation potential, immunomodulation and cardiac improvement after transplantation*. J Cell Mol Med, 2012. **16**(8): p. 1827-39.
252. Bharti, D., et al., *Research Advancements in Porcine Derived Mesenchymal Stem Cells*. Curr Stem Cell Res Ther, 2016. **11**(1): p. 78-93.
253. Xiao, J.Q., et al., *Administration of IL-1Ra chitosan nanoparticles enhances the therapeutic efficacy of mesenchymal stem cell transplantation in acute liver failure*. Arch Med Res, 2013. **44**(5): p. 370-9.
254. Wang, X., et al., *Bone marrow mesenchymal stem cells increase skin regeneration efficiency in skin and soft tissue expansion*. Expert Opin Biol Ther, 2012. **12**(9): p. 1129-39.
255. Forcheron, F., et al., *Autologous adipocyte derived stem cells favour healing in a minipig model of cutaneous radiation syndrome*. PLoS One, 2012. **7**(2): p. e31694.

-
256. Ando, W., et al., *Cartilage repair using an in vitro generated scaffold-free tissue-engineered construct derived from porcine synovial mesenchymal stem cells*. *Biomaterials*, 2007. **28**(36): p. 5462-70.
257. Bernardo, M.E. and W.E. Fibbe, *Safety and efficacy of mesenchymal stromal cell therapy in autoimmune disorders*. *Ann N Y Acad Sci*, 2012. **1266**: p. 107-17.
258. Ren, G., et al., *Species variation in the mechanisms of mesenchymal stem cell-mediated immunosuppression*. *Stem Cells*, 2009. **27**(8): p. 1954-62.
259. Spaggiari, G.M., et al., *Mesenchymal stem cells inhibit natural killer-cell proliferation, cytotoxicity, and cytokine production: role of indoleamine 2,3-dioxygenase and prostaglandin E2*. *Blood*, 2008. **111**(3): p. 1327-33.
260. Meisel, R., et al., *Human but not murine multipotent mesenchymal stromal cells exhibit broad-spectrum antimicrobial effector function mediated by indoleamine 2,3-dioxygenase*. *Leukemia*, 2011. **25**(4): p. 648-54.
261. Peister, A., et al., *Adult stem cells from bone marrow (MSCs) isolated from different strains of inbred mice vary in surface epitopes, rates of proliferation, and differentiation potential*. *Blood*, 2004. **103**(5): p. 1662-8.
262. Kern, S., et al., *Comparative analysis of mesenchymal stem cells from bone marrow, umbilical cord blood, or adipose tissue*. *Stem Cells*, 2006. **24**(5): p. 1294-301.
263. Anderson, P., et al., *CD105 (endoglin)-negative murine mesenchymal stromal cells define a new multipotent subpopulation with distinct differentiation and immunomodulatory capacities*. *PLoS One*, 2013. **8**(10): p. e76979.
264. Zhou, Y.F., et al., *Spontaneous transformation of cultured mouse bone marrow-derived stromal cells*. *Cancer Res*, 2006. **66**(22): p. 10849-54.
265. Li, Q., et al., *Transformation potential of bone marrow stromal cells into undifferentiated high-grade pleomorphic sarcoma*. *J Cancer Res Clin Oncol*, 2010. **136**(6): p. 829-38.
266. Armesilla-Diaz, A., G. Elvira, and A. Silva, *p53 regulates the proliferation, differentiation and spontaneous transformation of mesenchymal stem cells*. *Exp Cell Res*, 2009. **315**(20): p. 3598-610.
267. Li, H., et al., *Spontaneous expression of embryonic factors and p53 point mutations in aged mesenchymal stem cells: a model of age-related tumorigenesis in mice*. *Cancer Res*, 2007. **67**(22): p. 10889-98.
268. Aguilar, S., et al., *Murine but not human mesenchymal stem cells generate osteosarcoma-like lesions in the lung*. *Stem Cells*, 2007. **25**(6): p. 1586-94.
269. Bernardo, M.E., et al., *Human bone marrow derived mesenchymal stem cells do not undergo transformation after long-term in vitro culture and do not exhibit telomere maintenance mechanisms*. *Cancer Res*, 2007. **67**(19): p. 9142-9.
270. Meza-Zepeda, L.A., et al., *High-resolution analysis of genetic stability of human adipose tissue stem cells cultured to senescence*. *J Cell Mol Med*, 2008. **12**(2): p. 553-63.
271. Rosland, G.V., et al., *Long-term cultures of bone marrow-derived human mesenchymal stem cells frequently undergo spontaneous malignant transformation*. *Cancer Res*, 2009. **69**(13): p. 5331-9.
-

-
272. Rubio, D., et al., *Spontaneous human adult stem cell transformation*. *Cancer Res*, 2005. **65**(8): p. 3035-9.
273. Torsvik, A., et al., *Spontaneous malignant transformation of human mesenchymal stem cells reflects cross-contamination: putting the research field on track - letter*. *Cancer Res*, 2010. **70**(15): p. 6393-6.
274. de la Fuente, R., et al., *Retraction: Spontaneous human adult stem cell transformation*. *Cancer Res*, 2010. **70**(16): p. 6682.
275. *Guideline on quality, non-clinical and clinical aspects of medicinal products containing genetically modified cells*, E.M. Agency, Editor. 2012. p. 17.
276. Saalfrank, D.A., *Modelling the multi-step process of tumorigenesis in pigs*. 2015, Technische Universität München.
277. Loew, R., et al., *A new PG13-based packaging cell line for stable production of clinical-grade self-inactivating gamma-retroviral vectors using targeted integration*. *Gene Ther*, 2010. **17**(2): p. 272-80.
278. Zufferey, R., et al., *Woodchuck hepatitis virus posttranscriptional regulatory element enhances expression of transgenes delivered by retroviral vectors*. *J Virol*, 1999. **73**(4): p. 2886-92.
279. Hunt, C.J., *Cryopreservation of Human Stem Cells for Clinical Application: A Review*. *Transfus Med Hemother*, 2011. **38**(2): p. 107-123.
280. Stolzing, A., et al., *Hydroxyethylstarch in cryopreservation - mechanisms, benefits and problems*. *Transfus Apher Sci*, 2012. **46**(2): p. 137-47.
281. Uzbekova, S., et al., *Zygote arrest 1 gene in pig, cattle and human: evidence of different transcript variants in male and female germ cells*. *Reprod Biol Endocrinol*, 2006. **4**: p. 12.
282. Wilmut, I., et al., *Viable offspring derived from fetal and adult mammalian cells*. *Nature*, 1997. **385**(6619): p. 810-3.
283. Martin, I., et al., *A relativity concept in mesenchymal stromal cell manufacturing*. *Cytotherapy*, 2016. **18**(5): p. 613-20.
284. Smiler, D. and M. Soltan, *Bone marrow aspiration: technique, grafts, and reports*. *Implant Dent*, 2006. **15**(3): p. 229-35.
285. Fennema, E.M., et al., *The effect of bone marrow aspiration strategy on the yield and quality of human mesenchymal stem cells*. *Acta Orthop*, 2009. **80**(5): p. 618-21.
286. Schallmoser, K., et al., *Human platelet lysate can replace fetal bovine serum for clinical-scale expansion of functional mesenchymal stromal cells*. *Transfusion*, 2007. **47**(8): p. 1436-46.
287. Astori, G., et al., *Platelet lysate as a substitute for animal serum for the ex-vivo expansion of mesenchymal stem/stromal cells: present and future*. *Stem Cell Res Ther*, 2016. **7**(1): p. 93.
288. Peters, A.E. and A.E. Watts, *Biopsy Needle Advancement during Bone Marrow Aspiration Increases Mesenchymal Stem Cell Concentration*. *Front Vet Sci*, 2016. **3**: p. 23.
289. Bonab, M.M., et al., *Aging of mesenchymal stem cell in vitro*. *BMC Cell Biol*, 2006. **7**: p. 14.

-
290. Geissler, S., et al., *Functional comparison of chronological and in vitro aging: differential role of the cytoskeleton and mitochondria in mesenchymal stromal cells*. PLoS One, 2012. **7**(12): p. e52700.
291. Bosch, P., S.L. Pratt, and S.L. Stice, *Isolation, characterization, gene modification, and nuclear reprogramming of porcine mesenchymal stem cells*. Biol Reprod, 2006. **74**(1): p. 46-57.
292. Vacanti, V., et al., *Phenotypic changes of adult porcine mesenchymal stem cells induced by prolonged passaging in culture*. J Cell Physiol, 2005. **205**(2): p. 194-201.
293. Uren, A.G., et al., *Retroviral insertional mutagenesis: past, present and future*. Oncogene, 2005. **24**(52): p. 7656-72.
294. Vargas, J.E., et al., *Retroviral vectors and transposons for stable gene therapy: advances, current challenges and perspectives*. J Transl Med, 2016. **14**(1): p. 288.
295. Maetzig, T., et al., *Gammaretroviral vectors: biology, technology and application*. Viruses, 2011. **3**(6): p. 677-713.
296. Tailor, C.S., A. Nouri, and D. Kabat, *Cellular and species resistance to murine amphotropic, gibbon ape, and feline subgroup C leukemia viruses is strongly influenced by receptor expression levels and by receptor masking mechanisms*. J Virol, 2000. **74**(20): p. 9797-801.
297. Bahrami, S., M. Duch, and F.S. Pedersen, *Change of tropism of SL3-2 murine leukemia virus, using random mutational libraries*. J Virol, 2004. **78**(17): p. 9343-51.
298. Park, S.W., C.W. Pyo, and S.Y. Choi, *High-efficiency lentiviral transduction of primary human CD34(+) hematopoietic cells with low-dose viral inocula*. Biotechnol Lett, 2015. **37**(2): p. 281-8.
299. Everson, E.M. and G.D. Trobridge, *Retroviral vector interactions with hematopoietic cells*. Curr Opin Virol, 2016. **21**: p. 41-46.
300. Kusabuka, H., et al., *Highly efficient gene transfer using a retroviral vector into murine T cells for preclinical chimeric antigen receptor-expressing T cell therapy*. Biochem Biophys Res Commun, 2016. **473**(1): p. 73-9.
301. Stolzing, A., et al., *Age-related changes in human bone marrow-derived mesenchymal stem cells: consequences for cell therapies*. Mech Ageing Dev, 2008. **129**(3): p. 163-73.
302. Beausejour, C., *Bone marrow-derived cells: the influence of aging and cellular senescence*. Handb Exp Pharmacol, 2007(180): p. 67-88.
303. Zamai, L., et al., *Optimal detection of apoptosis by flow cytometry depends on cell morphology*. Cytometry, 1993. **14**(8): p. 891-7.
304. Nikolettou, V., et al., *Crosstalk between apoptosis, necrosis and autophagy*. Biochim Biophys Acta, 2013. **1833**(12): p. 3448-59.
305. Booth, L.A., et al., *The role of cell signalling in the crosstalk between autophagy and apoptosis*. Cell Signal, 2014. **26**(3): p. 549-55.
306. Schroder, K., et al., *Interferon-gamma: an overview of signals, mechanisms and functions*. J Leukoc Biol, 2004. **75**(2): p. 163-89.

-
307. de Bruin, A.M., et al., *Interferon-gamma impairs proliferation of hematopoietic stem cells in mice*. Blood, 2013. **121**(18): p. 3578-85.
308. Kim, Y.G., et al., *Ganciclovir-mediated cell killing and bystander effect is enhanced in cells with two copies of the herpes simplex virus thymidine kinase gene*. Cancer Gene Ther, 2000. **7**(2): p. 240-6.
309. Katsuda, T., et al., *The therapeutic potential of mesenchymal stem cell-derived extracellular vesicles*. Proteomics, 2013. **13**(10-11): p. 1637-53.
310. Rani, S., et al., *Mesenchymal Stem Cell-derived Extracellular Vesicles: Toward Cell-free Therapeutic Applications*. Mol Ther, 2015. **23**(5): p. 812-23.
311. Kordelas, L., et al., *MSC-derived exosomes: a novel tool to treat therapy-refractory graft-versus-host disease*. Leukemia, 2014. **28**(4): p. 970-3.
312. Lai, R.C., et al., *Exosome secreted by MSC reduces myocardial ischemia/reperfusion injury*. Stem Cell Res, 2010. **4**(3): p. 214-22.
313. Rani, S., et al., *Mesenchymal Stem Cell-derived Extracellular Vesicles: Toward Cell-free Therapeutic Applications*. Mol Ther, 2015. **23**(5): p. 812-823.
314. Horwitz, E.M. and W.R. Prather, *Cytokines as the major mechanism of mesenchymal stem cell clinical activity: expanding the spectrum of cell therapy*. Isr Med Assoc J, 2009. **11**(4): p. 209-11.
315. Jones, S., et al., *The antiproliferative effect of mesenchymal stem cells is a fundamental property shared by all stromal cells*. J Immunol, 2007. **179**(5): p. 2824-31.
316. Ramasamy, R., et al., *Mesenchymal stem cells inhibit proliferation and apoptosis of tumor cells: impact on in vivo tumor growth*. Leukemia, 2007. **21**(2): p. 304-10.
317. Caplan, A.I., *MSCs: The Sentinel and Safe-Guards of Injury*. J Cell Physiol, 2016. **231**(7): p. 1413-6.
318. Liu, Y., et al., *Cryopreservation of human bone marrow-derived mesenchymal stem cells with reduced dimethylsulfoxide and well-defined freezing solutions*. Biotechnol Prog, 2010. **26**(6): p. 1635-43.
319. Haack-Sorensen, M., A. Ekblond, and J. Kastrup, *Cryopreservation and Revival of Human Mesenchymal Stromal Cells*. Methods Mol Biol, 2016. **1416**: p. 357-74.
320. Ock, S.A. and G.J. Rho, *Effect of dimethyl sulfoxide (DMSO) on cryopreservation of porcine mesenchymal stem cells (pMSCs)*. Cell Transplant, 2011. **20**(8): p. 1231-9.
321. Yong, K.W., J.R. Choi, and W.K. Wan Safwani, *Biobanking of Human Mesenchymal Stem Cells: Future Strategy to Facilitate Clinical Applications*. Adv Exp Med Biol, 2016. **951**: p. 99-110.
322. Spaeth, E., et al., *Inflammation and tumor microenvironments: defining the migratory itinerary of mesenchymal stem cells*. Gene Ther, 2008. **15**(10): p. 730-8.
323. Rogers, C.S., et al., *The porcine lung as a potential model for cystic fibrosis*. Am J Physiol Lung Cell Mol Physiol, 2008. **295**(2): p. L240-63.

-
324. Fernandes-Platzgummer, A., et al., *Clinical-Grade Manufacturing of Therapeutic Human Mesenchymal Stem/Stromal Cells in Microcarrier-Based Culture Systems*. Methods Mol Biol, 2016. **1416**: p. 375-88.
325. Sart, S. and S.N. Agathos, *Large-Scale Expansion and Differentiation of Mesenchymal Stem Cells in Microcarrier-Based Stirred Bioreactors*. Methods Mol Biol, 2016. **1502**: p. 87-102.
326. Tsai, A.C. and T. Ma, *Expansion of Human Mesenchymal Stem Cells in a Microcarrier Bioreactor*. Methods Mol Biol, 2016. **1502**: p. 77-86.
327. de Soure, A.M., et al., *Scalable microcarrier-based manufacturing of mesenchymal stem/stromal cells*. J Biotechnol, 2016. **236**: p. 88-109.
328. Ketterl, N., et al., *A robust potency assay highlights significant donor variation of human mesenchymal stem/progenitor cell immune modulatory capacity and extended radio-resistance*. Stem Cell Res Ther, 2015. **6**: p. 236.
329. Thej, C., et al., *Development of a surrogate potency assay to determine the angiogenic activity of Stempeuceel(R), a pooled, ex-vivo expanded, allogeneic human bone marrow mesenchymal stromal cell product*. Stem Cell Res Ther, 2017. **8**(1): p. 47.
330. ; European Medicines Agency]. Available from: http://ec.europa.eu/health/human-use/advanced-therapies/developments_en.
331. *List of authorized ATMPs in the EU*. Dec 2016; Available from: <http://www.pei.de/EN/medicinal-products/advanced-therapy-medicinal-products-atmp/advanced-therapy-medicinal-products-atmp-node.html>.
332. Holm, I.E., A.K. Alstrup, and Y. Luo, *Genetically modified pig models for neurodegenerative disorders*. J Pathol, 2016. **238**(2): p. 267-87.
333. Flisikowska, T., et al., *A porcine model of familial adenomatous polyposis*. Gastroenterology, 2012. **143**(5): p. 1173-5 e1-7.

11 Supplemental

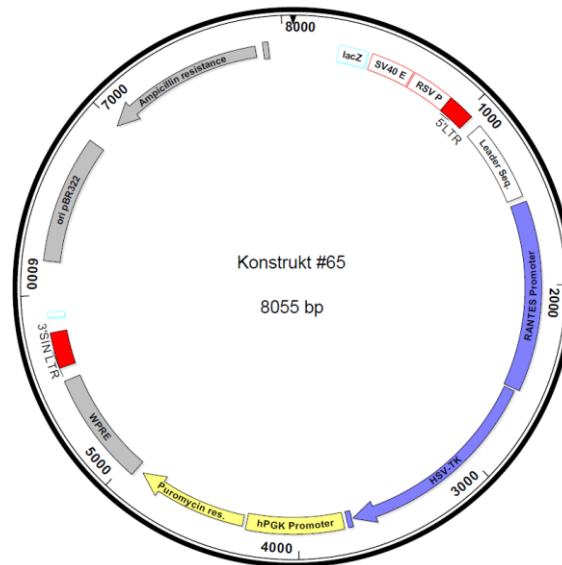


Figure 33: Construct #65 was used as plasmid for the clinical grad vector carrying the therapeutic gene **HSV-TK** under the control of the **Rantes promoter**. HSV-TK was fused with HA to allow an identification of the enzyme by flow cytometry mediated by antibodies. The selection gene for degrading the antibiotic puromycin is controlled under the constitutive promoter hPGK that shows continuous expression. The WPRE enhances the mRNA stability of the transcribed gene.

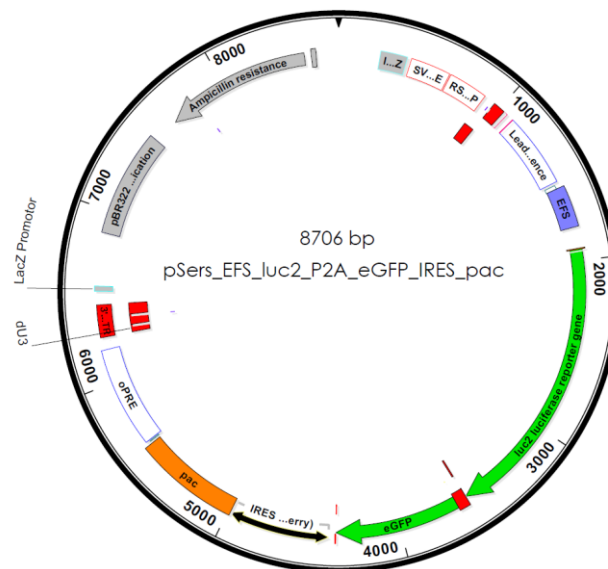


Figure 34: The eGFP containing plasmid was used to tag the cell lines HT1080 and K67. The GFP signal was used during flow cytometry analysis to distinguish cell lines and MSCs. The expression of GFP was under control of the EFS, a constitutive, promoter.